



**US Army Corps  
of Engineers®**  
Engineer Research and  
Development Center

*System-Wide Water Resources Research Program*

# **Carbon-Flow-Based Modeling of Ecophysiological Processes and Biomass Dynamics of Submersed Aquatic Plants**

Elly P. H. Best and William A. Boyd

September 2007

# **Carbon-Flow-Based Modeling of Ecophysiological Processes and Biomass Dynamics of Submersed Aquatic Plants**

Elly P. H. Best and William A. Boyd

*Environmental Laboratory  
U.S. Army Engineer Research and Development Center  
3909 Halls Ferry Road  
Vicksburg, MS 39180-6199*

Final report

Approved for public release; distribution is unlimited.

**Abstract:** A dynamic simulation modeling approach to describing carbon-flow-based, ecophysiological processes and biomass dynamics of freshwater submersed aquatic plant species has been developed. The models describe major, carbon-flow-based ecophysiological processes and biomass dynamics of four common freshwater species and how these are influenced by factors such as light, temperature, current velocity, dissolved inorganic carbon availability, oxygen concentration, and human influences such as management measures (changes in turbidity, mechanical harvesting, grazing, flooding). The model species are *Vallisneria americana* [model VALLA], *Potamogeton pectinatus* [POTAM], *Hydrilla verticillata* [HYDRIL], and *Myriophyllum spicatum* [MILFO]. These plant species are similar in growth strategy but differ significantly in morphology and physiology. The same modeling approach was followed for all species, with species-characteristic morphology and physiology incorporated in four separate models. *V. americana* and *P. pectinatus* are considered as desirable, and *H. verticillata* and *M. spicatum* as invasive species in parts of the United States. In the models, phenology is tied to day-degree sum. This enables simulations for different sites and climates facilitating model operation. The models contain unique descriptions of (1) species-characteristic vertical distribution of shoot biomass in the water column; (2) recalculation procedures of vertical distribution with daily changes in water level; (3) ibidem with daily removal of shoot biomass at various levels within the water column; (4) species-characteristic epiphytic light interception; (5) species-characteristic effects of current velocity on photosynthesis; (6) removal of periodic shoot and tuber/root crown biomass; and (7) relationships of plant process parameters with site-specific climate by linkage with formatted weather files and calculation of latitude-specific effects on day length. Sensitivity analysis showed that the models are very sensitive to changes in process parameters influencing carbon flow. A good fit was found between simulated and measured biomass in the field. The models can be used to simulate the daily changes in plant processes, biomass, and persistence under various site-specific conditions and management scenarios over a 1- to 5-year period of four submersed aquatic vegetation species, in climates varying from temperate to tropical.

**DISCLAIMER:** The contents of this report are not to be used for advertising, publication, or promotional purposes. Citation of trade names does not constitute an official endorsement or approval of the use of such commercial products. All product names and trademarks cited are the property of their respective owners. The findings of this report are not to be construed as an official Department of the Army position unless so designated by other authorized documents.

**DESTROY THIS REPORT WHEN NO LONGER NEEDED. DO NOT RETURN IT TO THE ORIGINATOR.**

# Contents

<b>Figures and Tables</b> .....	<b>v</b>
<b>Preface</b> .....	<b>vii</b>
<b>1 Introduction</b> .....	<b>1</b>
<b>2 Modeling Concepts</b> .....	<b>3</b>
<b>3 Description of Models</b> .....	<b>5</b>
Model approach, variables, and implementation.....	5
<i>Model approach</i> .....	5
<i>Variables</i> .....	6
<i>Implementation</i> .....	6
Model processes and parameter values.....	13
<i>Model processes</i> .....	13
<i>Parameter values</i> .....	27
<b>4 Simulations</b> .....	<b>59</b>
VALLA.....	59
VALLA calibration: Simulated and measured behavior of a <i>V. americana</i> community in Chenango Lake, NY.....	59
VALLA validation: Simulated and measured behavior of a <i>V. americana</i> community at other latitudes.....	61
VALLA example applications.....	63
POTAM.....	68
POTAM calibration: Simulated and measured behavior of a <i>P. pectinatus</i> community in the Western Canal near Zandvoort, NL.....	68
POTAM validation: Simulated and measured behavior of a <i>P. pectinatus</i> community in Lake Veluwe, NL, in two consecutive years with greatly different turbidities.....	70
POTAM example application: Simulated and measured behavior of a <i>P. pectinatus</i> community at other latitudes.....	71
HYDRIL.....	73
HYDRIL calibration: Simulated and measured behavior of the <i>H. verticillata</i> community in Lake Orange, FL.....	73
HYDRIL validation: Simulated and measured behavior of the <i>H. verticillata</i> community in Lake Trafford, FL.....	74
HYDRIL example applications.....	75
MILFO.....	76
MILFO calibration: Simulated and measured behavior of a <i>M. spicatum</i> community in Lake Wingra, WI.....	76
MILFO validation: Simulated and measured behavior of a <i>M. spicatum</i> community at a more southern latitude.....	78
MILFO example application: Simulated and measured behavior of a <i>M. spicatum</i> community at other latitudes.....	80

---

<b>5</b>	<b>Sensitivity Analysis of the Models</b> .....	<b>82</b>
<b>6</b>	<b>Discussion</b> .....	<b>85</b>
	Developmental cycle .....	85
	Carbon-flow-based aspects .....	86
	Unique characteristics of the models .....	86
	Application potential .....	87
<b>7</b>	<b>Conclusions</b> .....	<b>89</b>
	<b>References</b> .....	<b>90</b>
	<b>Report Documentation Page</b>	

# Figures and Tables

## Figures

Figure 1. Relational diagram illustrating the organization of each model and its subroutines in combination with the FSE shell. ....	12
Figure 2. Relational diagram illustrating wintering and sprouting of tubers in tuber-forming SAV. ....	17
Figure 3. Relational diagram illustrating wintering and sprouting of the rhizome/root crown of <i>M. spicatum</i> . ....	20
Figure 4. Relational diagram illustrating photosynthesis, respiration, and biomass formation in tuber-forming SAV. ....	24
Figure 5. Relational diagram illustrating translocation and senescence following anthesis in tuber-forming SAV. ....	26
Figure 6. Relationship between development phase and relative epiphytic light interception used for calibration of VALLA. ....	48
Figure 7. Relationship between current velocity and relative photosynthetic rate used for calibration of VALLA. ....	49
Figure 8. Relationship between development phase and relative epiphytic light interception used for calibration of POTAM, HYDRIL, and MILFO. ....	51
Figure 9. Relationship between current velocity and relative photosynthetic rate used for calibration of POTAM, HYDRIL, and MILFO. ....	52
Figure 10. Simulated biomass of plants (A), dormant and new tuber numbers (B), and measured plant biomass (C) of <i>V. americana</i> in Chenango Lake, NY. ....	60
Figure 11. Simulated photosynthetic rates of <i>V. americana</i> in Chenango Lake, NY, with water or air temperatures as input (initial plant parameter values as in nominal run). ....	60
Figure 12. Simulated biomass of plants and tubers of <i>V. americana</i> in Chenango Lake, NY, started from different initial biomass, but run in the same environmental and climatological, nominal, conditions. ....	61
Figure 13. Simulated biomass of plants and tubers of <i>V. americana</i> at sites differing in latitude. ....	63
Figure 14. Water level fluctuations over a 10-year period measured at the dam of Pool 8 of the Upper Mississippi River, WI. ....	65
Figure 15. Comparison of historical and simulated data on biomass of plants and tubers of <i>V. americana</i> in the Upper Mississippi River System, WI. ....	66
Figure 16. Simulated biomass of shoots (A) and tubers (B) of <i>V. americana</i> in Upper Mississippi River Pool 8 at Turtle Island (lat 43° 10' N, long 91° 30' W). ....	68
Figure 17. Simulated biomass of plants (A), dormant and new tuber numbers (B), and measured plant biomass (C) of <i>P. pectinatus</i> in the Western Canal near Zandvoort, NL. ....	69
Figure 18. Simulated and measured biomass of <i>P. pectinatus</i> plants and tubers in Lake Veluwe, NL (lat 52° 17' N, long 05° 19' E), during two successive years differing in water transparency. ....	71
Figure 19. Simulated biomass of plants and tubers of <i>P. pectinatus</i> at sites differing in latitude. ....	73

Figure 20. Simulated biomass of plants (A), dormant and new tuber numbers (B), and measured plant biomass (C) of <i>H. verticillata</i> in Lake Orange, FL. ....	74
Figure 21. Simulated biomass of plants and tubers of <i>H. verticillata</i> at sites differing in latitude. ....	75
Figure 22. Simulated biomass of shoots, roots (A), rhizomes/root crowns (B), and measured shoot biomass (C) of <i>M. spicatum</i> in Lake Wingra, WI.....	77
Figure 23. Simulated biomass with assimilate requirement for growth (ASRQ) value nominal (A) or as suggested for SAV (B), and measured shoot biomass (C) of a <i>M. spicatum</i> community in Lake Wingra, WI (SAV ASRQ data; Spencer et al. 1997). ....	78
Figure 24. Simulated biomass of shoots, roots (A), rhizomes/root crowns (B), and measured shoot biomass (C) of <i>M. spicatum</i> in Lake Guntersville, AL. ....	79
Figure 25. Simulated biomass of shoots, roots, and rhizomes of <i>M. spicatum</i> at sites differing in latitude, starting from a nominal initial biomass. ....	80

## Tables

Table 1. Variable listing of the models. ....	6
Table 2a. Parameter values used in VALLA. ....	27
Table 2b. Parameter values used in POTAM. ....	29
Table 2c. Parameter values used in HYDRIL. ....	30
Table 2d. Parameter values used in MILFO. ....	32
Table 3a. Relationship between development phase (DVS) of <i>V. americana</i> , day of year, at a reference temperature of 30 °C and 3 °C day-degree sum in a temperate climate (DVRVT= 0.015; DVRRT= 0.040).....	35
Table 3b. Relationship between development phase (DVS) of <i>P. pectinatus</i> , day of year, at a reference temperature of 30 °C and 3 °C day-degree sum in a temperate climate (DVRVT= 0.015; DVRRT= 0.040).....	35
Table 3c. Relationship between development phase (DVS) of <i>H. verticillata</i> , day of year, at a reference temperature of 30 °C and 3 °C day-degree sum in a temperate climate (DVRVT= 0.012; DVRRT= 0.012).....	36
Table 3d. Relationship between development phase (DVS) of <i>M. spicatum</i> , day of year, at a reference temperature of 30 °C and 3 °C day-degree sum in a temperate climate (DVRVT= 0.022; DVRRT= 0.015).....	36
Table 3e. Relationship between development phase (DVS) of <i>M. spicatum</i> , day of year, at a reference temperature of 30 °C and 3 °C day-degree sum in a tropical climate (DVRVT= 0.022; DVRRT= 0.015).....	37
Table 4. Relationship between tuber size and concurrently initiated tuber number in <i>V. americana</i> and <i>P. pectinatus</i> . ....	42
Table 5. Simulated effects of mechanical harvesting date and depth on <i>H. verticillata</i> plant biomass and tuber bank density.....	76
Table 6. Relative sensitivity (RS) of two state variables to deviations in parameter values from their nominal values as presented in Table 2. ....	83
Table 7. Environmental factor analysis, expressed as relative sensitivity (RS) of two state variables to deviations in parameter values from their nominal values as presented in Table 2.....	84

## Preface

This report summarizes the expanded development of aquatic plant growth models that can be used as stand-alone versions or linked with a variety of hydrologic and sediment modeling systems. This development effort was performed by the U.S. Army Corps of Engineers (USACE) Engineer Research and Development Center (ERDC), Environmental Laboratory (EL), Vicksburg, MS. Funding for this expansion effort was provided under the System-Wide Water Resources Program (SWWRP). Dr. Steven L. Ashby was Program Manager of SWWRP. Previous funding for the development of the versions 1.0 of these models was provided by the USACE Aquatic Plant Control Research Program (APCRP); and for the refinement of VALLA and POTAM for use in the Upper Mississippi River System was provided by the USACE Rock Island District.

Special thanks go to Drs. C. F. Cerco, Water Quality and Contaminant Modeling Branch, and D. M. Soballe (Environmental Processes Branch, USACE) who reviewed and provided comments on an earlier version of this report.

This study was performed by Dr. Elly P. H. Best, Principal Investigator, of the Environmental Risk Assessment Branch (ERAB), in cooperation with William A. Boyd, who assisted with programming and model runs, of the Ecosystem Processes and Engineering Branch, both of the Ecological Processes and Engineering Division (EPED). The study was conducted under the general supervision of Dr. Robert P. Jones, Chief, ERAB; Richard E. Price, Chief, EPED; Dr. Mike Passmore, Acting Deputy Director, and Dr. Beth C. Fleming, Director of EL.

COL Richard B. Jenkins was Commander and Executive Director of ERDC. Dr. James R. Houston was Director.

# 1 Introduction

Submersed aquatic vegetation (SAV) may play important roles in aquatic ecosystems. Roles attributed to desirable species are stabilization of sediment, amelioration of transparency and regulation of nutrient availability in the water column, and serving as habitat and food source for invertebrates, fish, and waterfowl. Many SAV communities in freshwater and marine environments have experienced dramatic losses during the past three to five decades. Most commonly declines are attributed to decreases in water transparency due to anthropogenic influences, but often they have been attributed to other factors such as high water levels, extended draw-downs, changes in current velocity, and epiphyte shading, or to combinations of factors. However, once the vegetation is lost from a given locale, increased sediment resuspension and current velocity may place significant constraints on plant recolonization of that site. Roles attributed to nuisance or invasive SAV species, however, are excessive biomass production interfering with human utilization of freshwater resources or displacing desirable indigenous communities.

The degree to which SAV influences the ecosystem is proportional to plant mass and depends on plant species and physical and chemical factors. Therefore, predictions of the environmental impact of management measures concerning the aquatic system in which SAV grows should be based on accurate estimates of plant (1) species, mass, and pertinent physiological properties; (2) contribution to various food chains (live and dead biomass); (3) contribution to biogeochemical cycling (carbon, nitrogen, phosphorus) and oxygen regime; and (4) contribution to habitat availability. Simulation models that include descriptions of SAV responses in terms of biomass dynamics to changes in physical and chemical factors in various climates can be useful tools for water resource managers because they can be used to evaluate key environmental conditions in which SAV would persist or produce excessive biomass, with ensuing consequences for the systems in which they grow, either affected or not affected by management scenarios (Carr et al. 1997; Best et al. 2001). Although the number of simulation models for production of monotypic SAV is increasing (e.g., Titus et al. 1975; Best 1981; Collins and Wlosinski 1985; Best and Jacobs 1990; Hootsmans 1994; Scheffer et al. 1993; Herb and Stefan 2003), it is still relatively low compared with that for terrestrial vegetation.

This technical report describes aquatic vegetation models that simulate major, carbon flow-based ecophysiological processes, biomass dynamics and persistence of four common freshwater species and how these are influenced by factors such as light, temperature, current velocity, dissolved inorganic carbon (DIC) availability, oxygen concentration, and human influences such as management measures (changes in turbidity, mechanical harvesting, grazing, flooding). The model species are *Vallisneria americana* (American wildcelery)-VALLA, *Potamogeton pectinatus* (sago pondweed)-POTAM, *Hydrilla verticillata* (dioecious hydrilla)-HYDRIL, and *Myriophyllum spicatum* (Eurasian watermilfoil)-MILFO. These plant species are similar in growth strategy, but they differ significantly in morphology and physiology. Therefore, the same modeling approach was followed for all species, with species-characteristic morphology and physiology incorporated in four separate models. *V. americana* and *P. pectinatus*<sup>1</sup> are considered as desirable, and *H. verticillata* and *M. spicatum* as invasive species in parts of the United States.

The models can be used to simulate the daily changes in plant processes and biomass under various site-specific conditions and management scenarios over a 1- to 5-year period of four SAV species, in climates varying from temperate to tropical.

---

<sup>1</sup> *P. pectinatus* has relatively recently moved from the Potamogetonaceae (Voss 1972) into the Stukeniaceae (Crow and Hellquist 2000), and its current taxonomic name is *Stukenia pectinata*. The authors use the taxonomic name commonly cited up to 2000 in this paper, since all literature references pertain to the formerly used name of *P. pectinatus* for this plant.

## 2 Modeling Concepts

Each model simulates growth of a typical SAV community. In the models growth is considered as the plant dry matter accumulation including subterranean tubers in tuber-forming plants or rhizome/root crown systems in *M. spicatum*, under ample supply of nitrogen and phosphorus, in a pest-, disease-, and competitor-free environment under the prevailing weather conditions. At least one plant cohort (a cohort is a plant group exhibiting the same phenological cycle) waxes and wanes per season in different climatological regions, varying from temperate to tropical. The rate of dry matter accumulation is a function of irradiance, temperature, carbon dioxide (CO<sub>2</sub>) availability, and plant characteristics. The rate of CO<sub>2</sub> assimilation (photosynthesis) of the SAV community depends on the radiant energy absorbed by the canopy, which is a function of incoming radiation, reflection at the water surface, attenuation by the water column, the epiphytes, plant shoots, and associated leaf area. The daily rate of gross CO<sub>2</sub> assimilation of the community is calculated from the absorbed radiation, the photosynthetic characteristics of individual shoot tips and the pH-determined CO<sub>2</sub> availability. Calculations are executed in a set of subroutines added to the model. Part of the carbohydrates produced is used to maintain the existing biomass. The remaining carbohydrates are converted into structural dry matter (plant organs). In the conversion process, part of the weight is lost in respiration. The dry matter produced is partitioned among the various plant organs using partitioning factors, defined as a function of the phenological cycle of the community. The dry weights (DW) of the plant organs are obtained by integration of their growth rates over time. The plant winters through tubers (rhizome/root crown for *M. spicatum*) in the sediment without or with biomass present. All calculations are performed on a square meter basis. Since environmental factors and plant growth characteristics vary with depth, in each model the water column and associated growth-related processes have been partitioned in 0.10-m depth classes.

Seed formation has not been included in the models because its role in maintaining existing SAV communities in a temperate climate is minimal. Dispersal and colonization of new habitats by seeds are recognized, important characteristics of SAV. The latter processes, however, are better described using other modeling approaches as discussed by Scheffer (1991),

i.e., based on logistic regression or on descriptions of population dynamics varying in time and space.

## 3 Description of Models

### Model approach, variables, and implementation

#### Model approach

The models follow a mechanistic approach explaining plant growth on the basis of the underlying processes, such as phenology, CO<sub>2</sub> assimilation, and respiration, as influenced by environmental conditions. They are carbon-flow-based mass balance models. This type of model follows the state-variable approach, in that it is based on the assumption that the state of each system can be quantified at any moment and that changes in the state can be described by mathematical equations. In this type of model, state, rate, and driving variables are distinguished. State variables are quantities such as biomass. Driving variables characterize the effect of environment on the system at its boundaries, such as climate and environmental conditions. Each state variable is associated with rate variables that characterize its rate of change at a certain instant, as a result of specific processes. These variables represent flows of material between state variables, the values of which are calculated from the state and driving variables according to knowledge of the physical, chemical, and biological processes involved. After all rate variables are calculated, these values are then used to calculate the state variables according to the following scheme: state variable at time  $t + \Delta t$  equals state variable at time  $t$  plus the rate at time  $t$  multiplied by  $\Delta t$ . This procedure, called numerical integration, gives the new values of the state variables, from which the calculation of rate variables is repeated. To avoid instabilities, the time interval  $\Delta t$  must be small enough so that the rates do not change materially within this period. This is generally the case when the time interval of integration is smaller than one-tenth of the time coefficient or response time. This characteristic time of a system is equal to the inverse of the most rapid relative rate of change of one of its state variables. The smaller the time coefficient, the smaller the time interval of integration (Rabbinge and De Wit 1989).

The predictive ability of mechanistic models does not always equal expectations. It should be realized, however, that each parameter estimate and process formulation has its own uncertainty, and that uncertainties in parameter estimates may accumulate in the prediction of the final yield. The

primary aim of this model approach is to increase insight in the system studied by quantitatively integrating the current knowledge in a dynamic simulation model. By studying the behavior of such a model, better insight in the real system is gained.

### **Variables**

A list of variables used in the models discussed in this report is presented in Table 1.

### **Implementation**

Each model is implemented as a FORTRAN77 program. For numerical integration, the Runge-Kutta technique is used, which allows employing a variable time-step. The program integrates the equations once per day in the main subroutine (MODEL), once per second in the subroutines calculating day length and instantaneous irradiance (ASTRO) and instantaneous gross assimilation (ASSIM), and at three times of the day in the subroutine calculating daily total gross assimilation (TOTASS; Gaussian integration). Instantaneous gross assimilation is calculated per second and converted to hourly rates within ASSIM.

Model organization is similar to that used for agricultural crops (SUCROS1; Goudriaan et al. 1992). Each model runs within a FORTRAN Simulation Environment (FSE) shell, Version 2.1, to enable easy handling of input and output files and rapid visualization of the simulation results (Van Kraalingen 1995). In the model input file, default values on plant characteristics and environmental conditions are provided. Users may enter site-specific data into this input file. In the weather file, data on irradiance, temperature, and latitude/longitude are provided. Users may enter site-specific data into this weather file. Two types of output files are generated, i.e., a binary file and an ASCII text file. The binary file is used for visualization of the results within the shell. The ASCII file can be imported in various software packages and serve as the basis for the preparation of publishable tables and graphics.

Each model can be executed on IBM PC-ATs and compatibles as a stand-alone version. Because of its language and simple structure, the model will generally be compatible with ecosystem models that accept FORTRAN. Executable model versions are available via the internet at <http://el.erd.c.usace.mil/products.cfm?Topic=model&Type=aquatic>. The organization of the

models and their subroutines in combination with the FSE shell is illustrated in Figure 1.

Table 1. Variable listing of the models.

Name	Explanation	Dimension
AH(i)	Absolute height of vegetation on top of stratum I, measured from the plant top	m
AMAX	Actual CO <sub>2</sub> assimilation rate at light saturation for shoots	g CO <sub>2</sub> g <sup>-1</sup> DW h <sup>-1</sup>
AMTMP	Daytime temperature effect on AMX (relative)	-
AMTMPT	Table of AMX as function of DVS	-, -
AMX	Potential CO <sub>2</sub> assimilation rate at light saturation for shoots	g CO <sub>2</sub> g <sup>-1</sup> DW h <sup>-1</sup>
ASRQ	Assimilate requirement for plant dry matter production	g CH <sub>2</sub> O g <sup>-1</sup> DW
ASRQSO	Assimilate requirement for storage component production	g CH <sub>2</sub> O g <sup>-1</sup> DW
ATMTR	Atmospheric transmission coefficient	-
COSLD	Intermediate variable in calculating solar height	-
CRIFAC	Critical shoot weight per 0.1-m depth layer	g DW per (0.1-m depth layer) plant <sup>-1</sup>
CRIGWT	Critical weight per 0.1-m depth layer	g DW per (0.1-m depth layer) m <sup>-2</sup>
CRRIZ*	Critical rhizome/root crown system weight	g DW m <sup>-2</sup>
CVT	Conversion factor for translocated dry matter into CH <sub>2</sub> O	-
DAVTMP	Daily average temperature	°C
DAY	Day number (January 1=1)	d
DAYEM	First Julian day number	d
DAYL	Day length	h
DDELAY	Integer value of DELAY	-
DDTMP	Daily average daytime temperature	°C
DEC	Declination of the sun	radians
DELAY	Lag period chosen to relate water temperature to air temp., in cases where water temp. has not been measured	d
DEPTH	Water depth	m
DLV	Death rate of leaves	g DW m <sup>-2</sup> d <sup>-1</sup>
DMPC(i)	Dry matter allocation to each plant layer (relative)	-
DMPCT	Table to read DMPC(i) as function of depth layer (relative)	-
DPTT	Table to read water depth as a function of day no.	m, d
DRT	Death rate of roots	g DW m <sup>-2</sup> d <sup>-1</sup>

DSINB	Integral of SINB over the day	s.d <sup>-1</sup>
DSINBE	Daily total of effective solar height	s.d <sup>-1</sup>
DSO	Daily extra-terrestrial radiation	J m <sup>-2</sup> d <sup>-1</sup>
DST	Death rate of stems	g DW m <sup>-2</sup> d <sup>-1</sup>
DTEFF	Daily effective temperature	°C
DTGA	Daily total gross CO <sub>2</sub> assimilation of the vegetation	g CO <sub>2</sub> m <sup>-2</sup> d <sup>-1</sup>
DTR	Measured daily total global radiation	J m <sup>-2</sup> d <sup>-1</sup>
DVR	Development rate as function of temperature sum	d <sup>-1</sup>
DVRT	Table of post-anthesis development rate as function of temperature sum	d <sup>-1</sup> , °C
DVRVT	Table of pre-anthesis development rate as function of temperature sum	d <sup>-1</sup> , °C
DVS	Development phase of the plant	-
EE	Initial light use efficiency for shoots	g CO <sub>2</sub> J <sup>-1</sup>
EPISHD	Table to read fraction of irradiation shaded by epiphytes as function of DVS	-, -
EPHSWT	Relative epiphyte shading switch (0=off, 1=on)	-
EPHY	Table to read relative epiphyte shading as function of DVS	-, -
FGROS	Instantaneous CO <sub>2</sub> assimilation rate of the vegetation	g CO <sub>2</sub> m <sup>-2</sup> h <sup>-1</sup>
FGL	Instantaneous CO <sub>2</sub> assimilation rate per vegetation layer	g CO <sub>2</sub> m <sup>-2</sup> h <sup>-1</sup>
FL	Leaf dry matter allocation to each layer of shoot (relative)	-
FLT	Table to read FL as function of DVS	-, -
FLV	Fraction of total dry matter increase allocated to leaves	-
FLVT	Table to read FLV as function of DVS	-
FRDIF	Diffuse radiation as a fraction of total solar radiation	-
FRT	Fraction of total dry matter increase allocated to roots	-
FRTT	Table to read FRT as function of DVS	-, -
FST	Fraction of total dry matter increase allocated to stems	-
FSTT	Table to read FST as function of DVS	-, -
GLV	Dry matter growth rate of leaves	g DW m <sup>-2</sup> d <sup>-1</sup>
GPHOT	Daily total gross assimilation rate of the vegetation	g CH <sub>2</sub> O m <sup>-2</sup> d <sup>-1</sup>
GRT	Dry matter growth rate of roots	g DW m <sup>-2</sup> d <sup>-1</sup>
GST	Dry matter growth rate of stems	g DW m <sup>-2</sup> d <sup>-1</sup>
GTW	Dry matter growth rate of the vegetation (plant excluding tubers or rhizomes)	g DW m <sup>-2</sup> d <sup>-1</sup>
HAR	Harvesting switch (0=off, 1=on)	-

HARDAY	Harvesting day number	d
HARDEP	Harvesting depth (measured from water surface)	m
HIG(i)	Height on top of stratum I (measured from water surface)	m
HOUR	Selected hour during the day	h
I	Counter in DO LOOP	-
IABS(i)	Total irradiance absorbed per depth layer i	$J m^{-2} s^{-1}$
IABSL(i)	Total irradiance absorbed by shoots per depth layer i	$J m^{-2} s^{-1}$
IDAY	Integer equivalent of variable DAY	d
INTUB	Tuber size	$g DW tuber^{-1}$
IREMOB	Initial value remobilization	$g CH_2O m^{-2}$
IRS	Total irradiance just under the water surface	$J m^{-2} s^{-1}$
IRZ(i)	Total photosynthetically active part of irradiance on top of depth layer i	$J m^{-2} s^{-1}$
IWGRIZ*	Initial rhizome weight	$g DW m^{-2}$
IWLVD	Initial dry matter of dead leaves	$g DW m^{-2}$
IWLVG	Initial dry matter of green (live) leaves	$g DW m^{-2}$
IWRD	Initial dry matter of dead roots	$g DW m^{-2}$
IWRG	Initial dry matter of green (live) roots	$g DW m^{-2}$
IWSTD	Initial dry matter of dead stems	$g DW m^{-2}$
IWSTG	Initial dry matter of green (live) stems	$g DW m^{-2}$
K	Plant species specific light extinction coefficient	$m^2 g^{-1} DW$
KCOUNT	Counter used to calculate number of consecutive days in which sprouts have a negative net photosynthesis	-
KT	Table to read K as function of DVS	$m^2 g^{-1} DW, -$
L	Water type specific light extinction coefficient	$m^{-1}$
LAT	Latitude of the site	degrees
LT	Table to read L as function of day number	d, $m^{-1}$
MAINRT*	Maintenance respiration rate rhizome/root crown system	$g CH_2O m^{-2} d^{-1}$
MAINT	Maintenance respiration rate vegetation	$g CH_2O m^{-2} d^{-1}$
MAINTS	Maintenance respiration rate vegetation at reference temperature	$g CH_2O m^{-2} d^{-1}$
NDTUB	Dormant tuber density (identical to NT)	dormant tubers $m^{-2}$
NGLV	Net growth rate of leaves	$g DW m^{-2} d^{-1}$
NGRT	Net growth rate of roots	$g DW m^{-2} d^{-1}$
NGST	Net growth rate of stems	$g DW m^{-2} d^{-1}$

NGTUB	Sprouting tuber number	spr. tubers m <sup>2</sup>
NINTUB	Tuber number concurrently initiated per plant	conc. in. tubers plant <sup>-1</sup>
NNTUB	New tuber number	new tubers m <sup>-2</sup>
NPL	Plant density	plants m <sup>-2</sup>
NTM	Tuber density measured (field site)	tubers m <sup>-2</sup>
NTMT	Table to read NTM as function of day number	tubers m <sup>-2</sup> , d
NTUBD	Dead tuber number	dead tubers m <sup>-2</sup>
NTUBPD	Dead tuber number previous day	dead p.d.tubers m <sup>-2</sup>
NUL	Zero (0)	-
PAR	Instantaneous flux of photosynthetically active radiation	J m <sup>-2</sup> s <sup>-1</sup>
PARDIF	Instantaneous flux of diffuse PAR	J m <sup>-2</sup> s <sup>-1</sup>
PARDIR	Instantaneous flux of direct PAR	J m <sup>-2</sup> s <sup>-1</sup>
PI	Ratio of circumference to diameter of circle	-
RAD	Factor to convert degrees to radians	radians degree <sup>-1</sup>
RC	Reflection coefficient of irradiance at water surface (relative)	-
RCSHST	Relation coefficient tuber weight-stem length	m g <sup>-1</sup> DW
RDR	Relative death rate of leaves (on DW basis)	d <sup>-1</sup>
RDRIZ*	Relative rhizome death rate	d <sup>-1</sup>
RDRT	Table to read RDR as function of DAVTMP	d <sup>-1</sup> , °C
RDS	Relative death rate of stems and roots (on DW basis)	d <sup>-1</sup>
RDST	Table to read RDS as function of DAVTMP	d <sup>-1</sup> , °C
RDTU	Relative tuber death rate (on number basis)	d <sup>-1</sup>
REDAM	Reduction factor to relate AMX to pH and oxygen levels of the water (relative)	-
REDAM1	Table to read factor relating AMX to water current velocity (relative)	-, cm s <sup>-1</sup>
REDF(i)	Relative reduction factor for AMX to account for senescence plant parts over vertical axis of vegetation (relative)	-
REMOB	Remobilization rate of carbohydrates	g CH <sub>2</sub> O m <sup>-2</sup> d <sup>-1</sup>
ROC	Relative conversion rate of tuber into plant material	g CH <sub>2</sub> O g <sup>-1</sup> DW d <sup>-1</sup>
RTR	Maximum relative tuber growth rate at 20 °C	g DW tuber <sup>-1</sup> d <sup>-1</sup>
RTRL	Relative tuber growth rate at ambient temperature	g DW tuber <sup>-1</sup> d <sup>-1</sup>
SC	Solar constant corrected for varying distance sun-earth	J m <sup>-2</sup> s <sup>-1</sup>
SC(i)	Shoot dry matter in depth layer i	g DW m <sup>-2</sup>
SHTBIO	Shoot biomass; one term for sum WLW + WST	g DW m <sup>-2</sup>

SINB	Sine of solar elevation	-
SINLD	Intermediate variable in calculating solar declination	-
STEMLE	Stem length	m
SURFAC	Expression of warning that plant canopy is not at water surface and tuber class has died	-
SSURPR	Integer value of SURPER	-
SURPER	Survival period for sprouts without net photosynthesis	d
TBASE	Base temperature for juvenile plant growth	°C
TEFF	Factor accounting for temperature effect on maintenance respiration, remobilization, maximum relative tuber growth and death rates	-
TEFFT	Table to read TEFF as function of temperature (Q10 of 2, up to 45 °C)	-, °C
TGRIZ*	Total live dry weight rhizome/root crown system of previous day	g DW m <sup>-2</sup>
TGW	Total live plant dry weight (excluding tubers)	g DW m <sup>-2</sup>
TGWM	Total live plant dry weight measured (field site)	g DW m <sup>-2</sup>
TGWMT	Table to read TGWM as function of day number	g DW m <sup>-2</sup> , d
TL	Thickness per depth layer	0.1 m
TMAX	Daily maximum temperature	°C
TMIN	Daily minimum temperature	°C
TMPSUM	Temperature sum after 1 January	°C
TRAFAC*	Translocation	-
TRANS	Translocation rate of carbohydrates	g CH <sub>2</sub> O m <sup>-2</sup> d <sup>-1</sup>
TREMOB	Total remobilization	g DW m <sup>-2</sup>
TW	Total live + dead plant dry weight (excluding tubers)	g DW m <sup>-2</sup>
TWCTUB	Total critical dry weight of new tubers	g DW m <sup>-2</sup>
TWGRIZ*	Total live dry weight rhizome/root crown system of current day	g DW m <sup>-2</sup>
TWGTUB	Total dry weight of sprouting tubers	g DW m <sup>-2</sup>
TWLD(1,2,3)*	Total dry weight of dead leaves	g DW m <sup>-2</sup>
TWLG(1,2,3)*	Total dry weight of live leaves	g DW m <sup>-2</sup>
TWLVD	Total dry weight of dead leaves	g DW m <sup>-2</sup>
TWLVG	Total dry weight of live leaves	g DW m <sup>-2</sup>
TWNTUB	Total dry weight of new tubers	g DW m <sup>-2</sup>
TWRD(1,2,3)*	Total dry weight of dead roots	g DW m <sup>-2</sup>
TWRG(1,2,3)*	Total dry weight of live roots	g DW m <sup>-2</sup>

TWRIZD*	Total weight dead rhizome/root crown system	g DW m <sup>-2</sup>
TWRTD	Total dry weight of dead roots	g DW m <sup>-2</sup>
TWRTG	Total dry weight of live roots	g DW m <sup>-2</sup>
TWSD(1,2,3)*	Total dry weight of dead stems	g DW m <sup>-2</sup>
TWSG(1,2,3)*	Total dry weight of live stems	g DW m <sup>-2</sup>
TWSTD	Total dry weight of dead stems	g DW m <sup>-2</sup>
TWSTG	Total dry weight of live stems	g DW m <sup>-2</sup>
TWTUB	Total dry weight of tubers	g DW m <sup>-2</sup>
VELSWT	Switch to relate AMX to current velocity (0=off, 1=on)	-
WLV	Dry weight of leaves (live + dead)	g DW m <sup>-2</sup>
WRT	Dry weight of roots (live + dead)	g DW m <sup>-2</sup>
WST	Dry weight of stems (live + dead)	g DW m <sup>-2</sup>
WTMP	Daily water temperature	°C
WTMPT	Table to read WTMP as function of day number	°C, d
WVEL	Water type specific current velocity	cm s <sup>-1</sup>
YRNUM	Year number simulation (1-5)	-

\*Variables unique for MILFO.

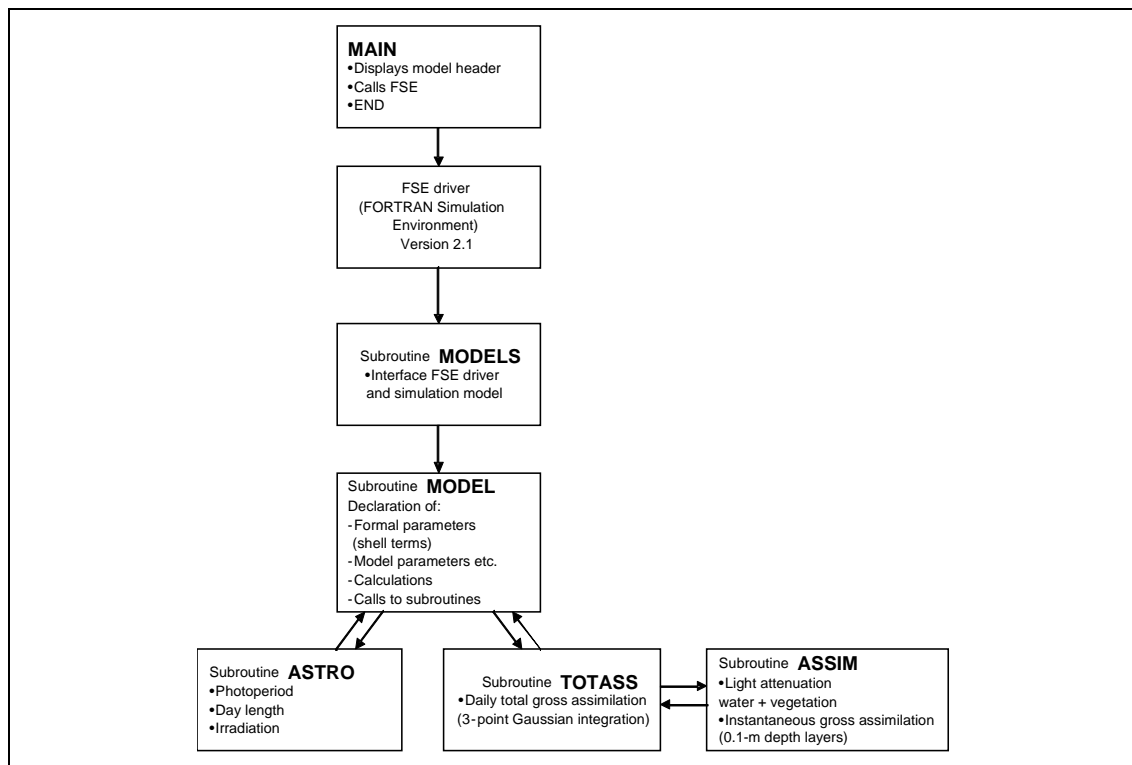


Figure 1. Relational diagram illustrating the organization of each model and its subroutines in combination with the FSE shell.

## Model processes and parameter values

### Model processes

*Morphology, phenological cycle, and development*

*Morphology and phenological cycle.* All four plant species are rooted into the sediment. Summer habit, reproduction strategy, flowering period, and frequency may vary strongly with plant species. Flowering usually coincides with peak biomass and is followed immediately by sloughing.

*Phenology and development.* The phenology of a plant community, for which development phase can be used as a measure, quantifies physiological age and is related to the plants' morphological appearance.

Development phase can not be expressed simply as chronological age because several environmental factors such as temperature and stress (e.g., nutrients, grazing) can speed up or reduce the rate of phenological development. Contrary to what is suggested by intuition, the rate of plant growth per se has no effect on phenological development, as long as the growth rate is not very low (Penning de Vries et al. 1989b, and citations therein). The concept of development phase is used to characterize the whole plant community; it is not appropriate for individual organs.

The response of developmental rate to temperature in the current models is in accordance with the degree-day hypothesis (Thornley and Johnson 1990a). The idea is as follows. The mean temperature  $\bar{T}_i$  for each day  $i$  is measured, and a sum  $h$  is formed according to the following equation:

$$h = \sum_{i=1}^j (\bar{T}_i - T_c) \quad (1)$$

which includes only those terms where  $\bar{T}_i$  is above some threshold value  $T_c$ . When  $h$  reaches a particular value, this signifies that a phase in development is complete, and this is generally associated with a biological event that occurs over a short period of time and is readily observed. The day-degree sum  $h$  essentially integrates some underlying temperature-dependent processes. For each plant species there are various phases in the development of the plant, and the temperature sum is found to have a certain value for the successful completion of each phase. The temperature threshold  $T_c$  may be different for each of these phases. The approach is

based on the notion of a developmental rate, whose response to temperature is approximately linear over a restricted temperature range. Comparison with actual temperature responses found in agricultural crops suggests that this is reasonable, and the method works well in practice. It is implicitly assumed that the organ possesses a developmental clock that is proceeding at the rate  $k_d$ . In general, it is to be expected that the development rate  $k_d$  may depend on a number of quantities. This can be represented by the following equation:

$$k_d = f(V, P, E) \quad (2)$$

in which  $f$  represents some function of the state variables  $V$ , parameters  $P$ , and environmental quantities  $E$ . The temperature-sum rule works because the most important environmental variable is temperature, and the response to temperature is approximately linear.

The phenological cycle in each model is described based on published field data collected in a temperate climate, and development rates have been generated by scaling the development phase to the pertinent climatological day-degree sum. In cases where climatological data were lacking for the year when the field data were collected, climatological data for the same or a nearby site of a different year were used, after verifying climatological conditions did not deviate from the usual at that site. Three plant species, i.e., *V. americana*, *P. pectinatus*, and *H. verticillata*, are modeled as if they propagate vegetatively by tubers with and without plant shoots present, because this is the predominant wintering mechanism supported by the calibration data that were collected in a temperate climate. Tubers are relatively small, dormant organs that develop on most stolons under special day length and temperature conditions in autumn, and that grow into the sediment. Tubers are composed of a small amount of dividing tissue surrounded by several fleshy leaves. The parent plants senesce and disintegrate at the end of the growth season, and only the tubers hibernate within the sediment until their emergence the following spring, which completes the annual growth cycle. Tubers are depleted and disintegrate during the summer in which they were formed in *V. americana* and *P. pectinatus*, but may survive several years in *H. verticillata* (Van and Steward 1990). The fourth plant species, *M. spicatum*, is modeled as if it propagates vegetatively by rhizome/root crowns with and without plant shoots present.

Development phase (DVS) is a state variable in the models. The development phase is dimensionless, and its value gradually increases within a growing season. The development rate has the dimension  $d^{-1}$ . The multiple of rate and time period yields an increment in phase. In the models, the temperature affecting plant development can be chosen as equal to the daily average air temperature at the height of the growing point of the shoots, with a user-defined lag-period to correct for deviations in temperature of the water body in which the SAV grows compared with air temperatures (7 days is nominal). It is more accurate to use water temperatures for this purpose, but since water temperatures are not always available for the site for which the user wants to run the model, the models can be run using either value.

The rate of phenological development can be affected by temperature differently in the vegetative phase and in the reproductive phase. These differences indicate that the physiological process of development may not be the same before and after flowering.

#### *Plant density and maximum biomass*

In each model, calculations are performed on a square meter basis assuming a typical plant density. Typical plant density indicates in this case, that it is possible that at some point in time under natural conditions plant densities may be different, but that an established, monotypic SAV optimizes at this typical number of plants per square meter. Lower densities may occur in the establishment phase, when some plants may not yet have neighbors and become relatively large, whereas higher plant densities may occur early in the season when more sprouts emerge but the plantlets are subsequently thinned to the typical number of plants per square meter by self-shading of the vegetation. In tuber-forming species, this implies also that the number of sprouting tubers in the tuber bank equals the typical number of plants per square meter, while the remaining tubers continue to senesce. However, at tuber bank densities lower than the typical number per square meter, the number of sprouting tubers is recalculated and set equal to the actual tuber bank density. If wintering plants are present, plant biomass is redistributed over the typical number of plants per square meter.

Seasonal plant biomass maxima may vary considerably over time and space. In the models maximum biomass is calculated as explained in “Light, photosynthesis, maintenance, growth, and assimilate partitioning”

up to a level that equals the highest published biomass value. Higher biomass values are considered as unrealistic and attributed to selective sampling or erroneous extrapolations of biomass measured on small surface areas to per square meter area.

*Wintering, sprouting in spring, and growth of sprouts to water surface*

*In tuber-forming SAV*, tubers in the tuber bank within the sediment are the main storage organs for carbohydrates during wintering in a temperate climate. Tuber bank weight is calculated by multiplication of tuber bank density and typical tuber weight. Tuber bank density may decrease by tuber death with a typical tuber death rate, and through grazing by waterfowl and other animals. Tuber bank weight may decrease by maintenance, tuber death and by the sprouting of tubers, which transform into plants. Both tuber bank weight and density may increase by the formation of new tubers. Tubers lie dormant if not disturbed (Van and Steward 1990), and it is, therefore, to be expected that maintenance processes proceed at a very low level of activity. Tuber death rate, maintenance, and growth increase with increasing temperature through a relative, effective temperature function (*TEFF*), being a Q10 of 2 with a 20 °C reference temperature.

A certain minimum weight is required for a tuber to sprout. The number of tubers that sprout is set equal to the typical plant density. Sprouting of tubers is a function of development phase (e.g., for *V. americana* a DVS of 0.291). Plantlets remobilize the tuber carbohydrate reserves by conversion into plant material, and elongate. The plant material is allocated to leaves, stems and roots following a fixed biomass partitioning pattern (see “Light, photosynthesis, maintenance, growth, and assimilate partitioning”).

These plantlets may survive at the plant height they can maximally reach, provided the balance of the carbohydrate influx from tuber carbohydrate reserves, efflux from tuber growth respiration, and influx from plantlet photosynthesis is positive. Sprouts/plantlets die if they have a negative net assimilation rate over a user-defined number of days, and the program stops with a warning “KCOUNT.” After the death of one tuber class, the next tuber class may sprout, provided more tubers are available in the tuber bank and DVS is lower than required for flowering (DVS 1). Up to three tuber classes may sprout annually. The program can resume running for the same year after the user’s pressing “ENTER” provided the proper conditions are met.



$$TWGTUB = NPL \times INTUB \quad (3)$$

$$NDTUB = NDTUB - (NTUBD - NTUBPD) \quad (3.a)$$

$$NTUBD = RDTU \times NDTUB \times TEFF \quad (3.a.1)$$

*IF (DVS. GE. 0.291. AND. DVS .LT. 1.) THEN*

*IF (TWGTUB .LE. (0.01 × NPL × INTUB)) NGTUB = 0.0*

$$NGTUB = NPL \quad (3.1)$$

$$TWGTUB = INTGRL (TWGTUB, -REMOB, DELT) \quad (3.2)$$

$$REMOB = TWGTUB \times ROC \times TEFF \quad (3.3)$$

*In M. spicatum*, rhizomes/root crowns in the sediment are the main storage organs for carbohydrates during wintering in a temperate climate. An initial biomass equal to the lowest biomass published (g DW m<sup>-2</sup>, measured) is used to enable the model plants to sprout. Rhizome weight may decrease by rhizome death with a typical rhizome death rate, and through grazing by waterfowl and other animals. Rhizome weight may also decrease by maintenance and by the sprouting of the growing points, which transform into plants. Rhizome weight may increase by downward translocation from shoots.

The number of plants that sprout is set equal to the typical plant density. Sprouting of growing points on the rhizome is a function of development phase. It occurs between DVS 0.375 and the flowering period for cohort 1, between DVS 1.001 and the flowering period for cohort 2. In a tropical climate, a third cohort may sprout between DVS 2.001 and the flowering period for cohort 3.

Plantlets remobilize the rhizome carbohydrate reserves by conversion into plant material and elongate. The plant material is allocated to leaves, stems, and roots following a fixed biomass partitioning pattern (see “Light, photosynthesis, maintenance, growth, and assimilate partitioning”).

These plantlets may survive at the plant height they can maximally reach, provided the balance of the carbohydrate influx from tuber carbohydrate reserves depletion, efflux from tuber growth respiration, and influx from plantlet photosynthesis is positive. Sprouting plantlets die if they have a negative net assimilation rate over a user-defined number of days, and the program stops with a warning “Vegetation is dying.” After initiation of flowering of plant cohort 1, the next plant cohort 2 may sprout, provided more rhizome mass is available and DVS is lower than required for flowering of cohort 2 (DVS 1.630). Up to three plant cohorts may sprout annually. The program can resume running for the same year after the user’s pressing “ENTER” provided the proper conditions are met.

$$TWGRIZ = INTGRL \left\{ TWGRIZ, - \left[ \left( \frac{-TRANS1 + REMOB1 + MAINRT}{1.242} \right) + (RDRIZ \times TGRIZ) \right], DELT \right\} \quad (3.4)$$

*IF (DVS. GE. 0.376. AND. DVS. LT. 1.0) THEN*

*IF (TWGRIZ. GT. CRRIZ) THEN*

$$REMOB1 = ROC \times TWGRIZ \quad (3.5)$$

$$TWRIZD = INTGRL (TWRIZD, RDRIZ, DELT) \quad (3.6)$$

where 1.242 equals assimilate requirement for rhizome dry matter production (g CH<sub>2</sub>O g DW<sup>-1</sup>).

A relational diagram illustrating the wintering and sprouting rhizomes/ root crowns of *M. spicatum* is shown in Figure 3.

*Light, photosynthesis, maintenance, growth, and assimilate partitioning*

**Light.** Light availability is an important factor controlling the distribution and abundance of SAV. In aquatic systems a small part of the irradiance can be reflected by the water surface, and further attenuation occurs by water and its suspended solids, by epiphytes, and by SAV itself. Measured daily total irradiance (wavelength 300-3,000 nm) is used as input in the model. Only half of the irradiance reaching the water surface is considered

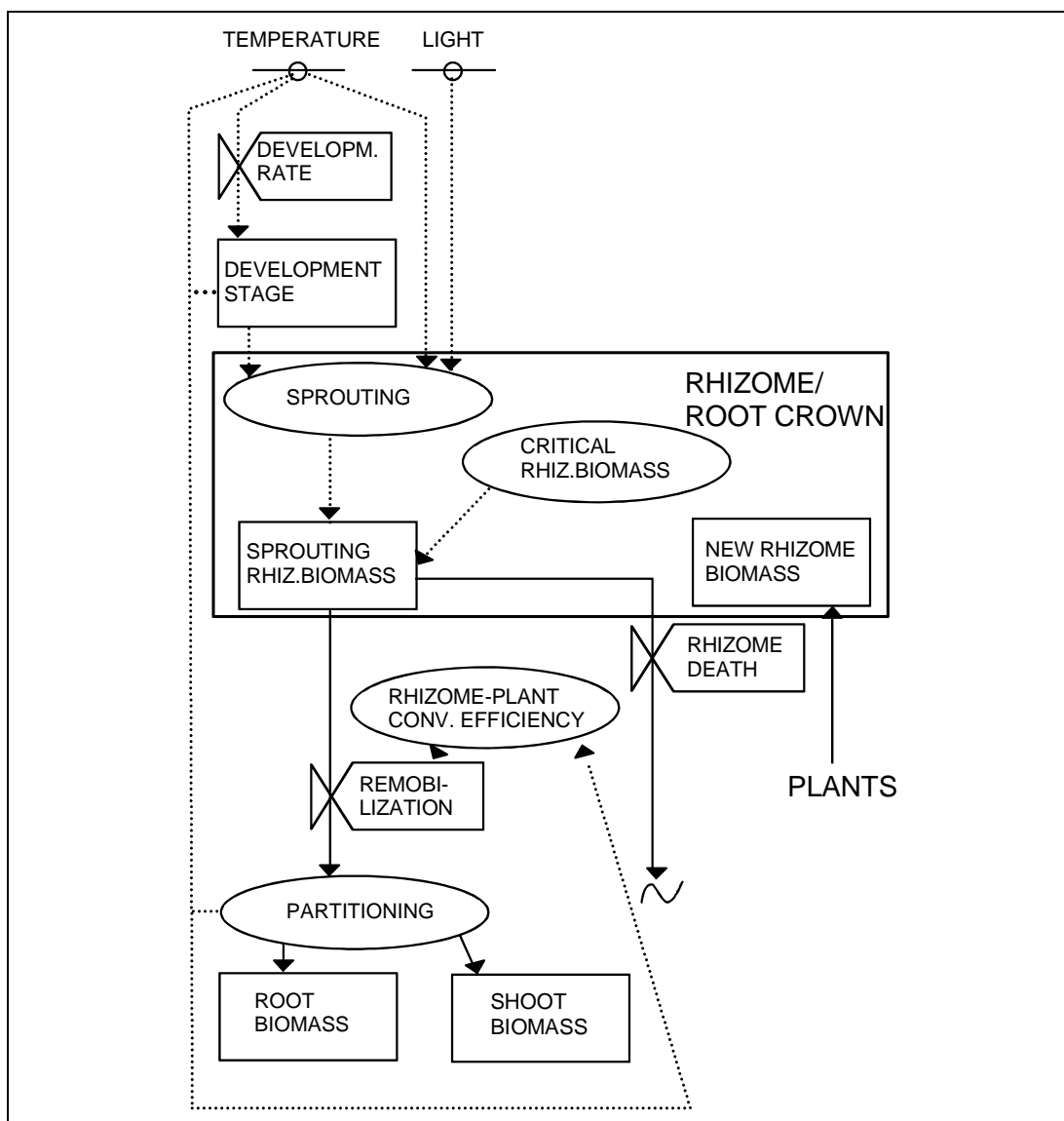


Figure 3. Relational diagram illustrating wintering and sprouting of the rhizome/root crown of *M. spicatum*.

to be photosynthetically active and is, therefore, used as a base for the calculation of  $\text{CO}_2$  assimilation. Six percent of the irradiance is reflected by the water surface (Golterman 1975). The subsurface irradiance is attenuated by dissolved substances and particles within the water column resulting in a site- and season-specific water extinction coefficient. The remaining radiation may be further reduced by epiphyte shading. Epiphyte shading can be activated and deactivated in the model input file. The vertical profiles of the radiation within the SAV layers are characterized also. The absorbed irradiance for each horizontal SAV layer is derived from these profiles. The SAV light extinction coefficient  $K$  is plant species-characteristic and assumed to be constant throughout the year. The in-

coming irradiance is attenuated by the shoots, part of which is absorbed by the photosynthetic plant organs, i.e. the leaves.

$$IRZ_{i+1} = IRZ_i \times e^{(-TL \times L - K \times SC_i)} \quad (4)$$

$$IABS_i = \frac{(IRZ_i - IRZ_{i+1}) \times SC_i \times K}{(K \times SC_i + TL \times L)} \times (1.0 - EPISHD) \quad (4.1)$$

$$IABSL_i = IABS_i \times FL \quad (4.2)$$

*Photosynthesis.* Instantaneous rates of gross assimilation are calculated from the absorbed light energy and the photosynthesis light response of individual shoots, here used synonymously to leaves.

The photosynthesis-light response of leaves is described by the following exponential function

$$FGL = SC_i \times AMAX \times \left[ 1 - \exp \left( \frac{-EE \times IABS_i \times 3600}{AMAX \times SC_i} \right) \right] \quad (4.3)$$

In the photosynthesis-light response equation, the value of potential photosynthetic activity at light saturation (AMX) is species-characteristic and the initial light-use efficiency (EE) typical for C<sub>3</sub> plants. AMX is affected by temperature via a fitted, relative function, AMTMPT, accounting for the measured effect of daytime temperature, and enabling the calculation of the actual photosynthesis rate (AMAX). AMAX is also affected by current velocity via a fitted, relative, function, REDAM1, accounting for the measured effect of current velocity on AMX. Senescence and daily changes in pH and oxygen concentrations may affect AMX. Substituting the appropriate value for the absorbed photosynthetically active radiation yields the assimilation rate for each specific shoot layer. The instantaneous rate of gross assimilation over the height of the vegetation is calculated by relating the assimilation rate per layer to the species-characteristic biomass distribution and by subsequent integration of all vegetation layers. The daily gross assimilation rate is calculated by using the Gaussian integration method. This method specifies the discrete points at which the value of the function to be integrated has to be calculated, and the weighting factors that must be applied to these values to attain minimum deviation

from the analytical solution. A three-point method performs well for calculating daily total assimilation (Goudriaan 1986; Spitters 1986).

*Maintenance, growth, and assimilate partitioning.* A portion of the carbohydrates formed is respired to provide energy for maintaining the existing plant components. The maintenance costs increase with metabolic activity, probably because of higher enzyme turnover and higher transport costs (Penning de Vries 1975). The maintenance cost can be estimated from the chemical composition of the plant. Typical maintenance coefficients for various plant organs have been derived, based on numerous chemical determinations in agricultural crops. They typically range from 0.010 to 0.016 g CH<sub>2</sub>O g AFDW<sup>-1</sup> d<sup>-1</sup> (Penning de Vries and Van Laar 1982b). These coefficients have been used in the current models. Maintenance respiration increases with increasing temperature through a relative effective temperature function (TEFF), as described under “Wintering, sprouting in spring, and growth of sprouts to water surface.”

Equations describing maintenance costs are:

$$MAINTS = 0.016 \times TWLG + 0.010 \times TWSG + 0.015 \times TWRG \quad (4.4)$$

$$MAINT = MAINTS \times TEFF \quad (4.4a)$$

The remainder of the carbohydrates is available for conversion into structural plant material, resulting in growth. In this conversion process of the glucose molecule, CO<sub>2</sub> and water are released. The assimilate requirement to produce one unit weight of any particular plant organ can be calculated from its chemical composition and the assimilate requirements of the various chemical components. Typical values are 1.46 g CH<sub>2</sub>O g DW<sup>-1</sup> for leaves, 1.51 for stems, and 1.44 for roots (Penning de Vries and Van Laar 1982b; Penning de Vries et al. 1989a), confirmed by Griffin (1994). At higher temperatures the conversion processes are accelerated, but the pathways are identical. The recently determined construction costs for several submersed plant species, using a different method (Williams et al. 1987), are generally lower and range from 0.99 to 1.11 (Spencer et al. 1997). However, some of the latter plants are relatively poor in nitrogen and transport costs have not been included, both factors which may have contributed to the lower cost found.

In the models the construction costs typical for agricultural plants have been used because construction costs calculated for *M. spicatum* leaves with an average chemical composition were similar to those in agricultural plants, i.e., 1.465 CH<sub>2</sub>O g DW<sup>-1</sup>, and those of stems and roots were presumed to be similar also.

The following equation describes growth:

$$GTW = \frac{[(REMOB \times CVT) + GPHOT - TRANS - MAINT]}{ASRQ} \quad (4.5)$$

Assimilate partitioning is the process by which assimilates available for growth are partitioned over leaves, stems, roots, and/or storage organs. It depends on physiological age. Assimilate partitioning patterns in most SAV species are unknown. However, partitioning of the biomass resulting from this process in full-grown plants has been published, and these values have been used for calibration in the models. The species-characteristic distribution of shoot biomass is allocated over the vertical axis via a dry matter partitioning coefficient function (DMPC), which allows changes in shoot biomass distribution with changes in water depth and differs significantly between species.

The following equation describes biomass partitioning over plant organs:

$$GLV = FLV \times GTW \quad (4.6)$$

$$GRT = FRT \times GTW \quad (4.7)$$

$$GST = FST \times GTW \quad (4.8)$$

A relational diagram illustrating photosynthesis, respiration, and biomass formation is shown in Figure 4.

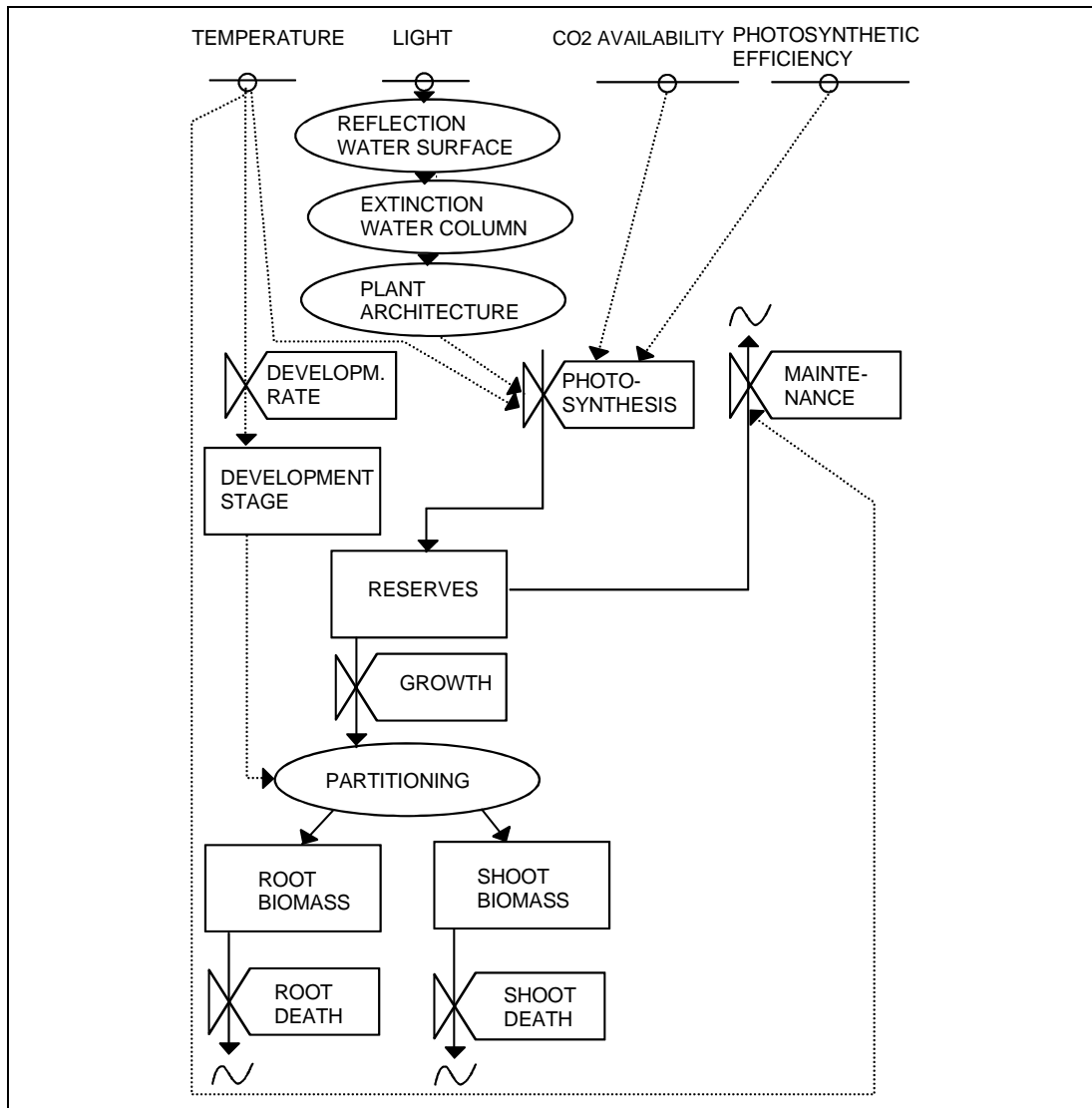


Figure 4. Relational diagram illustrating photosynthesis, respiration, and biomass formation in tuber-forming SAV.

#### *Flowering, translocation, senescence, and formation of wintering organs*

The flowering event affects subsequent metabolic activity of the vegetation. The timing of flowering is, therefore, extremely important for physiological activity and biomass formation, whereas the actual investment of dry matter in flowers and seeds is minor. In the models, a considerable part of net production is translocated downwards after flowering in the form of carbohydrates considered as equivalent to starch (Gijzen 1985). In tuber-forming species the translocation products are largely transported to the tubers, in *M. spicatum* to the rhizome/root crowns. The remainder of net production is allocated according to the species-characteristic biomass partitioning pattern. Senescence sets in resulting in loss of particulate

plant material via a species-characteristic relative death rate, which increases with an increase in temperature through the previously mentioned relative, effective temperature function (TEFF).

*In tuber-forming plants*, tubers are induced after flowering, i.e.,  $DVS > 1.0$ , and formed under short day conditions and within a certain temperature range. The combination of tuber size and concurrently initiated tuber number is species-characteristic (see “Wintering, sprouting in spring, and growth of sprouts to water surface”). Once initiated, a tuber class grows with a typical actual relative tuber growth rate (RTRL) from translocated material until a preselected critical weight of the new tuber class (TWCTUB) is reached. Temperature influences the maximum relative growth rate (RTR) of tubers through the TEFF function. Once finished, a tuber class is added to the dormant tuber bank, and the plant starts forming a new tuber class. Tuber initiation continues as long as environmental conditions permit, and tubers are formed as long as plants provide assimilates to fill them.

The following equations describe induction and formation of new tubers (illustrated for *V. americana*; DVS and temperature range differ between species).

*IF (REMOB . EQ. 0.0) THEN*

*IF (DVS . GT. 1.0 . AND. DAYL . LT. 14.7) THEN*

*IF (DDTMP . GT. 5.0 . AND. DDTMP . LT. 25.0) THEN*

*IF (TGW . GT. 0.1) THEN*

$$TRANS = AMAX1 [0., (RTRL \times 1. / CVT) \times (GPHOT - MAINT)] \quad (5)$$

$$NNTUB = NPL \times NINTUB \quad (5.1)$$

$$TWNTUB = INTGRL (TWNTUB, TRANS, DELT) \quad (5.2)$$

*IF (TWNTUB . GE. TWCTUB) THEN*

$$NDTUB = NDTUB + (NPL \times NINTUB) \quad (5.3)$$

A relational diagram illustrating translocation and senescence following anthesis in tuber-forming plants is shown in Figure 5.

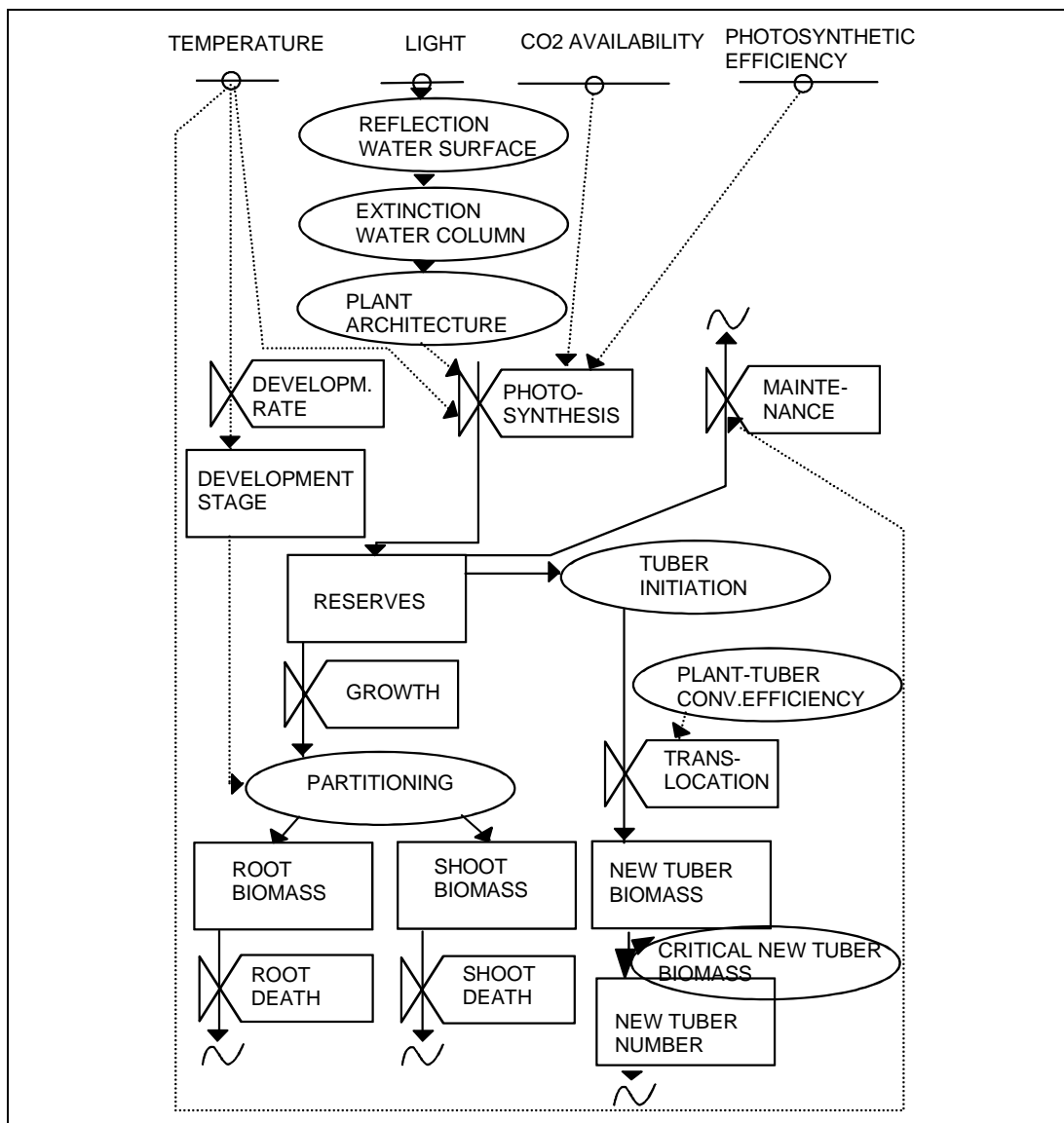


Figure 5. Relational diagram illustrating translocation and senescence following anthesis in tuber-forming SAV.

*In M. spicatum*, rhizomes increase in mass through translocation after flowering, i.e.,  $DVS > 1.0$ . Once started, the rhizomes grow with a typical relative translocation rate (*TRAFAC*) from translocated material that decreases exponentially to 0 with concomitantly decreasing biomass of the translocating plant cohort and increasing biomass of the successive growing plant cohort. New plant cohorts can only sprout until a *DVS* of 2.001 is reached.

Translocation is described by the following equation:

$$TRANS1 = CVT \times GPHOT \times \left[ \frac{(TWLG2 + TWSG2 + TWRG2)}{(TWLG1 + TWSG1 + TWRG1 + TWLG2 + TWSG2 + TWRG2) \times TRAFAC} \right] \quad (5.4)$$

### Parameter values

The relatively simple simulation model type described in this paper includes parameter values that can be defined with varying certainty. Most parameters have been calculated or estimated from published literature (Table 2). The choice of parameter values is summarized below. The parameter values are presented in four species- and model-characteristic tables: Table 2a pertains to *V. americana*, model VALLA, Table 2b to *P. pectinatus*, model POTAM, Table 2c to *H. verticillata*, model HYDRIL, and Table 2d to *M. spicatum*, model MILFO.

Table 2a. Parameter values used in VALLA.

Parameter	Name	Value	Reference
<b>Morphology, phenological cycle, and development</b>			
Fraction of total dry matter increase allocated to leaves	FLV(T)	0.718	1, 2
Fraction of total dry matter increase allocated to stems	FST(T)	0.159	1, 2
Fraction of total dry matter increase allocated to roots	FRT(T)	0.123	1, 2
Development rate as function of temperature*	DVRV	0.015 d <sup>-1</sup>	Calibrated
DVR prior to flowering DVRV, subsequently DVRR	DVRR	0.040 d <sup>-1</sup>	Calibrated
<b>Plant density and maximum plant biomass</b>			
Plant density	NPL	30 m <sup>-2</sup>	1
Maximum plant biomass		496 g DW m <sup>-2</sup>	2
<b>Wintering, sprouting, and growth of sprouts to water surface</b>			
Dormant tuber density	NDTUB	233 m <sup>-2</sup>	3
Tuber size	INTUB	0.090 g DW tuber <sup>-1</sup>	3, 4
Rel. tuber death rate (on number basis)	RDTU	0.018 d <sup>-1</sup>	1
Rel. conversion rate of tuber into plant material	ROC	0.0576 g CH <sub>2</sub> O. g <sup>-1</sup> DW d <sup>-1</sup>	5
Relation coefficient tuber weight-stem length	RCSHST	12 m g <sup>-1</sup> DW	5, 6
Critical shoot weight per 0.1-m depth layer	CRIFAC	0.0091g DW (0.1-m depth layer) <sup>-1</sup> plant <sup>-1</sup>	3, 4
Survival period for sprouts without net photosynthesis	SURPER	23 d	7, 8

<b>Light, photosynthesis, maintenance, growth, and assimilate partitioning</b>			
Plant species specific light extinction coefficient	K(T)	0.0235m <sup>2</sup> g <sup>-1</sup> DW	9
Fraction of irradiation shaded by epiphytes*	EPISHD	0-0.43	10
Potential CO <sub>2</sub> assimilation rate at light saturation for shoots	AMX	0.0165 g CO <sub>2</sub> . g <sup>-1</sup> DW h <sup>-1</sup>	9
Initial light use efficiency for shoots	EE	0.000011 g CO <sub>2</sub> J <sup>-1</sup>	11
Rel. reduction factor for AMX to account for senescence plant parts	REDF(T)	1.0	User def.
Reduction factor to relate AMX to water pH	REDAM	1	
Daytime temperature effect on AMX as function of DVS*	AMTMP(T)	0-1	12
Rel. factor to relate AMX to water current velocity*	REDAM1	0-1	10
Dry matter allocation to each plant layer*	DMPC	0-1	9
<b>Flowering, translocation, senescence, and formation of wintering organs</b>			
Max. relative tuber growth rate (part of net photosynthetic rate)	RTR	0.247 d <sup>-1</sup>	4, 12, 13
Conversion factor for translocated dry matter into CH <sub>2</sub> O	CVT	1.05	11
Tuber number concurrently initiated per plant	NINTUB	5.5 plant <sup>-1</sup>	13
Total critical dry weight of new tubers	TWCTUB	14.85 g DW m <sup>-2</sup>	1, 3, 13
Rel. death rate of leaves (on DW basis; Q <sub>10</sub> =2)	RDR(T)	0.021 d <sup>-1</sup>	1
Rel. death rate of stems and roots (on DW basis; Q <sub>10</sub> =2)	RDS(T)	0.021 d <sup>-1</sup>	1
<b>Site information</b>			
Water depth (field site)	DPT(T)	1.4 m	User def.
Daily water temperature (field site)	WTMP(T)	-, °C	User def.
Water type specific light extinction coefficient (field site)	L(T)	0.43-0.80 m <sup>-1</sup>	1
Water type specific current velocity (field site)	WVEL	0-100 cm s <sup>-1</sup>	User def.
Total live dry weight measured (field site)	TGWM(T)	-, g DM m <sup>-2</sup>	User def.
Tuber density measured (field site)	NTM(T)	233 m <sup>-2</sup>	1
<b>Harvesting</b>			
Harvesting	HAR	0 or 1	User def.
Harvesting day number	HARDAY	1-365	User def.
Harvesting depth (measured from water surface; 1-5 m)	HARDEP	0.1 m<DEPTH	User def.

\* Calibration function.

1. Titus and Stephens 1983. 2. Haller 1974. 3. Korschgen and Green 1988. 4. Korschgen et al. 1997. 5. Bowes et al. 1979. 6. Best and Boyd 1996. 7. Titus and Adams 1979b. 8. Best and Boyd 2003c. 9. Titus and Adams 1979a. 10. Best et al. 2005. 11. Penning de Vries and Van Laar 1982 a, b. 12. Donnermeyer,1982. 13. Donnermeyer and Smart 1985.

Table 2b. Parameter values used in POTAM.

Parameter	Name	Value	Reference
<b>Morphology, phenological cycle, and development</b>			
Fraction of total dry matter increase allocated to leaves	FLV(T)	0.731	1, 2
Fraction of total dry matter increase allocated to stems	FST(T)	0.183	1, 2
Fraction of total dry matter increase allocated to roots	FRT(T)	0.086	1
Development rate as function of temperature*	DVRV	0.015 d <sup>-1</sup>	Calibrated
DVR prior to flowering DVRV, subsequently DVRR	DVRR	0.040 d <sup>-1</sup>	Calibrated
<b>Plant density and maximum plant biomass</b>			
Plant density	NPL	30 m <sup>-2</sup>	1, 3
Maximum plant biomass		1,952 g DW m <sup>-2</sup>	4
<b>Wintering, sprouting, and growth of sprouts to water surface</b>			
Dormant tuber density	NDTUB	240 m <sup>-2</sup>	1
Tuber size	INTUB	0.083 g DW tuber <sup>-1</sup>	1
Rel. tuber death rate (on number basis)	RDTU	0.026 d <sup>-1</sup>	5
Rel. conversion rate of tuber into plant material	ROC	0.0576 g CH <sub>2</sub> O. g <sup>-1</sup> DW d <sup>-1</sup>	6
Relation coefficient tuber weight-stem length	RCSHST	12 m g <sup>-1</sup> DW	6, 7, 8
Critical shoot weight per 0.1-m depth layer	CRIFAC	0.0076 g DW (0.1-m depth layer) <sup>-1</sup> plant <sup>-1</sup>	7, 8
Survival period for sprouts without net photosynthesis	SURPER	27 d	1
<b>Light, photosynthesis, maintenance, growth and assimilate partitioning</b>			
Plant species specific light extinction coefficient	K(T)	0.095 m <sup>2</sup> g <sup>-1</sup> DW	1
Fraction of irradiance shaded by epiphytes*	EPISHD	0-1.0	9
Potential CO <sub>2</sub> assimilation rate at light saturation for shoots	AMX	0.019 g CO <sub>2</sub> . g <sup>-1</sup> DW h <sup>-1</sup>	10
Initial light use efficiency for shoots	EE	0.000011 g CO <sub>2</sub> J <sup>-1</sup>	11
Rel. reduction factor for AMX to account for senescence plant parts	REDF(T)	1.0	User def.
Reduction factor to relate AMX to water pH	REDAM	1	1
Daytime temperature effect on AMX as function of DVS*	AMTMP(T)	0-1	1
Rel. factor to relate AMX to water current velocity*	REDAM1	0-1	9
Dry matter allocation to each plant layer*	DMPC	0-1	1
<b>Flowering, translocation, senescence, and formation of wintering organs</b>			
Max. relative tuber growth rate (part of net photosynthetic rate)	RTR	0.19	1, 12
Conversion factor for translocated dry matter into CH <sub>2</sub> O	CVT	1.05	11
Tuber number concurrently initiated per plant	NINTUB	8 plant <sup>-1</sup>	1, 8

Total critical dry weight of new tubers	TWCTUB	19.92 g DW m <sup>-2</sup>	1, 3
Relative death rate of leaves (on DW basis; Q10 =2)	RDR(T)	0.047 d <sup>-1</sup>	1
Relative death rate of stems and roots (on DW basis; Q10=2)	RDS(T)	0.047 d <sup>-1</sup>	1
<b>Site information</b>			
Water depth (field site)	DPT(T)	1.3 m	User def.
Daily water temperature (field site)	WTMP(T)	-, °C	User def.
Water type specific light extinction coefficient (field site)	L(T)	1.07 m <sup>-1</sup>	1
Water type specific current velocity (field site)	WVEL	0-100 cm s <sup>-1</sup>	User def.
Total live dry weight measured (field site)	TGWM(T)	-, g DM m <sup>-2</sup>	User def.
Tuber density measured (field site)	NTM(T)	400 m <sup>-2</sup>	3
<b>Harvesting</b>			
Harvesting	HAR	0 or 1	User def.
Harvesting day number	HARDAY	1-365	User def.
Harvesting depth (measured from water surface; 1-5 m)	HARDEP	0.1 m<DEPTH	User def.

\* Calibration function.

- Best and Boyd 2003c.
- Sher-Kaul et al. 1995.
- Van Wijk 1989.
- Howard-Williams 1978.
- Van Wijk 1988.
- Best and Boyd 1996.
- Spencer 1987.
- Spencer and Anderson 1987.
- Best et al. 2005.
- Van der Bijl et al. 1989.
- Penning de Vries and Van Laar 1982a, b.
- Van Wijk et al. 1988.

**Table 2c. Parameter values used in HYDRIL.**

Parameter	Name	Value	Reference
<b>Morphology, phenological cycle and development</b>			
Fraction of total dry matter increase allocated to leaves	FLV(T)	0.34	1, 2, 3
Fraction of total dry matter increase allocated to stems	FST(T)	0.60	1, 2, 3
Fraction of total dry matter increase allocated to roots	FRT(T)	0.06	1, 2, 3
Development rate as function of temperature*	DVRV	0.012 d <sup>-1</sup>	Calibrated
DVR prior to flowering DVRV, subsequently DVRR	DVRR	0.012 d <sup>-1</sup>	Calibrated
<b>Plant density and maximum plant biomass</b>			
Plant density	NPL	35 m <sup>-2</sup>	4, 5
Maximum plant biomass		900 g DW m <sup>-2</sup>	4
<b>Wintering, sprouting, and growth of sprouts to water surface</b>			
Dormant tuber density	NT	500 m <sup>-2</sup>	4
Tuber size	INTUB	0.1 g DW tuber <sup>-1</sup>	6
Rel. tuber death rate (on number basis)	RDTU	0.36 d <sup>-1</sup>	7
Rel. conversion rate of tuber into plant material	ROC	0.0576 g CH <sub>2</sub> O. g <sup>-1</sup> DW d <sup>-1</sup>	8
Relation coefficient tuber weight-stem length	RCSHST	12 m g DW <sup>-1</sup>	3, 8

<b>Light, photosynthesis, maintenance, growth and assimilate partitioning</b>			
Plant species specific light extinction coefficient	K	0.01 m <sup>2</sup> g <sup>-1</sup> DW	4, 9
Fraction of irradiation shaded by epiphytes*	EPISHD	0-0.43	10
Potential CO <sub>2</sub> assimilation rate at light saturation for shoots	AMX	0.0158 g CO <sub>2</sub> . g <sup>-1</sup> DW h <sup>-1</sup>	4, 11
Initial light use efficiency for shoots	EE	0.000011 g CO <sub>2</sub> J <sup>-1</sup>	12
Rel. reduction factor for AMX to account for senescence plant parts	REDF(T)	1.0	User def.
Reduction factor to relate AMX to water pH	REDAM	0.581	4, 13
Daytime temperature effect on AMX as function of DVS*	AMTMP(T)	0-1	13
Rel. factor to relate AMX to water current velocity*	REDAM1	0-1	10
Dry matter allocation to each plant layer*	DMPC	0-1	4, 14
<b>Flowering, translocation, senescence, and formation of wintering organs</b>			
Max. relative tuber growth rate (part of net photosynthetic rate)	RTR	0.4 d <sup>-1</sup>	15
Conversion factor for translocated dry matter into CH <sub>2</sub> O	CVT	1.1	12
Tuber number concurrently initiated per plant	NINTUB	7 plant <sup>-1</sup>	4
Total critical weight new tubers	TWCTUB	24.5 g DW m <sup>-2</sup>	4, 6
Rel. death rate of leaves (on DW basis)	RDR(T)	0.033 d <sup>-1</sup>	8
Rel. death rate of stems and roots (on DW basis)	RDS(T)	0.033 d <sup>-1</sup>	8
<b>Site information</b>			
Water depth (field site)	DPT(T)	1.0 m	User def.
Daily water temperature (field site)	WTMP(T)	-, °C	User def.
Water type specific light extinction coefficient (field site)	L(T)	0.83 m <sup>-1</sup>	1, 4
Water type specific current velocity (field site)	WVEL	0-100 cm s <sup>-1</sup>	User def.
Total live dry weight measured (field site)	TGWM(T)	-, g DW m <sup>-2</sup>	User def.
Tuber bank density measured (field site)	NTM(T)	58-510 m <sup>-2</sup>	8
<b>Harvesting</b>			
Harvesting	HAR	0 or 1	User def.
Harvesting day number	HARDAY	1-365	User def.
Harvesting depth (measured from water surface; 1-5 m)	HARDEP	0.1 m<DEPTH	User def.

\* Calibration function.

1. Haller and Sutton 1975. 2. Van et al. 1978b. 3. Van der Zwerde 1981. 4. Bowes et al. 1979. 5. Barko and Smart 1981. 6. Van et al. 1977. 7. Sutton, pers. comm. 1995. 8. Bowes et al. 1977. 9. Ikusima 1970. 10. Best et al. 2005. 11. Van et al. 1978a. 12. Penning de Vries and Van Laar 1982a, b. 13. Van et al. 1976. 14. Ambasht and Ram 1976. 15. Haller et al. 1976.

Table 2d. Parameter values used in MILFO.

Parameter	Name	Value	Reference
<b>Morphology, phenological cycle and development</b>			
Fraction of total dry matter increase allocated to leaves	FLV(T)	0.47	1
Fraction of total dry matter increase allocated to roots	FRT(T)	0.06	1
Fraction of total dry matter increase allocated to stems	FST(T)	0.47	1
Development rate as function of temperature*	DVRV	0.015 d <sup>-1</sup>	Calibrated
DVR prior to flowering DVRV, subsequently DVRR	DVRR	0.022 d <sup>-1</sup>	Calibrated
<b>Maximum plant density and plant biomass</b>			
Plant density	NPL	11 m <sup>-2</sup>	2
Maximum plant biomass		2,283 g DW m <sup>-2</sup>	2
<b>Wintering and sprouting of rhizomes/root crowns, and growth of sprouts to water surface</b>			
Initial rhizome weight	IWGRIZ	50 g DW m <sup>-2</sup>	3
Rel. rhizome death rate	RDRIZ	0.00042 d <sup>-1</sup>	4
Rel. conversion rate of rhizome weight into plant material	ROC	0.0576 g CH <sub>2</sub> O. g <sup>-1</sup> DW d <sup>-1</sup>	5
Relation coefficient rhizome/root crown weight-stem length	RCSHST	12 m g DW <sup>-1</sup>	5, 6
Critical rhizome weight	CRRIZ	12 g DW m <sup>-2</sup>	7
<b>Light, photosynthesis, maintenance, growth and assimilate partitioning</b>			
Plant species specific light extinction coefficient	K(T)	0.006 m <sup>2</sup> g <sup>-1</sup> DW	8
Fraction of irradiation shaded by epiphytes*	EPISHD	0-0.43	9
Potential CO <sub>2</sub> assimilation rate at light saturation for shoot tips	AMX	0.0165 g CO <sub>2</sub> . g <sup>-1</sup> DW h <sup>-1</sup>	10, 11
Initial light use efficiency for shoot tips	EE	0.000011 g CO <sub>2</sub> J <sup>-1</sup>	12
Rel. reduction factor for AMX to account for senescence plant parts	REDF(T)	1.0	User def.
Reduction factor to relate AMX to water pH	REDAM	0.5	13, 14
Daytime temperature effect on AMX as function of DVS	AMTMP(T)	0 -1	8, 15
Rel. factor to relate AMX to water current velocity*	REDAM1	0-0.43	9
Dry matter allocation to each plant layer	DMPC(T)	0 -1	1
<b>Flowering, translocation, senescence, and formation of wintering organs</b>			
Translocation (part of net photosynthetic rate)	TRAFAC	0.35	5
Conversion factor for translocated dry matter into CH <sub>2</sub> O	CVT	1.05	12
Rel. death rate of leaves (on DW basis; Q <sub>10</sub> =2)	RDR(T)	0.042 d <sup>-1</sup>	10
Rel. death rate of stems and roots (on DW basis; Q <sub>10</sub> =2)	RDS(T)	0.042 d <sup>-1</sup>	10
<b>Site information</b>			
Water depth (field site)	DPTT(T)	1.5 m	User def.
Daily water temperature (field site)	WTMP(T)	-, °C	User def.
Water type specific light extinction coefficient (field site)	L(T)	1.15 - 2.00 m <sup>-1</sup>	13
Water type specific current velocity (field site)	WVEL	0-100 cm s <sup>-1</sup>	User def.
Total live dry weight measured (field site)	TGWM(T)	-, g DW m <sup>-2</sup>	User def.

Harvesting			
Harvesting	HAR	0 or 1	User def.
Harvesting day number	HARDAY	1-365	User def.
Harvesting depth (measured from water surface in m)	HARDEP	0.1 m<DEPTH	User def.

\* Calibration function.

1. Adams et al. 1974. 2. Budd et al. 1995. 3. Smith and Adams 1986. 4. Vogt et al. 1991. 5. Bowes et al. 1979. 6. Van der Zweerde 1981. 7. Madsen 1997. 8. Titus and Adams 1979a. 9. Best et al. 2005. 10. Adams and McCracken 1974. 11. Van et al. 1976. 12. Penning de Vries and Van Laar. 1982a, b. 13. Lee and Kluesener 1972. 14. Titus and Stone 1982. 15. Stanley and Nailor 1972. 16. Kooman 1995.

### *Morphology, phenological cycle, and development*

#### *Morphology and phenological cycle.*

- V. americana.*** *V. americana* plants have a short stem axis, bearing a variable number of stolons. The plant forms a rosette on top of the sediment (“meadow formation”) with up to 1.2-m-long, linear tape-shaped leaves, submersed or floating at the water surface (Lowden 1982; Titus and Stephens 1983; Korschgen and Green 1988). Typical partitioning of biomass—71.8 percent in leaves, 15.9 percent in stems, and 12.3 percent in roots—is based on summer habit of full-grown plants (Titus and Stephens 1983; Haller 1974; FLVT, FSTT, FRTT). This species propagates largely vegetatively by tubers in North America. The production of viable seeds is low and seedling establishment in the field is rare in the Northern U.S. (Choudhuri 1966; Titus and Stephens 1983; Kimber et al. 1995). Plants flower once a year, from late-June to August in the northern hemisphere (Donnermeyer 1982; Titus and Stephens 1983; Donnermeyer and Smart 1985).
- P. pectinatus.*** *P. pectinatus* plants have long, flexible stems with narrow, mostly filiform leaves near or at the water surface (“canopy formation”) and emergent flowers (Den Hartog 1982). Typical partitioning of biomass—73.1 percent in leaves, 18.3 percent in stems, and 8.6 percent in roots—is based on summer habit of full-grown plants (Best and Boyd 2003c; Sher-Kaul et al. 1995; FLVT, FSTT, FRTT). In shallow waters, this species usually behaves as an annual because it is sensitive to frost and decomposes rapidly in water (Lohammar 1938; Lapirova and Petukhova 1985). However, in deeper waters, green perennial shoots can be found (Hammer and Heseltine 1988). This species propagates largely by tubers. Regeneration from rhizomes, turions or seeds may occur also. Plants flower once a year, from late-June to August in the

- northern hemisphere (Yeo 1965). In mild climates flowering may extend up to five months (Gupta 1968; Ramirez and San Martin 1984).
- *H. verticillata*. *H. verticillata* plants have long, flexible, stems, that branch close to the water surface (“canopy formation”) and are surrounded by whorls of leaves. Typical partitioning of biomass—34 percent in leaves, 60 percent in stems, and 6 percent in roots—is based on summer habit of full-grown plants (Haller and Sutton 1975; Van et al. 1978b; Van der Zweerde 1981; FLVT, FSTT, FRTT). *H. verticillata* biotypes regenerate largely from tubers, but may have stem fragmentation, horizontal shoot formation in the sediment, and turion formation on the shoots in addition to this vegetative reproduction mechanism. Plants flower once a year, i.e., from early June to the end of August in near-subtropical Florida (Bowes et al. 1979).
  - *M. spicatum*. *M. spicatum* plants have long, flexible stems, that branch close to the water surface (“canopy formation”) and are surrounded by whorls of leaves. Typical distribution of biomass—47 percent in leaves, 47 percent in stems, and 6 percent in roots—is based on summer habit of full-grown plants (Adams et al. 1974; FLVT, FSTT, FRTT). This species is able to propagate in an evergreen condition, by vegetative fragmentation, and by seeds. It most frequently winters in an evergreen form, as root crowns/rhizome system (Grace and Wetzel 1978; Madsen et al. 1988; Madsen 1997) and may maintain considerable winter biomass (Stanley et al. 1976). Plants flower from June to November in the northern hemisphere; one (Aiken et al. 1979; Carpenter 1980), two (Nichols 1971; Lind and Cottam 1969) and three (Grace and Wetzel 1978) flowering periods per year have been reported. The timing of flowering is “less predictable” in more southern areas (Grace and Wetzel 1978), whereas it may last the whole growth season in the tropics (Zutschi and Vass 1973).

*Phenology and development.* Plant development rates were derived from field data, typical for temperate regions. They are all in the same order of magnitude (Tables 3a, b, c, d, e).

- *V. americana*: 0.015 d<sup>-1</sup> prior to the flowering period and 0.040 d<sup>-1</sup> subsequently, at a reference temperature of 30 °C and a temperature threshold of 3°C.
- *P. pectinatus*: 0.015 d<sup>-1</sup> prior to the flowering period and 0.040 d<sup>-1</sup> subsequently.

**Table 3a. Relationship between development phase (DVS) of *V. americana*, day of year, at a reference temperature of 30 °C and 3 °C day-degree sum in a temperate climate (DVRVT= 0.015; DVRRT= 0.040).**

Developmental Phase		Day Number	3 °C Day-Degree Sum
Description	DVS Value		
First Julian day number → tuber sprouting and initiation elongation	0 → 0.291	0 → 105	1 → 270
Tuber sprouting and initial elongation → Leaf expansion	0.292 → 0.875	106 → 180	271 → 1215
Leaf expansion → floral initiation and anthesis	0.876 → 1.000	181 → 191	1216 → 1415
Floral initiation and anthesis → induction of tuber formation, tuber formation and senescence	1.001 → 2.000	192 → 227	1416 → 2072
Tuber formation and senescence → senesced	2.001 → 4.008	228 → 365	2073 → 3167
Senesced	4.008	365	3167

Note: Calibration was on field data on biomass and water transparency from Chenango Lake, NY, 1978 (Titus and Stephens 1983) and climatological data from Binghamton (air temperatures) and Ithaca (irradiance), NY, 1978.

**Table 3b. Relationship between development phase (DVS) of *P. pectinatus*, day of year, at a reference temperature of 30 °C and 3 °C day-degree sum in a temperate climate (DVRVT= 0.015; DVRRT= 0.040).**

Developmental Phase		Day Number	3 °C Day-Degree Sum
Description	DVS Value		
First Julian day number → tuber sprouting and initiation elongation	0 → 0.210	0 → 77	1 → 193
Tuber sprouting and initial elongation → Leaf expansion	0.211 → 0.929	78 → 187	194 → 1301
Leaf expansion → floral initiation and anthesis	0.930 → 1.000	188 → 195	1302 → 1434
Floral initiation and anthesis → induction of tuber formation, tuber formation and senescence	1.001 → 2.000	196 → 233	1435 → 2077
Tuber formation and senescence → senesced	2.001 → 4.033	234 → 365	2078 → 3193
Senesced	4.033	365	3193

Note: Calibration was on field data on biomass and water transparency from the Western Canal near Zandvoort, NL, 1987 (Best and Boyd 2003c) and climatological data from De Bilt, NL, 1987.

**Table 3c. Relationship between development phase (DVS) of *H. verticillata*, day of year, at a reference temperature of 30 °C and 3 °C day-degree sum in a temperate climate (DVRVT= 0.012; DVRRT= 0.012).**

Developmental Phase		Day Number	3 °C Day-Degree Sum
Description	DVS value		
First Julian day number → tuber sprouting and initiation elongation	0 → 0.326	0 → 74	1 → 596
Tuber sprouting and initial elongation → Leaf expansion	0.327 → 0.360	75 → 78	597 → 673
Leaf expansion → floral initiation and anthesis	0.361 → 1.000	79 → 150	674 → 2063
Floral initiation and anthesis → induction of tuber formation	1.001 → 2.000	151 → 241	2064 → 4279
Induction tuber formation → tuber formation and senescence	2.001 → 2.200	242 → 260	4280 → 4744
Tuber formation and senescence → senesced	2.201 → 2.979	261 → 365	4745 → 6357
Senesced	2.979	365	6357

Note: Calibration was on field data on biomass and water transparency from Lake Orange, FL, 1977 (Bowes et al. 1979) and climatological data from Gainesville, FL, 1980. Sprouting was timed after Haller et al. (1976).

**Table 3d. Relationship between development phase (DVS) of *M. spicatum*, day of year, at a reference temperature of 30 °C and 3 °C day-degree sum in a temperate climate (DVRVT= 0.022; DVRRT= 0.015).**

Developmental Phase		Day Number	3 °C Day-Degree Sum
Description	DVS Value		
First Julian day number → sprouting, initiation elongation, and leaf expansion COHORT1	0 → 0.375	0 → 114	1 → 191
Sprouting, initiation elongation, and leaf expansion → floral initiation, anthesis, and induction of senescence COHORT1	0.376 → 1.000	115 → 162	192 → 900
Floral initiation, anthesis, and induction of senescence → senescence COHORT1	1.001 → 1.630	163 → 212	901 → 2012
Senescence → senesced COHORT1	1.631 → 2.000	213 → 245	2013 → 2669
Sprouting, initiation elongation, and leaf expansion → floral initiation, anthesis, and induction of senescence COHORT2	1.001 → 1.630	163 → 212	901 → 2012
Floral initiation, anthesis, and induction of senescence → anthesis and senescence COHORT2	1.631 → 2.000	213 → 245	2013 → 2669
Senescence → senesced COHORT2	2.001 → 2.570	246 → 365	2670 → 3508
Senesced COHORT 1 and 2	2.570	365	3508

Note: Calibration was on field data on biomass (Adams and McCracken 1974), and on water transparency, temperature, and irradiance from Lake Wingra, WI, 1970 (Lee and Kluesener 1972).

**Table 3e. Relationship between development phase (DVS) of *M. spicatum*, day of year, at a reference temperature of 30 °C and 3 °C day-degree sum in a tropical climate (DVRVT= 0.022; DVRRT= 0.015).**

Developmental Phase		Day Number	3 °C Day-Degree Sum
Description	DVS Value		
First Julian day number → sprouting, initiation elongation, and leaf expansion COHORT 1	0 → 0.375	0 → 25	1 → 431
Sprouting, initiation elongation, and leaf expansion → floral initiation, anthesis, and induction of senescence COHORT 1	0.376 → 1.000	115 → 61	432 → 1163
Floral initiation, anthesis, and induction of senescence → senescence COHORT 1	1.001 → 1.630	62 → 162	1164 → 3844
Senescence → senesced COHORT 1	1.631 → 2.000	163 → 188	3845 → 4490
Sprouting, initiation elongation, and leaf expansion → floral initiation, anthesis, and induction of senescence COHORT 2	1.001 → 1.630	62 → 162	1164 → 3844
Floral initiation, anthesis, and induction of senescence → anthesis and senescence COHORT 2	1.631 → 2.000	163 → 188	3845 → 4490
Senescence → senesced COHORT 2	2.001 → 2.570	164 → 233	4491 → 5492
Sprouting, initiation elongation, and leaf expansion → floral initiation, anthesis, and induction of senescence COHORT 3	2.001 → 2.447	164 → 223	4491 → 5273
Floral initiation, anthesis, and induction of senescence → anthesis and senescence COHORT 3	2.448 → 3.500	224 → 307	5274 → 7125
Senescence → senesced COHORT 3	3.501 → 4.141	308 → 365	7126 → 8254
Senesced COHORT 1, 2, and 3	4.141	365	8254

Note: Calibration was on field data on biomass from Kashmir lakes, India, 1970s (Zutschi and Vass 1973), and on climatological data from Patancheru, India, 1978.

- *H. verticillata*: 0.012 d<sup>-1</sup> prior to the flowering period and 0.012 d<sup>-1</sup> subsequently.
- *M. spicatum*: 0.022 d<sup>-1</sup> prior to the flowering period and 0.015 d<sup>-1</sup> subsequently.

Each simulation starts at the first Julian day number, i.e., January 1, when the development phase has the value 0.0 (Table 3). The quantities of leaves, stems, and roots are set equal to 0. For the tuber-producing species (Tables 2a, 2b, 2c), the simulation starts using an observed tuber bank density, with a certain, chosen (see “Wintering, sprouting in spring, and growth of sprouts to water surface”) individual tuber weight as initial values.

For *M. spicatum* (Tables 2d, 3e), the simulation starts using an observed rhizome weight at the beginning of the year. If simulation of a SAV at a

different site is desired, the simulation may start also with wintering plants present; first, however, initial quantities of plant organs must be calculated. Initiation of growth activity for a tuber-producing SAV in a temperate climate occurs by sprouting of the tubers, i.e., occurs at a DVS between 0.2 and 0.3 (Tables 2a, 2b, 2c). Sprouts of the first plant cohort develop through remobilization of carbohydrates from tubers. The sprouts elongate up to the preset maximum plant height (or to the water surface in cases where water depth is less than the maximum preset plant height), and subsequently follow a species-characteristic vertical distribution over the water column. Anthesis is initiated at DVS 1.000 and finishes at DVS 2.000 just before new tubers are initiated. Tubers can be formed directly at initiation in *V. americana* and *P. pectinatus*, or after a certain lag period in *H. verticillata*. Tuber formation, downward translocation, and senescence set in at DVS 2.001 (2.201 in *H. verticillata*) and continue until the end of the year (Tables 3a, 3b, 3c).

Initiation of growth activity for a *M. spicatum* community in a temperate climate (Table 2d) occurs by sprouting of the rhizome/root crown system, i.e., at DVS 0.376. Sprouts of plant COHORT 1 develop through remobilization of carbohydrates from the rhizome/root crown system. The sprouts elongate up to the water surface and form a canopy in the upper water layers. Anthesis of COHORT 1 is initiated at DVS 1.000 and finishes at DVS 1.630, just before downward carbohydrate translocation and senescence are initiated. Translocation and senescence of COHORT 1 set in at DVS 1.631 and continue until DVS 2.000. Sprouting of COHORT 2 starts when translocation and senescence of COHORT 1 have set in. This timing is based on the assumption that at that time, apical dominance by the existing, senescing shoots is broken and, consequently, new shoots develop. Sprouting of COHORT 2 occurs from growing points on the rhizome/root crown system. Anthesis of COHORT 2 is initiated at DVS 1.631 and finishes at DVS 2.000. Translocation and senescence of COHORT 2 set in at DVS 2.001 and continue until the end of the year. For a vegetation in the tropics (Table 3e), it proved impossible to generate the high levels of shoot and rhizome/root crown biomass reported (Zutschi and Vass 1973) with two plant cohorts active, since the second plant cohort had already senesced in May. However, proper biomass levels and timing were attained with three plant cohorts active, the third cohort being switched on at latitudes less than 33 °N. It is possible that a particular plant process, such as sprouting, is sensitive to day length, and that this process decides for the population to activate another cohort. However, since the authors

are not aware of publications on this topic for *M. spicatum*, the switch has been set at the cutoff latitude for tropical areas.

Plants in tropical regions behave similarly in terms of DVS to those in temperate regions, except that tropical plants require on average a 1.6 x higher 3 °C day-degree sum to complete their individual life cycle than temperate cohorts.

*Plant density and maximum biomass*

*V. americana*. For *V. americana*, typical plant density of 30 plants per square meter (NPL) was calculated by dividing the maximum standing crop of an established, monotypic vegetation (50.1 g DW m<sup>-2</sup>) by the average weight of an individual rosette with neighbor plants (1.65 g DW m<sup>-2</sup>) in Chenango Lake, NY (Titus and Stephens 1983). Maximum biomass ranged from 253 g DW m<sup>-2</sup> at a 0.73-m rooting depth in Lake Biwa, Japan, in 1969 (lat 35° 30' N; Ikusima 1970); to 344 g DW m<sup>-2</sup> at a 1.2-1.5-m rooting depth in University Bay, WI, in 1976 (lat 43° 08' N; Titus and Adams 1979b); to 496 g DW m<sup>-2</sup> in 1.5-m deep experimental ponds, in Orange County, FL (lat 28° 30' N; Haller 1974). For subtropical to tropical areas in Florida, a relatively constant, high biomass has been suggested (Godfrey and Wooten 1997). The highest published value on maximum biomass ( $\leq 496$  g DW m<sup>-2</sup>) was selected as upper limit of plant biomass in VALLA.

*P. pectinatus*. For *P. pectinatus*, typical plant density of 30 plants per square meter (NPL) was computed by dividing the maximum standing crop of an established, monotypic vegetation at a 2.5-m rooting depth (82.27 g DW m<sup>-2</sup>; Best and Boyd 2003c) by the highest average weight of an individual plant with neighbor plants (2.76 g DW plant<sup>-1</sup>) in shallow waters studied in NL and The Camargue, France (Best and Boyd 2003c; Van Wijk 1989). Other literature reviewed did not provide sufficiently detailed information to enable calculations of plant density. In a temperate climate, the highest biomass was found in brackish and saline lakes, i.e., 1,313 g DW m<sup>-2</sup> in a brackish pool near Yerseke, NL (lat 51° 30' N; Van Wijk et al. 1988); 1,568 g DW m<sup>-2</sup> in saline Lake Mariut, Egypt (lat 31° 10' N; Aleem and Samaan 1969); and 1,952 g DW m<sup>-2</sup> in the saline Swartvlei, between Port Elizabeth and Cape Town, South Africa (lat 34° 0' S; Howard-Williams 1978). A somewhat lower maximum of 712 g DW m<sup>-2</sup> occurred in freshwater Badfish Creek, WI (lat 43° 4' N; Madsen and Adams 1988). Maximum biomass in freshwater lakes in the tropics is similar to that in a temperate climate, i.e., 370-445 g DW m<sup>-2</sup> (lat 17° 27' N;

Sinha 1970; Sahai and Sinha 1973). The highest published value on maximum biomass ( $\leq 1,952$  g DW  $m^{-2}$ ) was selected as upper limit of plant biomass in POTAM.

*H. verticillata*. For *H. verticillata*, typical plant density of 35 plants per square meter (NPL) was considered as representative. A range of 34-53 plants  $m^{-2}$  was calculated by dividing the standing crop of an established vegetation (163 g DW  $m^{-2}$ ) in Lake Orange in August (1977; Bowes et al. 1979) by the weight range of individual plants (3.08-4.76 g DW plant $^{-1}$ ; Barko and Smart 1981). Maximum biomass varied from 163 g DW  $m^{-2}$  in Lake Orange, FL, in 1977 (Bowes et al., 1979); to 500 g DW  $m^{-2}$  in Lake Ramgarh, India, in 1967-68 (Sahai and Sinha 1973); to 890 g DW  $m^{-2}$  in Lake Trafford (shoots; Bowes et al. 1979).

The highest published value on maximum biomass (i.e., 890 g shoot biomass augmented with 10 g root biomass  $m^{-2}$ ) of 900 g DW  $m^{-2}$ ) was selected as upper limit of plant biomass in HYDRIL.

*M. spicatum*. For *M. spicatum*, typical plant density of 11 plants per square meter (NPL) was the average within a range of 3 to 32 "plant clumps" per square meter, consisting of a variable number of stems, measured in a vegetation in Fish Lake, WI, in 1990-92 (Budd et al. 1995). Maximum biomass was 2,283 g DW  $m^{-2}$  in the same lake and year, and similar values have been reported for the more southern Lake Guntersville, AL, in 1972 (Stanley et al. 1976). The latter value on maximum biomass ( $\leq 2,283$  g DW  $m^{-2}$ ) was selected as upper limit of plant biomass in MILFO.

*Wintering, sprouting in spring, and growth of sprouts to water surface*

*V. americana*. Tuber bank density in this species varies over a large range, from 0 in early summer to 450  $m^{-2}$  in autumn. The large range found may be attributed partly to the patchy spatial distribution of the community over the water body, limited number of replicate samples taken (Spencer et al. 1994), and between-site variation in rooting depth of the vegetation. Densities published are (1) 101  $m^{-2}$  in Lake Mendota, WI (Titus and Adams 1979b), (2) 170  $m^{-2}$  in Pool 9 of the Upper Mississippi River, WI (Donnermeyer 1982); (3) 233  $m^{-2}$  in the Lower Detroit River, MI (Korschgen and Green 1988); (4) 330-450  $m^{-2}$  in Chenango Lake, NY (Titus and Stephens 1983); and (5) 115-1,140  $m^{-2}$  in Lake Mattamuskeet, NC (Lovvorn and Gillingham 1996). A tuber bank density of 233  $m^{-2}$  with a tuber size of

0.09 g DW found in well-established tuber banks (Korschgen and Green 1988) was used for calibration.

Tuber sizes published are, in g DW tuber<sup>-1</sup>, (1) 0.04 to 0.18 (various north-american water bodies; Korschgen and Green 1988; Korschgen et al. 1997); (2) 0.055 (average, Chenango Lake, NY, 1.4-m rooting depth; Titus and Stephens 1983); (3) 0.07 (average, Lake George, NY, 2- to 4-m rooting depth, J. D. Madsen unpublished, Vicksburg, MS); and (4) 0.18 (maximum, just after tuber completion, Pool 9 Upper Mississippi River, WI, 1.1-m rooting depth; Donnermeyer 1982). Individual tuber weight decreased almost linearly with decreasing light level (from 0.102 to <0.01 g dry weight tuber<sup>-1</sup>), and parabolically with concurrently formed tuber number per plant (from 0.120 to 0.015; Korschgen et al. 1997). The latter phenomenon forms the basis of the hypothesis by the authors of this report that *V. americana* follows an optimization strategy aimed at producing the largest tubers for the light level experienced because large tubers have a greater survival value than smaller ones. Thus, an established vegetation experiencing a given light level will aim at producing one tuber size class only, i.e., with a size that allows new plants to survive at that site. Consequently, the differences in tuber size found in tuber banks may be attributed to, besides differences in environmental conditions, differences in age between tuber size classes with tubers in the oldest class weighing less because of remobilization processes, in the last-completed class being full-size, and in the youngest class weighing less because not yet finished. The combination of 5.5 concurrently initiated tubers and tuber size of 0.090 g DW tuber<sup>-1</sup> was selected as nominal. The typical relationship between tuber size and concurrently formed tuber number per plant has to be used to calculate the proper initial values for simulations started from a different tuber size than nominal (Table 4).

Tuber death rates have not been published. For use in VALLA, the value for the relative tuber death rate was determined by applying the same differential equation as commonly used for simple exponential growth to describe continuous exponential decrease in tuber number, with a negative specific decrease rate (Thornley and Johnson 1990b; Hunt 1982). A relative tuber death rate (*RDTU*) of 0.018 d<sup>-1</sup> (on number basis) was found for the vegetation in Chenango Lake, NY (Titus and Stephens 1983). Tuber loss from grazing is expected to be relatively low in this plant species because of its relatively low tuber bank density (compared to *H. verticillata*) which may discourage foraging by waterfowl because this species requires

a relatively long search time (Lovvorn 1989; Lovvorn and Gillingham 1996).

Table 4. Relationship between tuber size and concurrently initiated tuber number in *V. americana* and *P. pectinatus*.

<i>V. americana</i>		<i>P. pectinatus</i>	
Tuber Size (g DW tuber <sup>-1</sup> )	Concurrently Initiated Tuber Number (N plant <sup>-1</sup> )	Tuber Size (g DW tuber <sup>-1</sup> )	Concurrently Initiated Tuber Number (N plant <sup>-1</sup> )
0.015	0.6	0.002	0.5
0.035	2.0		
0.050	3.0		
0.070	4.0		
0.086	5.0	0.055	5.0
0.090	5.5	0.070	6.0
0.120	5.8	0.155	12.0

Sprouting frequency of tubers in the field has not been published. Potential sprouting frequency is high in a temperate climate, being  $\leq 80$  percent. Sprouting frequency in an established community is probably not important, unless it is very low, as long as the typical density of 30 plants per square meter is somehow reached, since density tends to play a lesser role in biomass production compared to space availability. Sprouting frequency is not affected by day length, but is higher in light than in darkness. Sprouting is prevented by temperatures  $\leq 5$  °C, optimal between 15 and 25 °C, and maximal at 20 and 25 °C (J. D. Madsen unpub., Vicksburg, MS), and occurs early in the growth season, i.e., mid-April to end-of-May in Pool 9 of the Upper Mississippi River, WI, in 1980-81 (Donnermeyer 1982). In VALLA, sprouting is governed by DVS and, thus, indirectly by temperature.

Minimum weight required for a tuber to sprout is 0.003 g DW tuber<sup>-1</sup> (Donnermeyer and Smart 1985; J. D. Madsen unpub., Vicksburg, MS). In VALLA the minimum tuber weight has been set at 0.003 g dry weight tuber<sup>-1</sup>.

The derivations of the parameters *CRIFAC* and *SURPER* in VALLA are described in this paragraph; those of *ROC* and *RCHST* are described under *H. verticillata*. The elongation potential of plantlets emerging from tubers is limited, i.e. 0.44 m (range 0.04 to 0.18 g DW tuber<sup>-1</sup>; Korschgen and Green 1988; Korschgen et al. 1997). Thus, plants can rise one 0.1-m depth layer in the water column after filling that layer with a minimum of 0.0091 or maximum of 0.041 g DW. Elongation is modeled by filling each successive water layer from the sediment to a 1.2-m water column with the minimum required shoot biomass (0.0091 g DW plant<sup>-1</sup>, termed *CRIFAC*). Respiration of dormant tubers is low. Measured respiration in dormant *P. pectinatus* tubers was 0.003623 g CO<sub>2</sub> g DW<sup>-1</sup> h<sup>-1</sup> at 20 °C (Best and Boyd 2003c). Respiration is expected to decrease by a factor of 2 with a 10 °C-decrease in temperature (Q<sub>10</sub>). Thus, daily respiration of a dormant tuber at 10 °C would be 0.043476 g CO<sub>2</sub> g DW<sup>-1</sup> d<sup>-1</sup> (multiplication by 1/2 and 24), and yield 0.00391 g CO<sub>2</sub> tuber<sup>-1</sup> d<sup>-1</sup> of the nominal 0.09-g-DW tuber size. A tuber of this size would survive 23 days (*SURPER*), not taking conversion costs of CO<sub>2</sub> into dry weight into consideration (0.00391 g CO<sub>2</sub> tuber<sup>-1</sup> d<sup>-1</sup> x 23 days = 0.09 g dry weight) without net photosynthesis taking place. Larger tubers have longer, and smaller tubers shorter survival periods.

*P. pectinatus*. Tuber bank density in this species ranges from 0 in early summer to 3,975 m<sup>-2</sup> in autumn (Van Wijk 1989). Potential causes for the large range found have been outlined under *V. americana*. The following densities have been published: (1) 45-115 m<sup>-2</sup> on a wave-exposed shallow site within the brackish Baltic Sea, Sweden (Kautsky 1987); (2) 270-385 m<sup>-2</sup> in the shallow, fresh, Lake Veluwe, NL (Van Dijk et al. 1992); (3) 1,330 and 3,975 m<sup>-2</sup> in an oligohaline, sheltered ditch Salin De Badon and shallow pool Les Garcines, respectively, both in the Camargue, France (Van Wijk 1988). A tuber bank density of 240 m<sup>-2</sup> with a tuber size of 0.083 g DW found in well-established tuber banks, in the Western Canal near Zandvoort, NL (Best and Boyd 2003c) was used for calibration.

Tuber sizes published are, in g DW tuber<sup>-1</sup>, (1) 0.005 to 0.155 (average 0.013 g, laboratory study in CA; Spencer and Anderson 1987); (2) 0.017 (derived from 0.056 g fresh weight, and DW:FW ratio of 0.299±0.034; freshwater canals, CA; Spencer 1987); (3) 0.083 (Best and Boyd 2003c). Tubers may be formed in classes, as suggested by the formation of 10 tuber size classes with an average fresh weight of 0.061 ± 0.006 g tuber<sup>-1</sup> (range 0.02 to 0.3 g) and 18 tuber size classes with an average fresh weight of

$0.017 \pm 0.003$  g tuber<sup>-1</sup> (range 0.02 to 0.46 g) in the fresh Lake Veluwe and a brackish Texel ditch, respectively, both in NL (Hootsmans 1994). Tuber size decreased almost linearly with tuber number concurrently formed per plant (from 0.155 to 0.002; Spencer and Anderson 1987, Table 3). The combination of 8.0 concurrently initiated tubers and tuber size of 0.083 g DW tuber<sup>-1</sup> was selected as nominal. The typical relationship between tuber size and concurrently formed tuber number per plant is used to calculate the proper initial values for simulations started from a different tuber size than nominal (Table 4).

Tuber death rates have not been published. For use in POTAM, the value for the relative tuber death rate (*RDTU*) was found using the same approach as followed for VALLA. A *RDTU* of 0.026 d<sup>-1</sup> (on number basis) was found for the SAV in a shallow ditch in Yerseke, NL (Van Wijk 1988). Tuber loss from grazing is expected to be in the same order of magnitude as in *V. americana*.

Sprouting frequency of tubers in the field has not been published. Potential sprouting frequency is high in a temperate climate, being  $\leq 80$  percent. It is increased by cold stratification (Van Wijk 1989). Sprouting frequency decreases with tuber burial depth, for instance (a) small tubers in the range of 0.003 to 0.012 g DW tuber<sup>-1</sup> proved less likely to emerge when planted at 5 and 10 cm than at 2.5 cm depth, whereas (b) only 30 percent of large tubers of 0.017 g DW sprouted at 20 cm depth (Spencer 1987). Abundant sprouting was observed between 5.5 °C and 10 °C (Western Canal, NL; Best and Boyd 2003c) and 25 °C (Spencer and Anderson 1987, CA; Van Wijk 1989, France), but sprouting was lower at 25 °C than at 20 °C (Van Wijk 1989). Sprouting occurs early in the growth season, i.e., in the beginning of April in the Western Canal, NL, in 1987 (Best and Boyd 2003c). In POTAM, sprouting is governed by DVS and, thus, indirectly by temperature. Minimum weight required for a tuber to sprout in POTAM has been set at 10 percent of the initial tuber size.

The derivations of the parameters *CRIFAC* and *SURPER* in POTAM are described in this paragraph; those of *ROC* and *RCHST* are described under *H. verticillata*. The elongation potential of plantlets emerging from tubers is limited, i.e., 0.00714 m (for tubers ranging from 0.0054 to 0.155 g DW tuber<sup>-1</sup> (Spencer 1987; Spencer and Anderson 1987)). Thus, plants can rise one 0.1-m depth layer in the water column when they can fill that layer with a minimum of 0.0076 or maximum of 0.2170 g DW. Elongation is

modeled by filling each successive water layer from the sediment to a 1.3-m water column with the minimum shoot biomass required (0.0076 g plant dry weight plant<sup>-1</sup>, termed *CRIFAC*). A tuber survival period (*SURPER*) of 23 days for the nominal 0.083-g-DW tuber size was calculated, following the same approach as used for VALLA. A slightly higher *SURPER* of 27 days was selected for use in POTAM since this value allowed the simulated SAV to survive and produce biomass similar to populations in the field, while with a *SURPER* of 23 days the SAV became extinct. Larger tubers have longer, and smaller tubers shorter survival periods.

*H. verticillata*. Tuber bank density in this species ranges from 0 in early summer to 1,000 m<sup>-2</sup> in autumn (Haller et al. 1976; Bowes et al. 1979). A tuber bank density of 500 m<sup>-2</sup> with a tuber size of 0.1 g DW found in well-established tuber banks, in Lake Orange, FL (Bowes et al. 1979) was used for calibration.

Tubers of various size classes have been found in the field, usually around 0.1 g DW tuber<sup>-1</sup> (Van et al. 1978a). Larger tubers have been found also (Bowes et al. 1977). The largest tubers of 0.5 g DW tuber<sup>-1</sup> were reported in plants cultivated in the laboratory and fertilized (McFarland and Barko 1990). The number of tubers concurrently formed per plant was derived from tubers collected from the *H. verticillata* tuber bank in Lake Orange, FL (Bowes et al. 1979), and ranged from 7 to 11. The combination of 7.0 concurrently initiated tubers (*NINTUB*) and tuber size of 0.1 g DW tuber<sup>-1</sup> (*INTUB*) was selected as nominal. A typical relationship between individual tuber weight and concurrently formed tuber number per plant, which was identified in both other tuber-forming plants, was not found in this plant species.

Tuber death rates have not been published. For use in HYDRIL, the value for the relative tuber death rate (*RDTU*) of 0.36 d<sup>-1</sup> (on number basis) was found by linear extrapolation from a density of 500 m<sup>-2</sup> (representative for Lake Orange, FL) to 0 m<sup>-2</sup> in 3 years (field observation North New River Canal, FL; D.L. Sutton, personal communication 1995). This value is similar to that reported for a potato crop in Florida (Ingram and McCloud 1984). Tuber loss from grazing is expected to be substantial because of the high tuber bank density, and relatively high compared to other tuber-forming species.

Sprouting frequency of tubers in the field has not been published. Potential sprouting frequency is high under experimental conditions, i.e., up to 100 percent (Bowes et al. 1977; Spencer and Anderson 1986; Steward and Van 1986; Sutton and Portier 1992). Sprouting may be triggered by a certain red-far red ratio in the light reaching the plants' photosensitive pigments (Spencer and Anderson 1986); however, the latter phenomenon can only play a role when wintering shoot biomass is present. Phytochrome is not expected to trigger tuber sprouting in the spring for *H. verticillata* in Lake Orange, since it winters in the form of tubers in the sediment without shoot biomass. Sprouting occurs at a day length greater than 13 h, as for potatoes (Hahn and Hozyo 1983), within a temperature range between 18 °C and 33 °C (Haller et al. 1976), and may start early in the growth season, i.e., mid-March in Florida lakes (Haller et al. 1976). Minimum weight required for a tuber to sprout in POTAM has been set at 10 percent of the initial tuber size.

The derivations of the parameters *ROC* and *RCHST* in HYDRIL are described in this paragraph. *CRIFAC* and *SURPER* are not used in HYDRIL. Sprouting tubers deplete tuber carbohydrate reserves. Tuber carbohydrates are converted into plant material following a relative tuber-to-plant conversion rate (*ROC*) of 0.0576 g CH<sub>2</sub>O g tuber DW<sup>-1</sup> d<sup>-1</sup>. This value was derived from the light compensation point (*LCP<sub>t</sub>*) of 12 μE m<sup>-2</sup> s<sup>-1</sup> in young, 35-d old, *H. verticillata* shoots (Bowes et al. 1977), assuming that the originally high *LCP<sub>0</sub>* of 100 decreases exponentially to the far lower *LCP<sub>t</sub>* due to conversion of tuber into plant material, according to the following equation.

$$LCP_t = LCP_0 \times e^{-ROC(35 \times 24)} \quad (6)$$

The elongation potential of plantlets emerging from tubers is large, i.e., 12 m g<sup>-1</sup> DW on average (range 8.8 to 18.8 m g<sup>-1</sup> DW (tuber size range of 0.011-0.056; derived from Bowes et al. 1977)). Elongation is modeled by allowing each tuber to elongate from the sediment as far as possible or up to the water surface, according to the relation coefficient tuber weight-stem length (*RCSHST*) of 12 m g<sup>-1</sup> DW.

*M. spicatum*. In MILFO, initial rhizome/root crown biomass has been set at 50 g AFDW m<sup>-2</sup>, i.e., equal to the lowest shoot biomass found in Lake Wingra, WI, in 1970 (Adams and McCracken 1974), and equal to the belowground biomass measured at the beginning of the year at a 1.5-m

rooting depth in the same lake in 1977 (Smith and Adams 1986). Rhizome/root crown biomass of *M. spicatum* fluctuated between 12 and 400 g DW m<sup>-2</sup> in a temperate climate (Madsen 1997), and between 32 and 48 g DW m<sup>-2</sup> in a tropical climate (Zutschi and Vass 1973).

Sprouting or regrowth of the rhizome/root crown in the field has not been published. Sprouting potential is usually high. Sprouting frequency in an established community is probably not important, unless it is very low, as long as the typical plant density of 11 plants m<sup>-2</sup> is somehow reached because plant density tends to play a lesser role in biomass production compared to space availability. In southern areas such as Texas (lat 33° N), sprouting occurs already in March (Madsen 1997). In northern areas, the timing of sprouting may be similar, but no observations confirming this have been published, probably because at that time water temperatures are still very low impeding field work. Minimum weight required for a rhizome to sprout (*CRRIZ*) is 12.0 g dry weight m<sup>-2</sup>, i.e., the lowest published value (Madsen 1997).

The derivation of the parameter *RDRIZ* in MILFO is described in this paragraph; those of *ROC* and *RCHST* are described under *H. verticillata*. The relative rhizome death rate was not derived from field data because the data availability was insufficient. Instead, a relative rhizome death rate has been derived from observations on terrestrial rhizome systems where annual turnover rates were found to be approximately four times less than those of aboveground plant biomass in the growth season, but dropping by a factor of 1/100 in inactive periods (Vogt et al. 1991). Following this approach, a tentative relative rhizome death rate (*RDRIZ*) of 0.00042 d<sup>-1</sup> was calculated (on weight basis), being 1/100 of the *M. spicatum* plant death rate. Effects of grazing by waterfowl on the milfoil rhizome/root crown systems are unknown, but they are expected to be far lower than on *H. verticillata* tubers.

*Light, photosynthesis, maintenance, growth, and assimilate partitioning*

*V. americana*. *VALLA* is calibrated using field data on biomass and water transparency (*L*) from Chenango Lake, NY, 1978 (Titus and Stephens 1983) and climatological data from Binghamton (air temperatures) and Ithaca (irradiance), NY, 1978. For the plant community-specific light extinction coefficient (*K*) in *VALLA*, the value of 0.0235 m<sup>2</sup> g<sup>-1</sup> DW was used, measured in the canopy of a SAV in Lake Mendota, WI (Titus and Adams 1979a). Other, lower, community-specific extinction coefficients of 0.0051,

0.013-0.019, and  $0.018 \text{ m}^2 \text{ g}^{-1} \text{ DW}$  have been published by Blanch et al. (1998), Titus and Adams (1979a, “vertical  $K$ ”) and Ikusima (1970).

The reduction in light interception by the plant through epiphyte shading in VALLA is derived from measured epiphyte shading up to a 0.43-fraction in *V. americana* populations in the Upper Mississippi River, WI (Best et al. 2005; Figure 6). Light interception by the plant is multiplied by a factor of  $(1-EPISHD)$ , that ranges from 1 at DVS 0 to 0.57 at DVS 1.0 during flowering, to 1 at DVS 2.3 in a temperate climate (and  $DVS >2.3$  in a warmer climate). This fraction may be typical for this particular plant species and site. For SAV growing in aquatic systems with less epiphyte shading than in the Mississippi River, the maximum epiphyte shading may have to be reduced in the model input file.

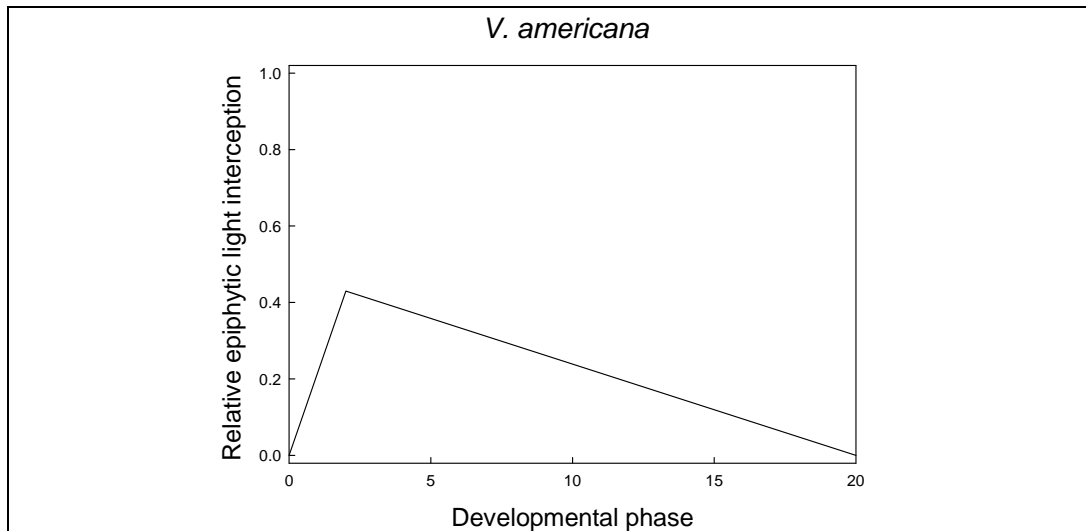


Figure 6. Relationship between development phase and relative epiphytic light interception used for calibration of VALLA.

For photosynthetic activity at light saturation ( $AMX$ ) in VALLA, the value of  $0.0165 \text{ g CO}_2 \text{ g}^{-1} \text{ DW h}^{-1}$  was used, measured in *V. americana* in the laboratory (Titus 1977). Light- and carbon-saturated photosynthetic rates can be far higher (Titus and Stone 1982; Titus et al. 1990), suggesting that photosynthetic activity in lakes such as Lakes Chenango and Mendota, where DIC concentrations are in the range of 0.8 to 3.5 mmol and pH 7.6 - 9.4, can be carbon-limited. For photosynthetic light-use efficiency ( $EE$ ) in VALLA, a value of  $11 \times 10^{-6} \text{ g CO}_2 \text{ J}^{-1}$  and typical for  $C_3$  plants was used (Penning de Vries and Van Laar 1982a). Gross assimilation rate at light saturation shows a distinct seasonal pattern and tends to decrease with aging (Titus 1977). Although a relative function describing the effect of

aging on gross assimilation (*REDFT*) has been included in VALLA, it is not active in the nominal version (set to 1) because in simulations this effect was negligible compared to that of changes in irradiance. Daily changes in pH and oxygen concentrations may affect *AMX*. In VALLA, a reduction factor, *REDAM*, can be used to take effects of daily changes in pH and oxygen concentration into account by reducing the *AMX* by a factor between 0 and 1. *AMX* and actual photosynthesis are similar at pH 8.5 found in *V. americana* communities in Chenango Lake (Titus and Stephens 1983; Titus and Stone 1982), and, therefore, *REDAM* currently has the value of 1. *AMX* in this species is not affected by changes in oxygen concentration. In VALLA, the effect of daytime temperature on *AMX* is accounted for via a fitted, relative function, *AMTMPT*, which is based on the measured photosynthetic response of *V. americana* to temperature and has its optimum at 35 °C (Titus and Adams 1979a). A similar relationship between temperature and chlorophyll concentration was found by Barko and Filbin (1982).

The relationship between photosynthesis and current velocity in VALLA is derived from measured typical plant photosynthesis in the related *Elodea nuttallii* at low current velocity (Best and Boyd 2003a), and typical biomass production of *V. americana* in the Red Cedar River, WI, at high current velocity (Best et al. 2005). *AMX* is multiplied by the relative photosynthetic rate (*REDAMI*), which ranges between 1 at a current velocity of 7 cm s<sup>-1</sup> and 0 at a current velocity of 81 cm s<sup>-1</sup> (Figure 7).

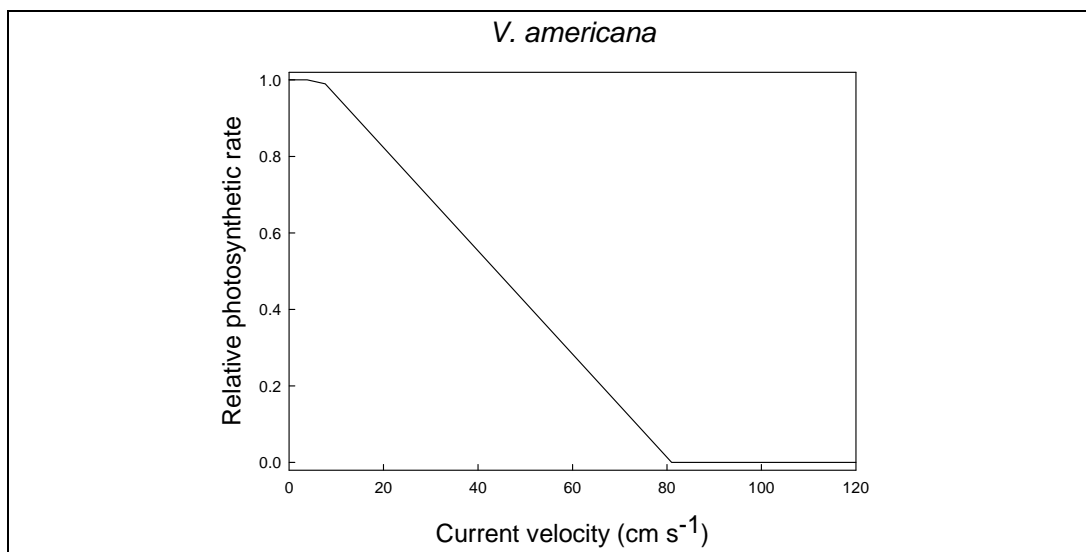


Figure 7. Relationship between current velocity and relative photosynthetic rate used for calibration of VALLA.

In VALLA, assimilates are partitioned typically over the plant parts, with 71.8 percent as leaves, 15.9 percent as stems, and 12.3 percent as roots (Titus and Stephens 1983; Haller 1974). Vertical distribution of shoot biomass is governed by a dry matter partitioning coefficient function (*DMPC*) following the typical meadow type shape. Distribution proceeds as follows. First plant biomass is distributed at 18.4 percent over the three depth layers above the sediment surface and at 11.4 percent over layers 4 and 5 above these. Subsequently, the remaining shoot biomass is distributed over maximally seven depth layers above this 0.5 m up to a total share of 9.7 percent. When five depth layers or less are present, first the lowest layers are filled according to the typical distribution pattern, and subsequently the remaining shoot biomass is added by equal distribution over the found layers. Vertical biomass distribution pattern is recalculated and redistributed by VALLA when a rooting depth other than nominal (1.4 m) is chosen by the user. In the model, roots always contribute 12.3 percent to total plant biomass.

*P. pectinatus*. POTAM is calibrated using field data on biomass and water transparency (*L*) from the Western Canal near Zandvoort, NL, 1987 (Best and Boyd 2003c) and climatological data from De Bilt, NL, 1987. For the plant community-specific light extinction coefficient in POTAM (*K*), the value of 0.095 m<sup>2</sup> g DW<sup>-1</sup>, measured in the canopy of a SAV in the same canal, was used (Best and Boyd 2003c). Other community-specific extinction coefficients of 0.0183, 0.020, and 1.79 m<sup>2</sup> g DW<sup>-1</sup> have been published by Sher-Kaul et al. (1995), Westlake (1965), and Best et al. (2005).

The reduction in light interception by the plant through epiphyte shading in POTAM is derived from measured epiphyte shading up to complete light extinction, i.e., a 1.00-fraction, in *P. pectinatus* populations in the Upper Mississippi River, WI (Best et al. 2005; Figure 8). Light interception by the plant is multiplied by a factor of (*1-EPISHD*), that ranges from 1 at DVS 0 to 0 at DVS 1.0 during flowering, to 1 at DVS 2.3 in a temperate climate (and DVS >2.3 in a warmer climate). This fraction may be typical for this particular plant species and site. For SAV growing in aquatic systems with less epiphyte shading than the Mississippi River, the maximum epiphyte shading may have to be reduced in the model input file.

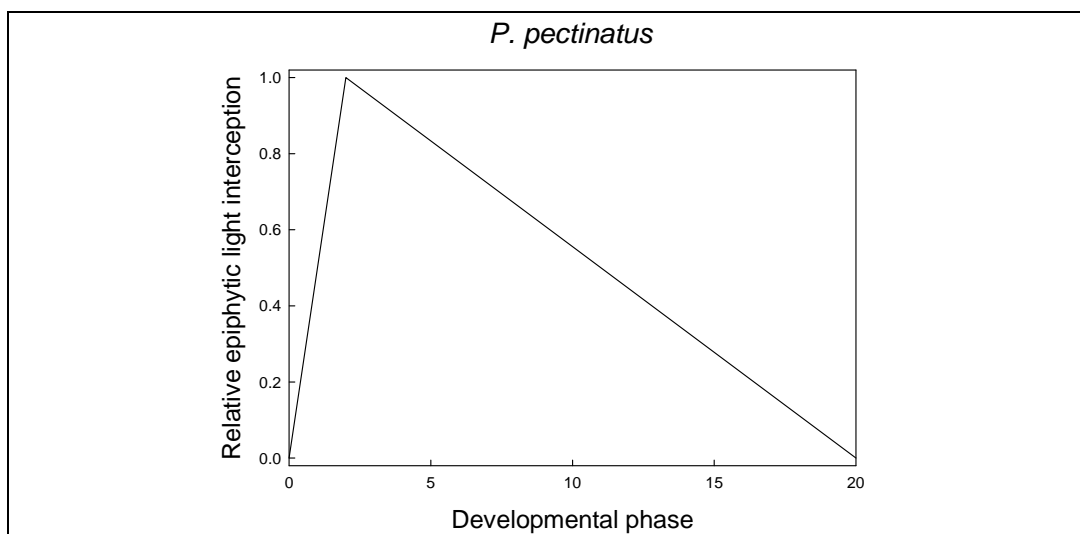


Figure 8. Relationship between development phase and relative epiphytic light interception used for calibration of POTAM, HYDRIL, and MILFO.

For photosynthetic activity at light saturation ( $AMX$ ) in POTAM, the value of  $0.019 \text{ g CO}_2 \text{ g}^{-1} \text{ DW h}^{-1}$  was used, measured in *P. pectinatus* shoot apices in May in the shallow, fresh, River Susa, Denmark (Van der Bijl et al. 1989;  $AMX$ ). Other, lower,  $AMX$  values of  $0.0099$  and  $0.012 \text{ g CO}_2 \text{ g DW}^{-1} \text{ h}^{-1}$  were determined under laboratory conditions (Hootsmans and Vermaat 1994; Hootsmans 1994; Madsen and Adams 1988). Light- and carbon-saturated photosynthetic rates of *P. pectinatus* can be far higher (Best and Boyd 2003c), suggesting that photosynthetic activity in waters with low DIC concentrations ( $<3.5 \text{ mmol L}^{-1}$ ) or high pH ( $>8$ ) can be carbon-limited. For photosynthetic light-use efficiency ( $EE$ ) in POTAM, the same value as for VALLA was used.  $REDFT$  and  $REDAM$  have been modeled as in VALLA. In POTAM, the effect of daytime temperature on  $AMX$  is accounted for via a fitted, relative function,  $AMTMPT$ , which is based on the measured photosynthetic response of *P. pectinatus* to temperature and has its optimum at  $30.0 \text{ }^\circ\text{C}$  (Best and Boyd 2003c).

The relationship between photosynthesis and current velocity in POTAM is derived from measured typical plant photosynthesis at low current velocity (Best and Boyd 2003c), and biomass production in the shallow Canadian rivers at high current velocity (Chambers et al. 1991).  $AMX$  is multiplied by the relative photosynthetic rate ( $REDAMI$ ), which ranges between 1 at a current velocity of  $7 \text{ cm s}^{-1}$  and 0 at a current velocity of  $94 \text{ cm s}^{-1}$  (Figure 9).

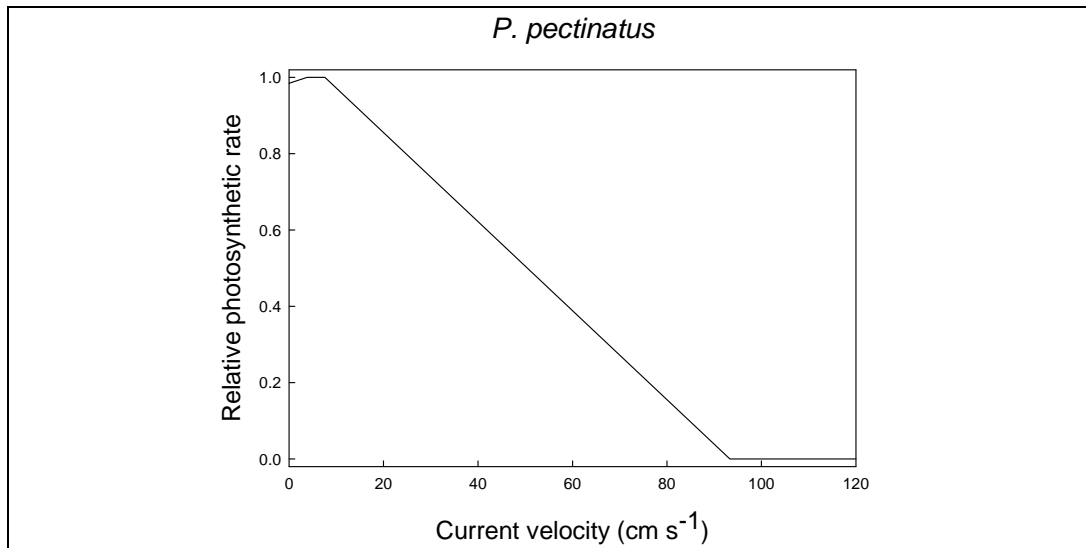


Figure 9. Relationship between current velocity and relative photosynthetic rate used for calibration of POTAM, HYDRIL, and MILFO.

In POTAM, assimilates are partitioned typically over the plant parts, with 73.1 percent as leaves, 18.3 percent as stems and 8.6 percent as roots (Best and Boyd 2003c; Sher-Kaul et al. 1995). Vertical distribution of shoot biomass is governed by a dry matter partitioning coefficient function (*DMPC*) following the typical canopy type shape. Distribution proceeds as follows. First plant biomass is distributed for 4.4 percent over the upper depth layer 1, for 4.3 percent over layer 2, for 23.1 percent over layer 3, for 25.4 percent over layer 4, and for 21.3 percent over layer 5 (78.4 percent of total plant biomass; Best and Boyd 2003c). Subsequently, the remaining shoot biomass is distributed equally over the depth layers below this 0.5 m up to a total share of 13 percent. When the biomass in a layer is lower than the critical biomass, the total number of layers is reduced by one and the distribution procedure is redone. When five depth layers or less are present, first the upper layers are filled according to the typical distribution pattern, and subsequently the remaining shoot biomass is added by equal distribution over the found layers. Vertical biomass distribution pattern is recalculated and redistributed by POTAM when a rooting depth other than nominal (1.3 m) is chosen by the user. In POTAM, roots always contribute 8.6 percent to total plant biomass.

*H. verticillata*. HYDRIL is calibrated using field data on biomass and water transparency (*L*) from Lake Orange, FL, 1977 (Bowes et al. 1979) and climatological data from Gainesville, FL, 1980. For the plant community-specific light extinction coefficient (*K*) in HYDRIL, the value of 0.01 m<sup>2</sup> g<sup>-1</sup> DW, measured in the canopy of a *H. verticillata* community in Lake

Trafford, FL, was used (Bowes et al. 1979). The same value was reported for a *H. verticillata* Caspary community in Lake Biwa, Japan (Ikusima 1970).

The reduction in light interception by the plant through epiphyte shading, and the relationship between photosynthesis and current velocity have been modeled as in POTAM based on calibration data pertaining to VALLA because calibration data on *H. verticillata* were lacking. Once pertinent calibration data are available, these can be inserted in the model input file.

For photosynthetic activity at light saturation (*AMX*) in HYDRIL, the value of 0.0158 g CO<sub>2</sub> g<sup>-1</sup> DW h<sup>-1</sup> was used, measured in shoot apices in Lake Orange, FL, in May (Bowes et al. 1979; Van et al. 1978a). Light- and carbon-saturated photosynthetic rates can be far higher (Van et al. 1976), suggesting that photosynthetic activity in waters with low DIC concentrations (<3.5 mmol L<sup>-1</sup>) or high pH (>8) can be carbon limited. For photosynthetic light-use efficiency (*EE*) in HYDRIL, the same value as for VALLA was used.

*REDFT* has been modeled as in VALLA. In HYDRIL, a reduction factor, *REDAM*, can be used to take effects of daily changes in pH and oxygen concentration into account by reducing the *AMX* by a factor between 0 and 1 for the whole day. Daily changes in pH and oxygen concentrations affect *AMX* in *H. verticillata* significantly. *REDAM* currently has the value of 0.581 because changes in pH in the SAV in Florida lakes inhibited photosynthesis by a factor of 0.83 and changes in O<sub>2</sub> concentration by a factor of 0.7 (Van et al. 1976; Bowes et al. 1979). In HYDRIL, the effect of daytime temperature on *AMX* is accounted for via a fitted, relative function, *AMTMPT*, which is based on the measured photosynthetic response of *H. verticillata* to temperature and has its optimum at 24.0 °C (Barko and Smart 1981). A higher optimum of 36.5 °C, found by W.T. Haller, IFAS, Gainesville, FL (unpublished results 1984) and by Van et al. (1976), generated unrealistically high biomass in simulations, and was, therefore, not used for model calibration.

In HYDRIL, assimilates are partitioned typically over the plant parts, with 34 percent as leaves, 60 percent as stems, and 6 percent as roots (Haller and Sutton 1975; Van et al. 1978b; Van der Zwerde 1981). Vertical distribution of shoot biomass is governed by a dry matter partitioning

coefficient function (*DMPC*) following the typical canopy type shape. Distribution proceeds as follows. First, plant biomass is distributed for 21 percent over the two upper depth layers 1 and 2, for 10 percent over the two successive layers 3 and 4, and for 9 percent over the two successive layers 5 and 6 (80 percent of total plant biomass; Ambasht and Ram 1976; Bowes et al. 1979). Subsequently, the remaining shoot biomass is allocated equally to the depth layers below this 0.6 m up to a total share of 14 percent. Vertical biomass distribution pattern is recalculated and redistributed by HYDRIL when a rooting depth other than nominal (1.0 m) is chosen by the user. In HYDRIL, roots always contribute 6 percent to total plant biomass.

*M. spicatum*. MILFO is calibrated as follows: (1) For a SAV in a temperate climate, using field data on biomass (Adams and McCracken 1974), water transparency (*L*), temperature and irradiance from Lake Wingra, WI, 1970 (Lee and Kluesener 1972); (2) For a SAV in a tropical climate, using field data on biomass from Kashmir lakes, India (Zutschi and Vass 1973) and climatological data from Patancheru, India, 1978. For the plant community-specific light extinction coefficient (*K*) in MILFO, the value of 0.006 m<sup>2</sup> g<sup>-1</sup> DW, measured in the canopy of a SAV in Lake Wingra, WI, was used (Titus and Adams 1979a). Another, higher, extinction coefficient of 0.01 m<sup>2</sup> g<sup>-1</sup> DW has been published by Ikusima (1970).

The reduction in light interception by the plant through epiphyte shading, and the relationship between photosynthesis and current velocity have been modeled as in POTAM based on calibration data pertaining to POTAM because calibration data on *M. spicatum* were lacking. Once pertinent calibration data are available, these can be inserted in the model input file.

For photosynthetic activity at light saturation (*AMX*) in MILFO, the value of 0.0165 g CO<sub>2</sub> g<sup>-1</sup> DW h<sup>-1</sup> was used, measured in *M. spicatum* in Lake Wingra, WI, in May (Adams and McCracken 1974; pH 8 and a total alkalinity of 190 mg L<sup>-1</sup>; *AMX*). For photosynthetic light-use efficiency (*EE*) in POTAM, the same value as for VALLA was used. *REDFT* has been modeled as in VALLA. Daily changes in pH and oxygen concentrations may affect *AMX*. A reduction factor, *REDAM*, can be used to take effects of daily changes in pH and oxygen concentration into account by reducing the *AMX* by a factor between 0 and 1. In MILFO, actual photosynthesis is reduced by 50 percent compared to *AMX* at pH 8.8 found in *M. spicatum*

SAV in Lake Wingra (Titus and Stone 1982; Adams and McCracken 1974), and, therefore, *REDAM* currently has the value of 0.5. *AMX* in this species is negligibly affected by changes in oxygen concentration (Van et al. 1976). In MILFO, the effect of daytime temperature on *AMX* is accounted for via a fitted, relative function, *AMTMPT*, which is based on the measured photosynthetic response of *M. spicatum* to temperature and has its optimum at 35.0 °C (Titus and Adams 1979a; confirmed by Stanley and Nailor 1972).

In MILFO, assimilates are partitioned typically over the plant parts, with 47 percent as leaves, 47 percent as stems and 6 percent as roots (Adams et al. 1974). Vertical distribution of shoot biomass is governed by a dry matter partitioning coefficient function (*DMPC*) following the typical canopy type shape. Distribution proceeds as follows. First, plant biomass is distributed for 10 percent over the upper depth layer 1, for 16 percent over layer 2, for 17 percent over layer 3, for 10 percent over layer 4, and for 8 percent over layer 5 (61 percent of total plant biomass; Adams et al. 1974). Shoot biomass distribution over the lower water layers is equal up to a total biomass share of 5 percent. The remaining shoot biomass of 34 percent is distributed equally over all layers. Vertical biomass distribution pattern is recalculated and redistributed by MILFO when a rooting depth other than nominal (1.5 m) is chosen by the user. In MILFO, roots always contribute 6 percent to total plant biomass.

*Flowering, translocation, senescence, and formation of wintering organs*

*V. americana*. Flowering starts late in June (Titus and Stephens 1983).

Translocation has not been measured directly in SAV. In *V. americana* translocation products end up largely in tubers, and, thus, in VALLA translocation rate is based on relative tuber growth rate (see below). A translocation rate of 24.7 percent of net photosynthesis generated realistic biomass production in simulations and was used for calibration. The total transport “cost” of downward translocation was estimated at a factor of 1.05 ( $10/9 \times 36/38$ ; CVT) because transport of glucose costs dry matter (decrease by a factor of 36/38), whereas conversion of starch into glucose increases it (by a factor of 10/9). Translocation estimates in other plant species range from 19 percent of net production in seagrasses (Wetzel and Neckles 1996), 29 percent in cassava (Gijzen 1985) to 35 percent in certain potato varieties (Kooman 1995).

Senescence rates of SAV have not been published. The value for the relative death rate in VALLA was determined using the same approach as followed for the tuber death rate. Thus, a relative death rate (RDRT, RDST) of  $0.021 \text{ d}^{-1}$  was calculated for the SAV in Chenango Lake, NY (Titus and Stephens 1983).

In VALLA, tubers are formed after flowering, under short day conditions (<14.7 h) and within a temperature range between  $5 \text{ }^{\circ}\text{C}$  and  $25 \text{ }^{\circ}\text{C}$ , based on field data from Titus and Stephens (1983) and Donnermeyer (1982). The intensity of translocation is governed by the actual relative tuber growth rate, RTRL, consuming 24.7 percent of net production and corrected for the total transport “cost” CVT and temperature. In VALLA, the maximum relative tuber growth rate (RTR) was determined by applying the same differential equation as commonly used for simple exponential growth (Thornley and Johnson 1990b; Hunt 1982) to tuber data collected in the field (Titus and Stephens 1983). Thus, a RTR of  $0.247 \text{ d}^{-1}$  at a reference temperature of  $20 \text{ }^{\circ}\text{C}$  was computed. Tubers grow until the preselected critical weight of the new tuber class (TWCTUB) is reached. The value of TWCTUB is calculated by multiplication of the individual tuber weight with the concomitantly initiated tuber number and plant density ( $5.5 \times 0.09 \times 30$ ).

*P. pectinatus*. Flowering starts in mid-July (Best and Boyd 2003c).

Translocation rate in POTAM could not be based on tuber growth rate because the availability of tuber growth data was insufficient. A translocation rate of 19 percent of net photosynthesis, typical for the related seagrasses (Wetzel and Neckles 1996), generated realistic biomass production in simulations and was used for calibration. The total transport “cost” of downward translocation was estimated at a factor of 1.05 (CVT).

The value for the relative death rate in POTAM was determined using the same approach as followed for the tuber death rate. Thus, a relative death rate (RDRT, RDST) of  $0.047 \text{ d}^{-1}$  was calculated for the SAV in the Western Canal near Zandvoort, NL (Best and Boyd 2003c).

In POTAM, tubers are formed after flowering under short-day conditions (<16 h) and within a temperature range between  $5 \text{ }^{\circ}\text{C}$  and  $25 \text{ }^{\circ}\text{C}$  (Spencer and Anderson 1987; Van Wijk 1988). In POTAM, the maximum relative tuber growth rate (RTR) at was set equal to the translocation rate at

0.19 d<sup>-1</sup> at a reference temperature of 20 °C. Tubers grow until the pre-selected critical weight of the new tuber class (TWCTUB) is reached. TWCTUB is calculated by multiplication of the individual tuber weight with the concomitantly initiated tuber number, and plant density ( $8 \times 0.083 \times 30$ ).

*H. verticillata*. Flowering starts at the end of May (Haller et al. 1976).

Translocation rate in HYDRIL could not be based on tuber growth rate because the availability of tuber growth data was insufficient. A translocation rate of 40 percent of net production, slightly higher than measured in potato (Kooman 1995), generated realistic biomass production in HYDRIL and was used for calibration. In this case, only the dry matter cost of glucose transport of glucose was included in the model, i.e., a factor of 1.1 (CVT).

The value for the relative death rate in HYDRIL was determined using the same approach as followed for the tuber death rate. A relative death rate (RDRT, RDST) of 0.033 d<sup>-1</sup> was calculated for the SAV in Lake Orange, FL (Bowes et al. 1979).

In HYDRIL, tubers are formed after flowering under short-day conditions (>10 h and <16 h) and within a temperature range between 14 °C and 33 °C (Van et al. 1978b). In HYDRIL, the maximum relative tuber growth rate (RTR) at was set equal to the translocation rate at 0.40 d<sup>-1</sup> at a reference temperature of 20 °C. Tubers grow until the preselected critical weight of the new tuber class (TWCTUB) is reached. TWCTUB is calculated by multiplication of the individual tuber weight with the concomitantly initiated tuber number and plant density ( $7 \times 0.1 \times 35$ ).

*M. spicatum*. Flowering starts in the first half of June in temperate conditions (Adams and McCracken 1974), and may last the whole growth season in the tropics (Zutschi and Vass 1973).

Translocation rate (TRAFAC) in MILFO could not be based on rhizome/root crown growth rate because the availability of growth data was insufficient. A translocation rate of 35 percent of net production, equal to that measured in potato (Kooman 1995), generated realistic biomass production in MILFO and was used for calibration. Costs of glucose transport and conversion of starch into glucose (CVT) have been modeled as in VALLA.

In MILFO, the value for the relative death rate was determined using the same approach as followed for the death rates of other modeled SAV. A relative death rate (RDRT, RDST) of  $0.042 \text{ d}^{-1}$  was determined for the SAV in Lake Wingra, WI (Adams and McCracken 1974).

## 4 Simulations

### VALLA

#### **VALLA calibration: Simulated and measured behavior of a *V. americana* community in Chenango Lake, NY**

The seasonal changes in biomass of plants and tubers, as simulated by VALLA, are shown in Figure 10. Simulated plant biomass compared well with average plant biomass measured in Chenango Lake, NY (Titus and Stephens 1983). Plant biomass reached its maximum at the same time, and peak biomass was somewhat higher in the simulated than in the measured SAV, notably 56.1 versus 50.1 g DW m<sup>-2</sup>. The latter may be due to the relatively large tuber size /concurrently initiated tuber number combination (0.09 g DW tuber<sup>-1</sup>, 5.5 tubers plant<sup>-1</sup>) used to initiate this nominal run. Measured tuber size was 0.055 g DW tuber<sup>-1</sup>, and another model run starting with the measured tuber size generated a peak biomass of 48 g DW m<sup>-2</sup> (see also Figure 12). Simulated transport of carbohydrates was substantial in the beginning of the growth season when upward carbohydrate remobilization from the tubers supports initial sprouting, but far higher after flowering when downward carbohydrate translocation from plant organs supports the filling of the tubers. Carbohydrate transport could be in the same range as net assimilation at the beginning and end of the growth season. Maintenance respiration was usually considerably lower than assimilation but could be in the same range of translocation just after flowering (data not shown).

Running VALLA with (24-h average) air temperatures with a lag-period of 1 day instead of with measured water temperatures as forcing variables yielded higher assimilation (Figure 11) and plant biomass values than found in the nominal case. This difference was attributed to the fact that water temperatures in the lake were relatively low compared to air temperatures because of the large inflow of groundwater (Titus and Stephens 1983). In the authors' experience, a lag period of 7 days between model daily air and measured temperatures usually describes this relationship well for shallow, up to 5- or 6-m deep water bodies with a relatively small inflow of groundwater.

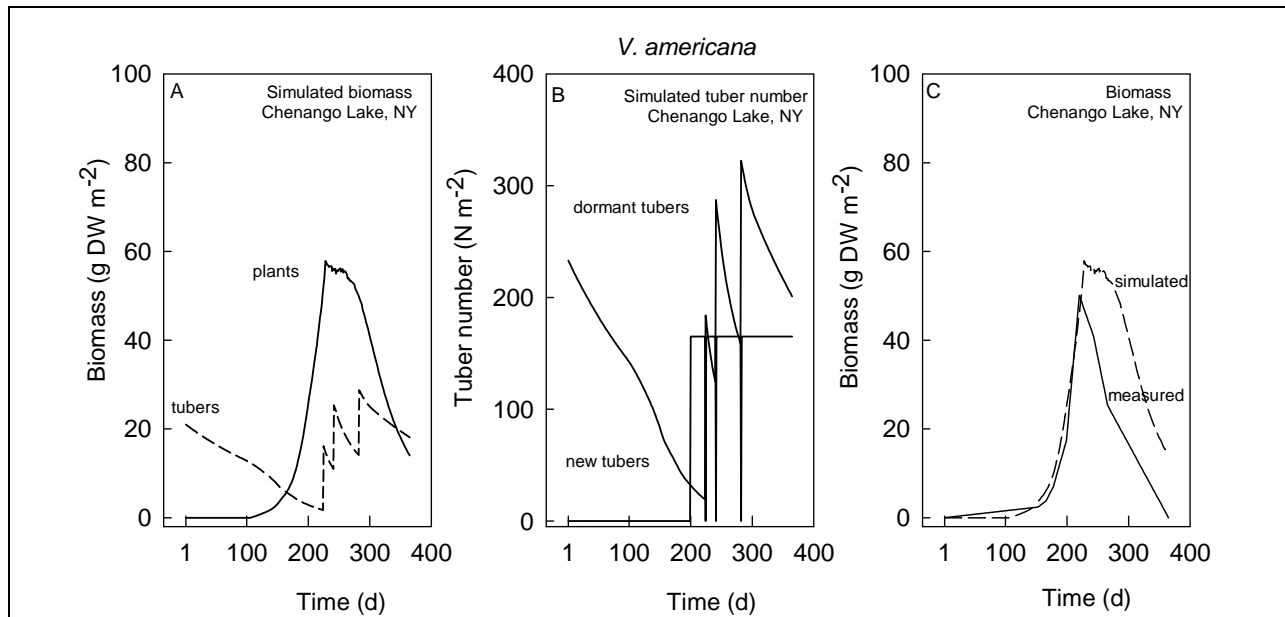


Figure 10. Simulated biomass of plants (A), dormant and new tuber numbers (B), and measured plant biomass (C) of *V. americana* in Chenango Lake, NY. Nominal run. Field data 1987 from Titus and Stephens (1983); climatological data 1987, Binghamton, NY (lat 42° 15' N, long 75° 50' W); water depth 1.4 m; light extinction coefficient 0.43 m<sup>-1</sup>.

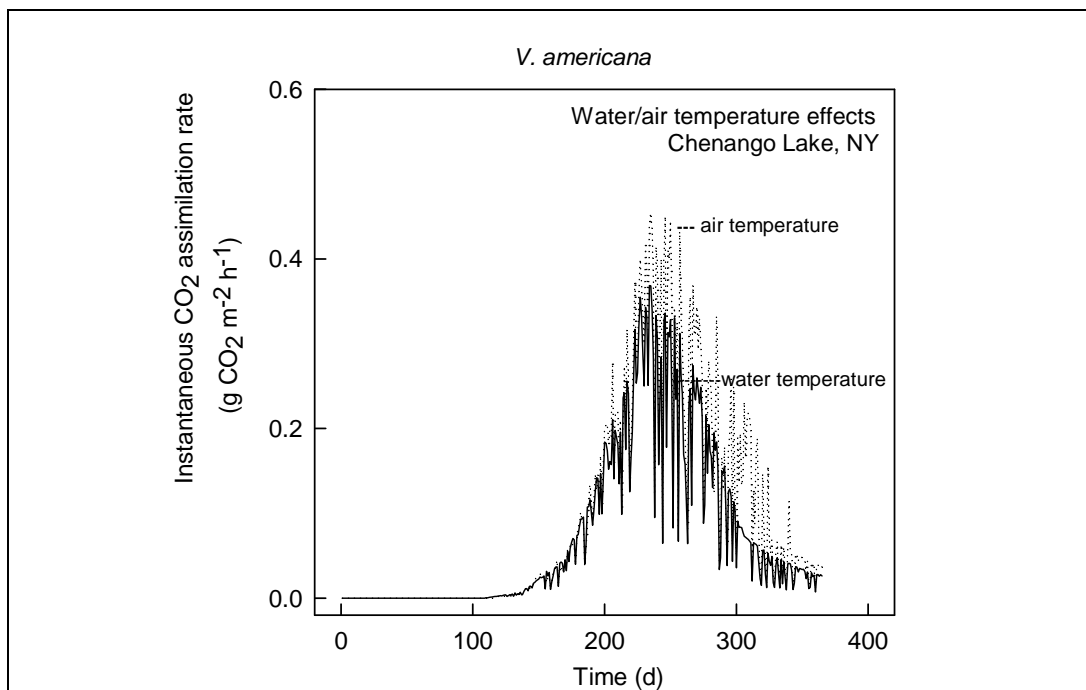


Figure 11. Simulated photosynthetic rates of *V. americana* in Chenango Lake, NY, with water or air temperatures as input (initial plant parameter values as in nominal run).

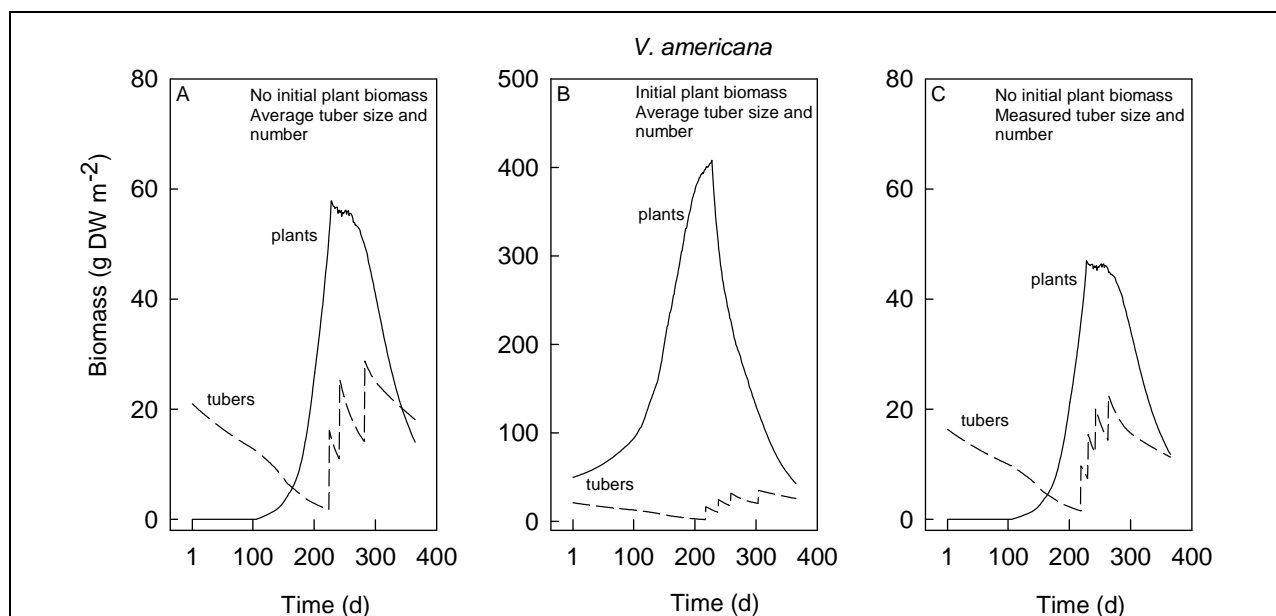


Figure 12. Simulated biomass of plants and tubers of *V. americana* in Chenango Lake, NY, started from different initial biomass, but run in the same environmental and climatological, nominal, conditions. (A) Plant biomass 0; tuber size 0.09 g DW; tuber bank 233 m<sup>-2</sup>; (B) Plant biomass 50 g DW m<sup>-2</sup>; tuber size 0.09 g DW; tuber bank density 233 m<sup>-2</sup>; (C) Plant biomass 0; tuber size 0.055 g DW; tuber bank density 233 m<sup>-2</sup>.

Running VALLA for the same lake and year, but with both plants and tubers initially present, showed that peak plant biomass was then far higher and more tuber classes were finished (4 instead of 3 in the nominal case; Figure 12). This large difference in peak biomass is due to the ability of the plant community to fully capture the high spring irradiance at this latitude of 43° N, which they can not without wintering shoots. Thus, wintering shoots would provide a distinct advantage for this plant species. However, wintering shoots have only been reported to occur in a tropical climate. A simulation started from the measured tuber size/chosen concurrently initiated tuber number combination yielded peak plant biomass that was almost equal in simulated and measured plant community (Figure 12C; Figure 10), and the simulated tuber numbers were within the range found in a *V. americana* community in the same lake (Titus and Stephens 1983).

#### VALLA validation: Simulated and measured behavior of a *V. americana* community at other latitudes

To explore whether VALLA could be used to simulate behavior of a *V. americana* community at other sites besides the nominal one, runs were made for one more western site, Lake Mendota, WI, and another, tropical more southern site, ponds at Fort Lauderdale, FL.

A simulation was performed of SAV in Lake Mendota, WI, starting from site-specific community, water depth, transparency, and climatological data. Plant community-specific data included the following: initial plant biomass absent, tuber size 0.03 g DW, concurrently initiated tuber number 1.5 plant<sup>-1</sup>, and tuber bank density 233 m<sup>-2</sup>. Site-specific environmental data included the following: water depth 1.2 m and light extinction coefficient 0.7 m<sup>-1</sup>. In these conditions simulated plant biomass remained low, maximally 25 g DW m<sup>-2</sup>, and no tuber classes were finished. Because the simulated maximum plant biomass was far lower than published (average peak biomass 344, and minimum 266 g DW m<sup>-2</sup>; Titus and Adams 1979a), and *V. americana* populations in Lake Mendota have been described as stable, several other simulations were done to explore community- and site-specific characteristics favoring such a sustainable population. Increasing the tuber size from 0.03 to 0.09 g DW increased peak biomass from 25 to 105 g DW m<sup>-2</sup> and the number of finished tuber classes to 5. Increasing water transparency by decreasing the light extinction coefficient from 0.7 to 0.4 m<sup>-1</sup> increased peak biomass from 25 to 130 g DW m<sup>-2</sup> and the number of finished tuber classes to 7. Introduction of the largest tuber size published, 0.11 g DW, increased peak biomass to 150 g DW m<sup>-2</sup> but allowed only 5 tuber classes to be finished. Even in very clear water (extinction coefficient 0.4 m<sup>-1</sup>), a very shallow, 0.2-m water depth, and with the most profitable tuber size, the SAV would only be able to produce maximally 195 g DW m<sup>-2</sup> in Lake Mendota (Figure 13B). The latter result led the authors to believe that the high plant biomass range of 266 to 344 g DW m<sup>-2</sup> published (Titus and Adams 1979a) is either an overestimate, or that spring growth starts partly from wintering shoots.

A simulation was performed of a *V. americana* community in earthen ponds near Fort Lauderdale, FL, starting from site-specific community, water depth, transparency, and climatological data. Plant community-specific data included the following: initial plant biomass 50 g DW m<sup>-2</sup>, tuber size 0.09 g DW, concurrently initiated tuber number 5.5 plant<sup>-1</sup>, tuber bank density 233 m<sup>-2</sup>. Site-specific environmental data included the following: water depth 1.5 m and light extinction coefficient 0.4 m<sup>-1</sup>. In these conditions, simulated plant biomass was high, maximally 403 g DW m<sup>-2</sup>, and three tuber classes were finished at the very end of the year. Tuber weights and numbers of the Fort Lauderdale community were not published, so comparison between simulated and measured tuber data is not possible. Simulated maximum plant biomass in this case was within the measured peak biomass range of 298 to 496 g DW m<sup>-2</sup> (Figure 13C).

Maximum plant biomass was enhanced to  $450 \text{ g DW m}^{-2}$  by decreasing the K value from  $0.0235$  to  $0.019 \text{ m}^2 \text{ g DW}^{-1}$ , and even surpassed the maximum measured value by decreasing the K value further to  $0.0051 \text{ m}^2 \text{ g DW}^{-1}$ .

Comparison of simulated biomass produced in the various climatological conditions (Figure 13) indicates that in a temperate climate generally less biomass is produced and investment in vegetative reproduction is relatively higher than in a tropical climate.

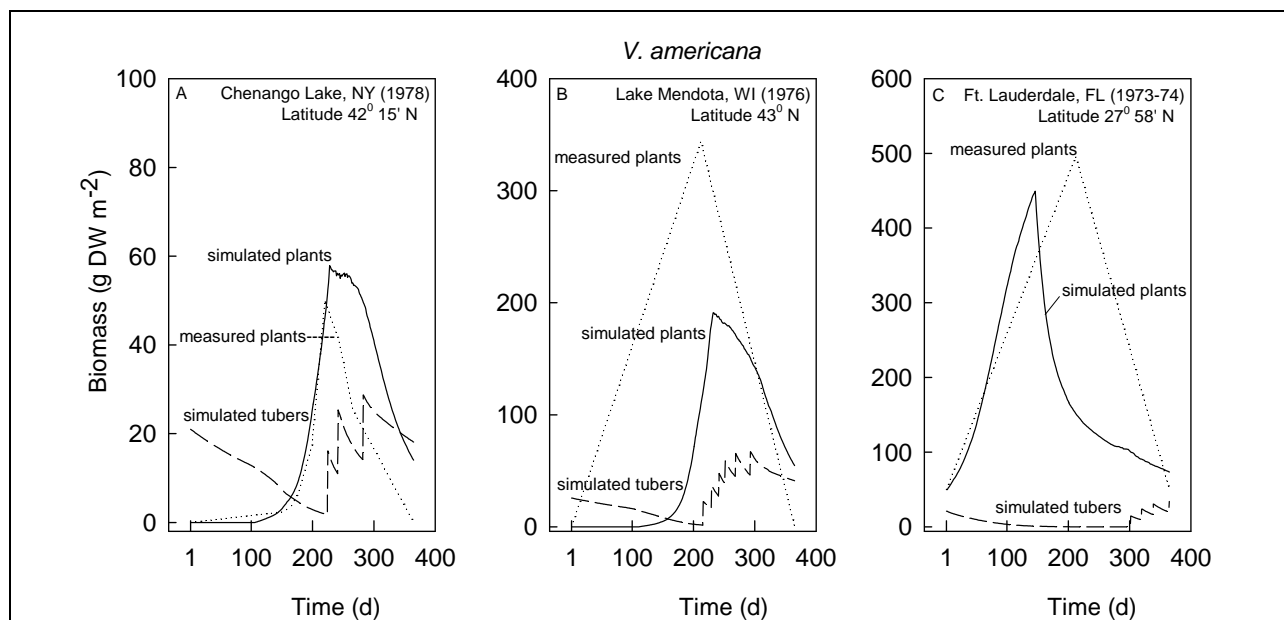


Figure 13. Simulated biomass of plants and tubers of *V. americana* at sites differing in latitude. (A) Chenango Lake, NY (lat  $42^{\circ} 15' \text{ N}$ , long  $75^{\circ} 50' \text{ W}$ ); tuber size  $0.09 \text{ g DW}$ , tuber bank density  $233 \text{ m}^{-2}$ ; water depth  $1.4 \text{ m}$ ; light extinction coefficient  $0.43 \text{ m}^{-1}$ ; climatological data 1987; measured data 1978, Titus and Stephens (1983). (B) Lake Mendota, WI (lat  $43^{\circ} 08' \text{ N}$ , long  $89^{\circ} 20' \text{ W}$ ); tuber size  $0.11 \text{ g DW}$ , tuber bank density  $233 \text{ m}^{-2}$ ; water depth  $0.2 \text{ m}$ ; light extinction coefficient  $0.4 \text{ m}^{-1}$ ; climatological data 1971-75; measured data 1976, Titus and Adams (1979a). (C) Fort Lauderdale ponds, FL (lat  $27^{\circ} 58' \text{ N}$ , long  $82^{\circ} 32' \text{ W}$ ); plant biomass  $50 \text{ g DW m}^{-2}$ ; tuber size  $0.09 \text{ g DW}$ , tuber bank density  $233 \text{ m}^{-2}$ ; K value  $0.018 \text{ m}^2 \text{ g}^{-1} \text{ DW}$ ; water depth  $1.5 \text{ m}$ ; light extinction coefficient  $0.4 \text{ m}^{-1}$ ; climatological data 1975-84; measured data 1973-74, Haller (1974).

### VALLA example applications

*Application 1: Historical and simulated behavior of a *V. americana* community in a riverine environment subject to flooding*

*V. americana* is an important riverine macrophyte that provides food and habitat resources for waterfowl, fishes, and invertebrates in the Upper Mississippi River (UMR), WI. Navigation pools along the Mississippi Flyway have historically been used by migrating waterfowl as staging areas in

part because of abundant populations of *V. americana* (Bellrose et al. 1983; Korschgen and Green 1988). Recent declines in these populations have caused concern and have been attributed to eutrophication, competition by other macrophytes such as *M. spicatum* L. and *Nelumbo lutea* Willd., drought, and flooding. It is desirable to improve management programs aimed at enhancing *V. americana* populations, but these programs require an improved understanding of the population dynamics of the latter and factors affecting these. Detailed biomass dynamics of *V. americana* have been recorded in the early 1980s, when populations were still substantial (Pool 9; Donnermeyer 1982). Subsequently, populations have been included in regular surveys of several navigation pools, but only by species presence or absence, not characterized by plant and tuber biomass.

Simulations using VALLA were carried out to evaluate the effects of daily changes in water level during different hydrological years on a typical *V. americana* in Pool 8 of the UMR. Stage data collected at the dam of Pool 8 were used to document water level fluctuations over a 10-year period, i.e. from 1985 to 1994. In this period, 1985 is considered as a normal hydrological year, 1986 as a normal flood year with floods in spring and autumn, 1993 as an abnormal flood year with one flood in summer, and 1986 as a drought year (Figure 14). Disappearance of large portions of *V. americana* populations in 1993 and 1988 have been reported (Rogers 1994; Spink and Rogers 1996). The simulations were done starting from a nominal SAV, site-specific environmental data, and site- and year-specific climatological data. Site-specific environmental data included the following: water depth daily varying as would be experienced by a community at 0.5-m rooting depth; light extinction coefficient ranging from 2.619 to 3.173  $\text{m}^{-1}$  during the period of May to October, and set to 2.0  $\text{m}^{-1}$  the rest of the year (converted via Giesens relationship from Secchi disk readings, cf Giesen et al. (1990), correlated with 10-year data on total suspended solids concentrations). Historical data indicate that in 1980 plant biomass peaked in mid-August at 217  $\text{g DW m}^{-2}$ , and that tuber biomass was low (maximally 14-16  $\text{g DW m}^{-2}$ ; Donnermeyer 1982; Figure 15A).

Running VALLA with nominal initial plant biomass and tuber bank data at a constant 1.1-m water depth (annual average in the historical dataset) with a 10-year average climate, indicated that a peak biomass of only 60  $\text{g DW m}^{-2}$  was formed, but no tubers. Water fluctuations were substantial in

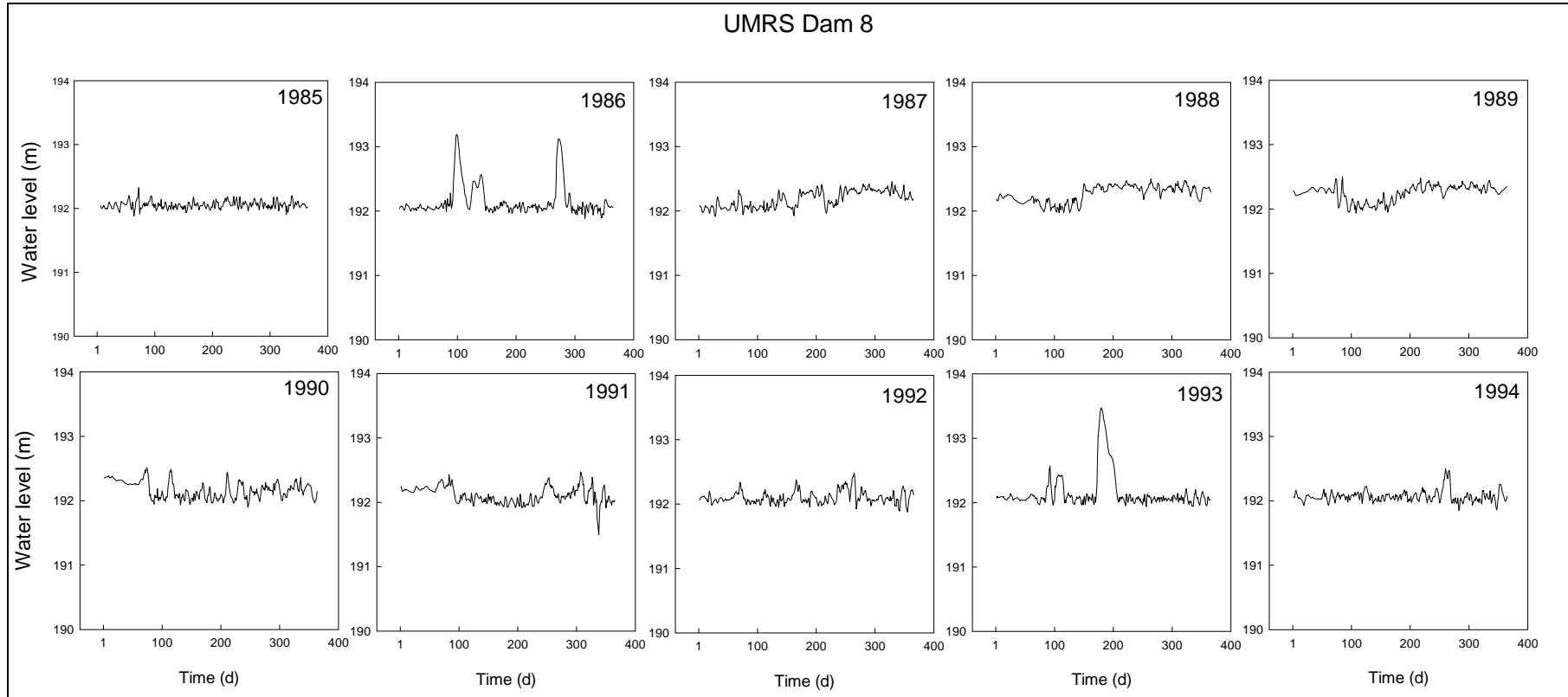


**Figure 14.** Water level fluctuations over a 10-year period measured at the dam of Pool 8 of the Upper Mississippi River, WI (long 91° 30' E, lat 43° 10' N); data J. H. Wlosinski, La Crosse, WI. Flat pool is considered to be the average summer (June, July, August) value during normal hydrological years over the 1985-94 period; abnormal hydrological years were 1986, 1988, and 1993.

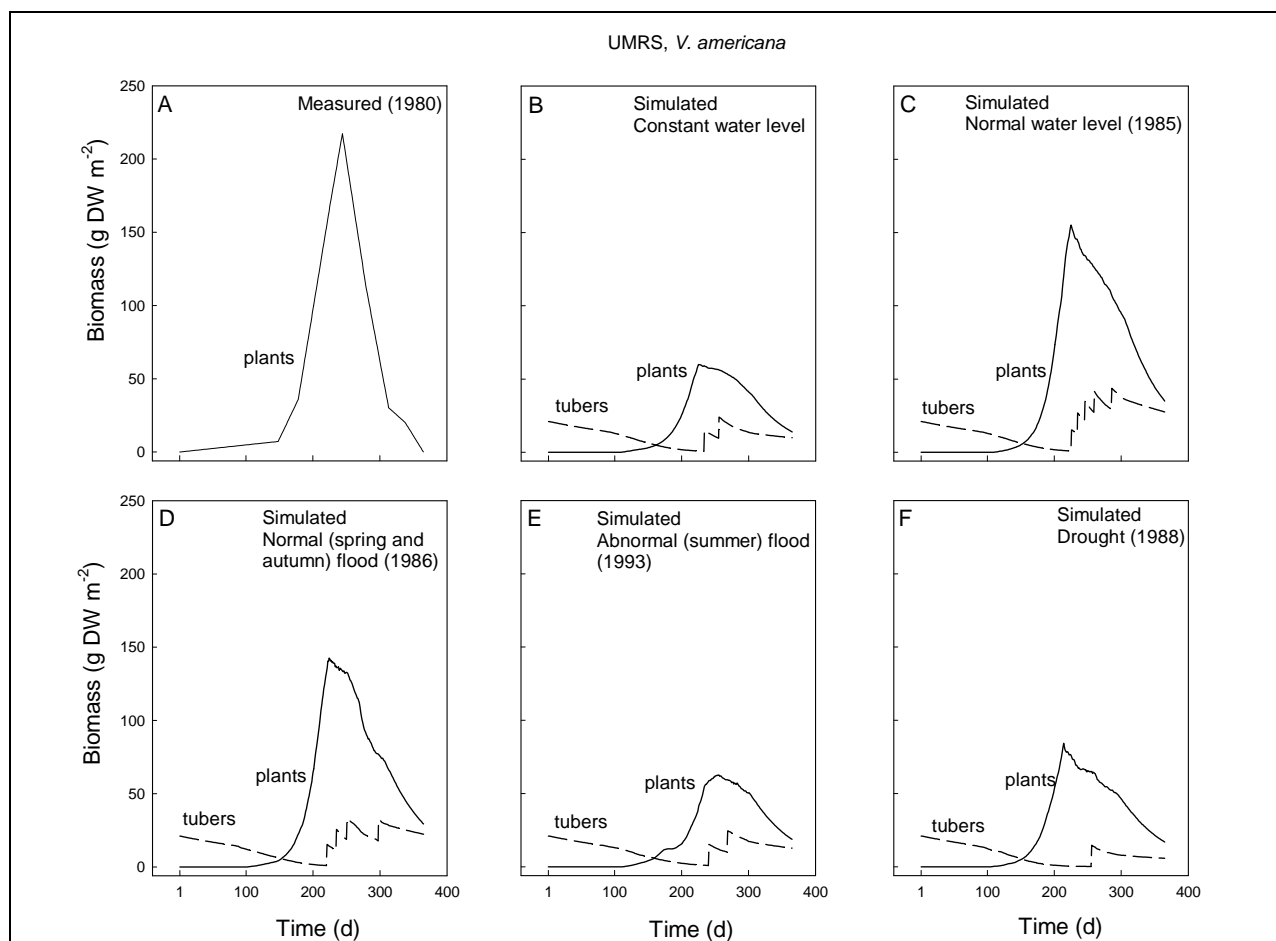


**Figure 15.** Comparison of historical and simulated data on biomass of plants and tubers of *V. americana* in the Upper Mississippi River System, WI. (A) Historical data: measured plant data Pool 9, 1980, average water depth 1.1 m (lat 43° 10' N, long 91° 30' W; Donnermeyer 1982). Simulations: Nominal initial biomass data; light extinction coefficients derived from 10-year average background total suspended solids values measured in the nearby Pool 4 in the 1980s (Bartell et al. 1999); climatological data, Minnesota/St. Paul, WI (long 93° W, lat 45° N). (B) Water level, annual average historical data set; climate, average 1985-94; (C) Water level, daily values 0.5 m depth class; climate 1985; (D) Water level, daily values 0.5 m depth class; climate, 1986; (E) Water level: daily values 0.5-m depth class; climate 1993; (F) Water level, daily values 0.5-m depth class; climate, 1986.

1980, and it was, therefore, concluded that calculation of the annual average water depth from Pool 9 historical data might have yielded an erroneous, probably too high, average depth and, therefore, the simulated plant biomass was too low. The next simulation at a constant, shallower 0.5-m water depth indicated that in this case more biomass was produced and that two tuber classes were finished (Figure 15B). Surprisingly, far more biomass could be produced and five tuber classes were finished under a normal water level fluctuation regime in Pool 8 pointing to a tentative positive influence of relatively small water level fluctuations (Figure 15C). Normal flooding inhibited biomass and tuber production somewhat,

allowing only four tuber classes to be finished but the population to persist (Figure 15D). The relatively small size of this effect was attributed to the fortuitous timing of the high water levels that occurred only in spring and autumn, still allowing the plants to fully benefit from the high summer irradiance at normal water levels. Abnormal flooding, however, reduced the finished number of tuber classes by a factor of  $>2$  in the 0.5-m depth class (Figure 15 E), and completely prevented tuber formation in the 1-m depth class. The harshness of this effect was attributed to the fact that the plants could not fully benefit from the high summer irradiance due to the high summer water levels. The effect of the 1988 drought was most surprising and detrimental. In this year substantial plant biomass could be produced peaking relatively early in the growth season. However, tuber formation was severely inhibited because (1) water levels were kept relatively high later in summer, possibly as a water conservation measure, causing increased extinction of light within the water column, and (2) temperatures were relatively high causing increased respiration and senescence. The increased light extinction in the water column may even have been larger in situ than in the simulation because during droughts not only water levels may change but also extinction within the water column increases by stimulation of algal blooms. The seasonal changes in the light extinction coefficient were kept the same in all simulations.

*Application 2: Importance of current velocity and epiphyte cover for a V. americana community in a riverine environment*

VALLA was used to explore the habitat quality at a site in the UMR, Turtle Island (WI) for *V. americana*. This site is characterized by shallow water (depth of 0.2 m at the day of harvest), current velocities tolerable for SAV (ranging from 0.03 to 0.37 m s<sup>-1</sup>), and high turbidity in the plant growth season (light extinction coefficients ranging from 3.00 to 4.23 m<sup>-1</sup>). Results of a run performed for this site with a temperate climate in 2001 indicated that simulated shoot biomass at the day of harvest, without and with corrections for epiphyte shading effects, was within the range of the measured shoot biomass, but with corrections for current velocity and both epiphyte shading and current velocity it was below the measured range (Figure 16A). All simulated peak shoot biomass values were within the range of the measured values. Peak shoot biomass, without corrections for the effects of current velocity and epiphyte shading, was similar to mean shoot biomass measured at the day of harvest, but was about 30 days delayed in time. Peak biomass generated by runs corrected for current velocity effects was 50 percent lower, corrected for epiphyte shading

10 percent lower, and corrected for both effects 64 percent lower than peak biomass without corrections. Thus, simulated plant biomass was greatly decreased by onsite current velocity and epiphyte cover. Simulated end-of-year tuber number was always substantial, ranging from 80 to around 350 tubers  $m^{-2}$ . This indicates that the *V. americana* population would persist because the end-of-year tuber number was  $>1$ , and the tuber size was large enough to enable sprouts to become self-supporting in their carbon gain at shallow sites (0.5 m depth at relatively turbid water common in the UMR; Best et al. 2005).

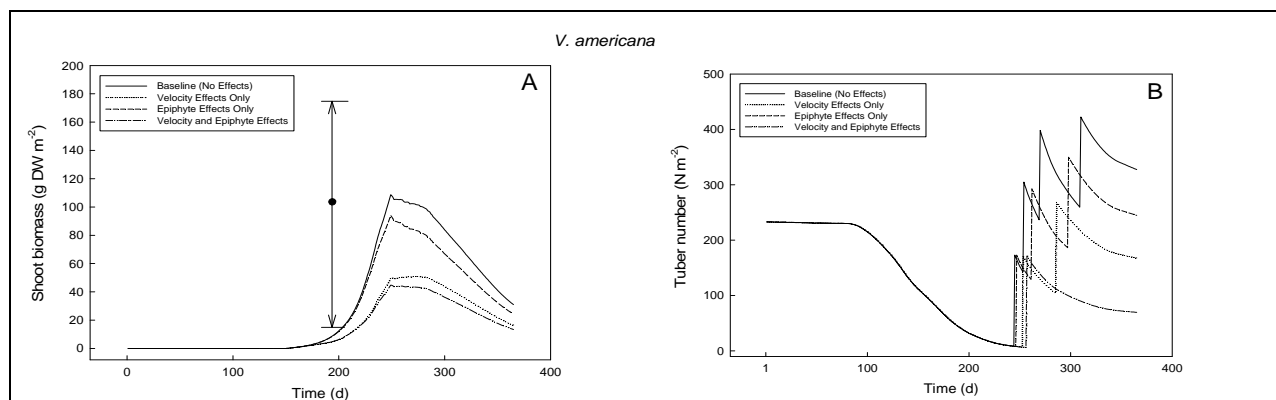


Figure 16. Simulated biomass of shoots (A) and tubers (B) of *V. americana* in Upper Mississippi River Pool 8 at Turtle Island (lat 43° 10' N, long 91° 30' W). Plant biomass 0; tuber size 0.09 g DW; tuber bank density 233  $m^{-2}$ ; site-specific field data on light extinction coefficient (3.00-4.23  $m^{-1}$ ), water temperature (5 °C -30.5 °C), current velocity (0.03-0.37  $m s^{-1}$ ), water depth (0.20 m), 2001; climatological data LaCrosse, WI, 2001 (long and lat as above); measured shoot biomass values are indicated by the mean (solid circle) and range (between arrows; Best et al. 2005).

## POTAM

### POTAM calibration: Simulated and measured behavior of a *P. pectinatus* community in the Western Canal near Zandvoort, NL

The seasonal changes in biomass of plants and tubers, as simulated by POTAM, are shown in Figure 17. Simulated plant biomass compared well with average plant biomass measured in the Western Canal near Zandvoort, NL (Best and Boyd 2003c). Plant biomass reached its maximum 13 days later, and peak biomass was somewhat higher in the simulated than in the measured SAV, notably 101.9 versus 78.5  $g DW m^{-2}$ . The higher simulated than measured biomass was attributed to the use of air temperatures for this nominal run instead of the measured water temperatures. Air temperatures with a lag-period of 7 days (default) were used because the temperature of the water surrounding the majority of the

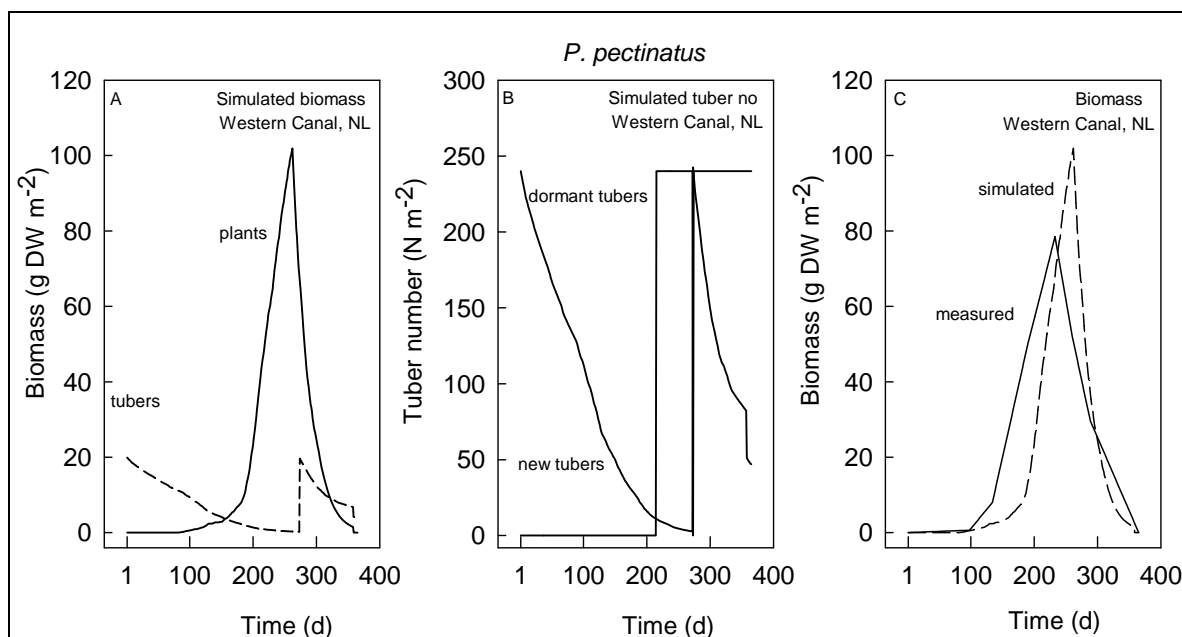


Figure 17. Simulated biomass of plants (A), dormant and new tuber numbers (B), and measured plant biomass (C) of *P. pectinatus* in the Western Canal near Zandvoort, NL. Nominal run. Field data 1987 from Best and Boyd (2003a); climatological data 1987, De Bilt, NL (lat 52° 06' N, long 05° 11' E); water depth 1.3 m; light extinction coefficient 1.07 m<sup>-1</sup>.

plant shoots in summer was closer to the temperature of the air than to the temperature of the water filling the canals via upward seepage. Another explanation may be that actual maximum plant biomass occurred at the end of August, as found for the 2.5-m depth class (Best and Boyd 2003c), but since biomass was measured only once a month the actual peak was missed.

Running POTAM for the same canal and year, but with both plants and tubers initially present, showed that peak plant biomass was greatly increased but no tuber class was finished. The large increase in peak biomass is due to the ability of the plant community to fully capture the high spring irradiance at this latitude (52° N), which they can not without wintering shoots. However, since maintenance respiration increased proportionally to plant biomass and light extinction due to self-shading was high, carbohydrate reserves invested in tubers were insufficient to finalize a large-sized tuber class and, consequently, such a plant population would become extinct the next year. Thus, wintering shoots would not provide a distinct advantage for this plant species in a temperate climate. A simulation started with initial plant biomass but from a smaller tuber size/concurrently initiated tuber number combination (a 0.07 g DW and 6 tubers per plant) yielded a far higher peak plant biomass and 50 percent reduced tuber

numbers (data not shown) compared to the values measured in the Western Canal (Best and Boyd 2003c).

**POTAM validation: Simulated and measured behavior of a *P. pectinatus* community in Lake Veluwe, NL, in two consecutive years with greatly different turbidities**

Lake Veluwe, located in the center of NL, is a man-made, shallow wind-exposed, eutrophic lake in which remnants of *P. pectinatus* populations remained at the end of the 1770s (Bick and Van Schaik 1980). The decline in SAV coverage area was attributed to increased turbidity due to eutrophication, and management strategies were sought to reverse this decline. Management, including regular flushing of the lake and a reduction in external phosphorus loading, resulted in a more transparent water column and a slow increase in the area colonized by *P. pectinatus*. Because this management scenario did not lead to a full recovery of the SAV, several studies have been undertaken to quantify the relationship between light availability within the water column and the production of plant biomass and tubers in this lake. Field data on plant and tuber biomass, and on local water transparency generated by the studies mentioned above have been used to validate the data simulated using POTAM (Van Dijk et al. 1992; Van Dijk and Achterberg 1992).

POTAM was run for two consecutive years greatly differing in turbidity, i.e., 1986 and 1987, using as initial values the measured tuber bank densities and predominant tuber sizes. Model results indicated that a higher plant biomass but lower tuber class number (four classes in 1986 versus seven classes in 1987) would be expected in 1986 than in 1987, with plant biomass and newly produced tuber densities similar to measured ones (Figure 18). The timing at which the simulated maxima in plant biomass and tuber density occurred coincided with the measured values in 1986, but were delayed in 1987 (Figure 18). This example illustrates that although intuitively it would be expected that a larger peak plant biomass would lead to a higher tuber density, it is possible that in reality less tubers are formed since the latter process does not only depend on plant biomass but also on the critical combination of day length and temperature.

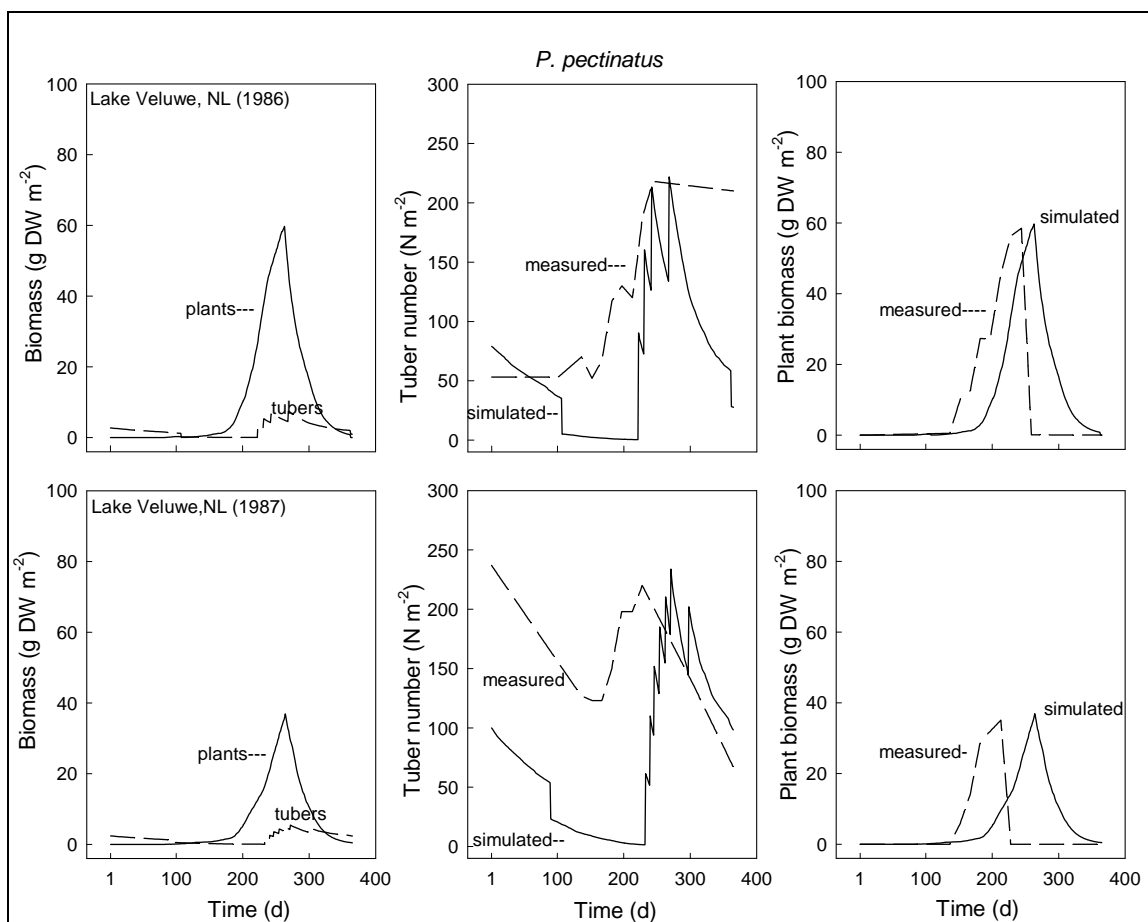


Figure 18. Simulated and measured biomass of *P. pectinatus* plants and tubers in Lake Veluwe, NL (lat 52° 17' N, long 05° 19' E), during two successive years differing in water transparency. Field data from Van Dijk et al. (1992); 1986, tuber size 0.034 g DW, tuber bank density 79 m<sup>-2</sup>, water depth 0.5 m; 1987, tuber size 0.024 g DW, tuber bank density 100 m<sup>-2</sup>, water depth 0.5 m. Light extinction coefficients: 1986, average May-September 2.58 m<sup>-1</sup>; 1987, average 4.30 m<sup>-1</sup> (Van Dijk and Achterberg 1992). Climatological data 1986, 1987, De Bilt, NL (lat 52° 06' N, long 05° 11' E).

### POTAM example application: Simulated and measured behavior of a *P. pectinatus* community at other latitudes

To investigate whether POTAM could be used to simulate the behavior of a *P. pectinatus* community at other sites besides the nominal one, runs were made for one more western site, the Byrne Canal, CA, and one more southern site, tropical Lake Ramgarh, India.

A simulation was performed of a *P. pectinatus* community in the Byrne Canal, CA, starting from site-specific community, water depth, transparency, and climatological data. For this site, plant community-specific data included the following: initial plant biomass absent, tuber size 0.025 g DW, concurrently initiated tuber number 3 plant<sup>-1</sup>, and tuber bank density

700 m<sup>-2</sup>. Environmental data included the following: water depth 0.2 m and light extinction coefficient 0.4 m<sup>-1</sup>. In these conditions simulated plant biomass showed a maximum of 130 g DW m<sup>-2</sup> using the nominal self-shading coefficient ( $K$ ) of 0.095 m<sup>2</sup> g DW<sup>-1</sup>, but a maximum close to the measured biomass of 175 g DW m<sup>-2</sup> at a lower self-shading coefficient of 0.0183 m<sup>2</sup> g DW<sup>-1</sup> (as reported by Sher-Kaul et al. 1995, for clear Lake Geneva, Switzerland). In both simulations many tuber classes were finished, giving rise to extremely high tuber densities - just as found in situ (Figure 19B; D. F. Spencer 1990, unpub. results). Another simulation was performed of a *P. pectinatus* community in Lake Ramgarh, India, starting from a nominal community, water depth, transparency, but climatological data pertaining to Patancheru, India. For this site, plant community-specific data included the following: no initial plant biomass, tuber size 0.083 g DW, concurrently initiated tuber number 8 plant<sup>-1</sup>, and a tuber bank density of 240 m<sup>-2</sup>. In these conditions simulated plant biomass was high, maximally 375 g DW m<sup>-2</sup>, and only two tuber classes were finished within a year. Tuber weights and numbers of the Lake Ramgarh SAV were not published, so comparison between simulated and measured tuber data is not possible. However, simulated maximum plant biomass in this case was in the same order of magnitude as the measured peak biomass of 445 g DW m<sup>-2</sup> (Figure 19C). Comparison of biomass production characteristics in the various climatological conditions (Figure 19) indicates that in a temperate climate generally less biomass is produced, but investment in vegetative reproduction is higher than in a tropical climate. The criteria for tuber formation, of (a) timed just after flowering, (b) day length between 12 and 16 hours, and (c) temperature between 5.5 °C and 25 °C, were met for long continuous periods in NL and CA, but only occasionally in India because the temperature usually exceeded the critical range. In NL, tubers could be initiated from day 215 to 250 at relatively moderate irradiance, allowing only one tuber class to be finished; in CA from day 161 to 250 at far higher irradiance giving rise to many tuber classes; in India from day 150 to 220 only two tuber classes might be finished. The extremely limited window for tuber formation in tropical regions was confirmed by Pilon (1999), who reported that the number of tubers formed per plant decreases from around 0 at a latitude of 25° N to 8 at 68° N, but predominant tuber size decreases from 0.022 to 0.006 g DW tuber<sup>-1</sup>. Although the latter characteristics were suggested at first to have a genetic basis, it was reported later that they may be environmentally regulated (Pilon and Santamaria 2002).

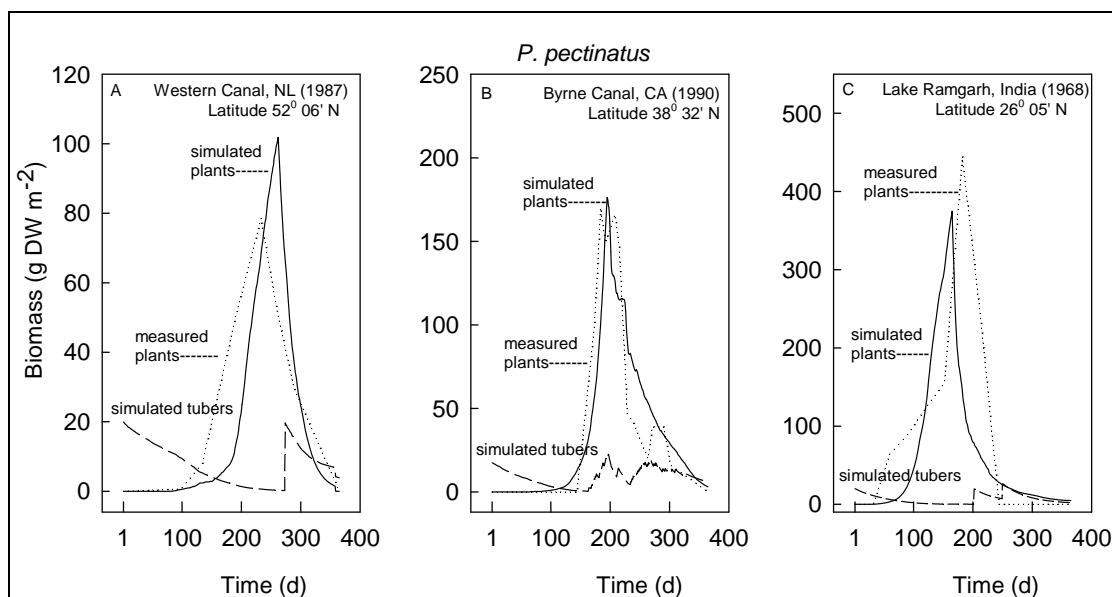


Figure 19. Simulated biomass of plants and tubers of *P. pectinatus* at sites differing in latitude. (A) The Western Canal near Zandvoort, NL (lat 52° 06' N, long 05° 11' E); tuber size 0.083 g DW, tuber bank density 240 m<sup>-2</sup>; water depth 1.3 m; light extinction coefficient 1.07 m<sup>-1</sup>; climatological data 1987; measured data 1987, Best and Boyd (2003a). (B) Byrne Canal, CA (lat 38° 32' N, long 121° 47' W); tuber size 0.025 g DW, tuber bank density 700 m<sup>-2</sup>; K value 0.0183 m<sup>2</sup> g DW<sup>-1</sup>; water depth 0.2 m; light extinction coefficient 0.4 m<sup>-1</sup>; climatological data 1990; measured data 1990, D. W. Spencer, USDA-ARS, Davis, CA, unpublished). (C) Lake Ramgarh, India (lat 26° 05' N, long 83° 26' E); tuber size 0.083 g DW, tuber bank density 240 m<sup>-2</sup>; K value 0.0183 m<sup>2</sup> g DW<sup>-1</sup>; water depth 1.3 m; light extinction coefficient 1.07 m<sup>-1</sup>; climatological data Patancheru, India, 1978 (lat 17° 27' N, long 78° 28' E); measured data 1968, Sahai and Sinha (1973).

## HYDRIL

### HYDRIL calibration: Simulated and measured behavior of the *H. verticillata* community in Lake Orange, FL

The seasonal changes in biomass of plants and tubers, as simulated by HYDRIL, are shown in Figure 20. Simulated plant biomass compared well with measured plant biomass found in the lake (Bowes et al. 1979). Plant biomass reached its maximum somewhat earlier in the simulated than in the measured SAV. The lower simulated than measured biomass was attributed to the rather low frequency of field observations (no measurements between September and November). Simulated tuber number was well within the tuber number range of approximately 500 m<sup>-2</sup> found in the lake.

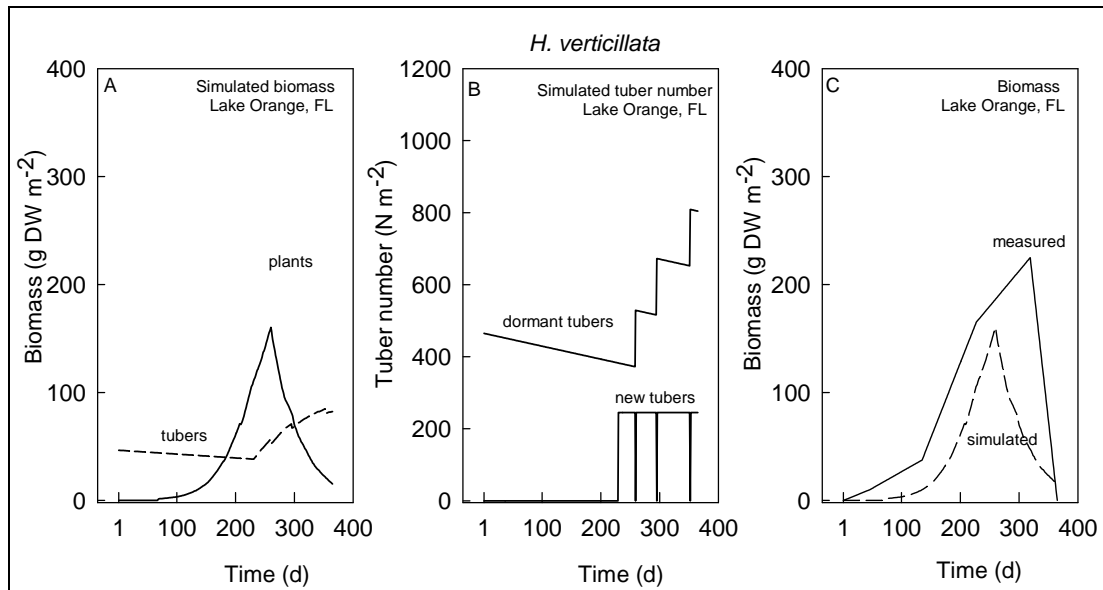


Figure 20. Simulated biomass of plants (A), dormant and new tuber numbers (B), and measured plant biomass (C) of *H. verticillata* in Lake Orange, FL. Nominal run. Field data 1977 from Bowes et al. (1979); climatological data 1980, Gainesville, FL (lat 29° 38' N, long 82° 22' W); water depth 1.0 m; light extinction coefficient 0.83 m<sup>-1</sup>.

#### HYDRIL validation: Simulated and measured behavior of the *H. verticillata* community in Lake Trafford, FL

To investigate whether HYDRIL could be used to simulate the behavior of a *H. verticillata* community at other sites, a run was made using initial values of another Florida lake at a similar latitude, Lake Trafford. The simulated biomass compared well with the measured biomass (Figure 21). Comparison of the tuber behavior is not useful in this case since measured tuber data had such a wide scatter that no conclusions could be drawn.

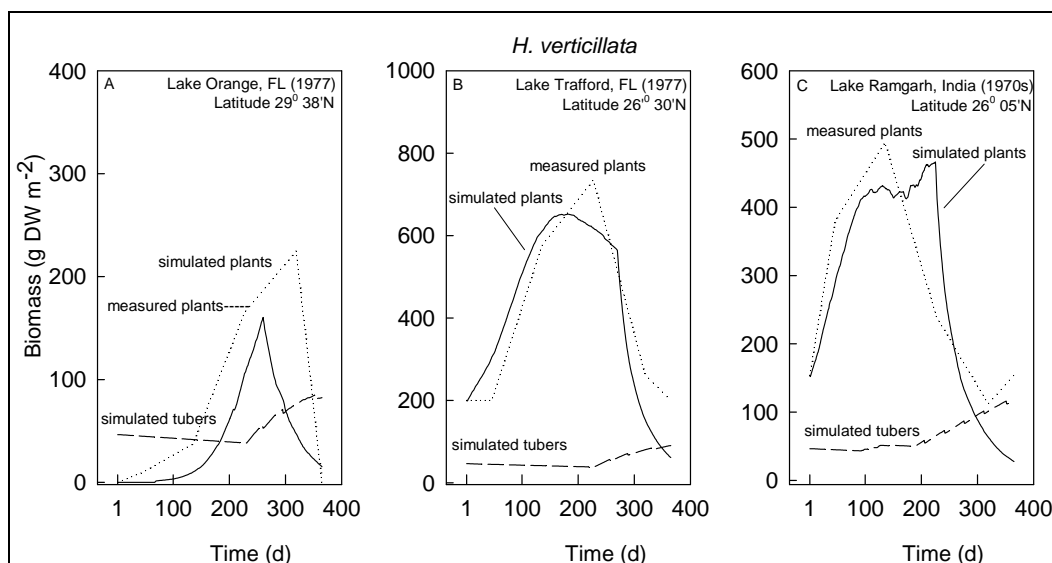


Figure 21. Simulated biomass of plants and tubers of *H. verticillata* at sites differing in latitude. (A) Lake Orange, FL (lat 29° 38' N, long 82° 22' W); tuber size 0.1 g DW, tuber bank density 500 m<sup>-2</sup>; water depth 1.0 m; light extinction coefficient 0.83 m<sup>-1</sup>; climatological data Gainesville 1980 (long and lat as above); measured data 1977, Bowes et al. (1979). (B) Lake Trafford, FL (lat 26° 30' N, long 82° 30' W); initial plant biomass 200 g DW m<sup>-2</sup>; climatological data Tampa (lat 27° 58' N, long 82° 32' W), average 1980-85; measured data 1977, Bowes et al. (1979). (C) Lake Ramgarh, India (lat 26° 05' N, long 83° 26' E; initial plant biomass 154 g DW m<sup>-2</sup>; climatological data Patancheru, India (lat 17° 27' N, long 78° 28' E), 1978; measured data 1970s, Sahai and Sinha (1973).

### HYDRIL example applications

*Application 1: Simulated and measured behavior of the H. verticillata community at other latitudes*

Simulation of a *H. verticillata* community in Lake Ramgarh, India, indicated that usually lower peak biomass than in FL is reached, when started merely from subterranean tubers. This was attributed to the formation of more tubers and their inherent sink function for assimilates in India. A simulation started from wintering plant biomass in addition to tubers generated a far higher peak biomass (Figure 21C). The latter simulation showed biomass curves that agreed well with the onsite measured biomass (Figure 21C). Using the model calibrated on North Florida to calculate the timing of phenological events in other climatological conditions indicated postponement of anthesis and reduced tuber formation in autumn only in temperate areas, but earlier anthesis and extensive tuber formation in two periods of the year in the tropics. Both of these model results are confirmed by literature data from India and Ireland, respectively (data not shown; Sahai and Sinha 1973; Scannel and Webb 1976).

*Application 2: Simulated effects of cutting and grazing*

Effects of man-made control activities, such as plant biomass harvesting at different times and at various water depths to prevent excessive biomass production can also be calculated using the HYDRIL model (Table 5).

Thus, in the latter case the model can be used as a tool for aquatic plant management agencies. From the data in this table it can be concluded that harvesting at the end of July to a water depth of 0.8 m requires removal of a relatively low amount of biomass but yields the lowest tuber bank density at the end of the year. This situation can be seen as favorable to control *H. verticillata*. In contrast, harvesting later in the year requires removal of relatively more plant biomass and allows for a relatively higher tuber bank density. Removing only the top layer of the plant community later in the year may lead even to increased numbers of tubers at the end of the year, probably due to a higher light penetration within the community in the period of tuber formation. Effects of plant biomass control through grazing of tubers by waterfowl can be calculated also by reducing the initial tuber bank density in the simulations.

Table 5. Simulated effects of mechanical harvesting date and depth on *H. verticillata* plant biomass and tuber bank density. Results of a 1-year simulation starting from a tuber bank density of 500 tubers m<sup>-2</sup> without wintering shoot biomass present, in Lake Orange, FL; climatological data 1980, Gainesville, FL.

Harvest Day	Depth (m)	Live Biomass Day 260 (g DW m <sup>-2</sup> )	Preharvest Biomass (g DW m <sup>-2</sup> )	Postharvest Biomass (g DW m <sup>-2</sup> )	Day with Zero Biomass	Final Tuber Biomass (g DW m <sup>-2</sup> ; (no))
212	0.8	0.0	72.8	7.65	257	51 (330)
243	0.8	6.3	127.5	13.2	273	56 (490)
273	0.8	160.3	124.0	12.3	287	65 (490)
273	0.1	160.3	124.0	95.5	>365	82 (804)
304	0.8	160.3	65.2	6.5	316	73 (647)

## MILFO

### **MILFO calibration: Simulated and measured behavior of a *M. spicatum* community in Lake Wingra, WI**

The seasonal changes in biomass of plant shoots and roots, and of the rhizome/root crown system, as simulated by MILFO, are shown in Figure 22. Simulated shoot biomass compared well with shoot biomass measured in Lake Wingra. Peak biomass appeared to be reached somewhat earlier in

the simulation than found in the lake. The latter was attributed to the low frequency of field observations (no measurements between September and November). The simulated biomass of the rhizome/root crown system showed two maxima per year. Variation was within the range found in a *M. spicatum* community in the same lake in later years (Smith and Adams, 1986).

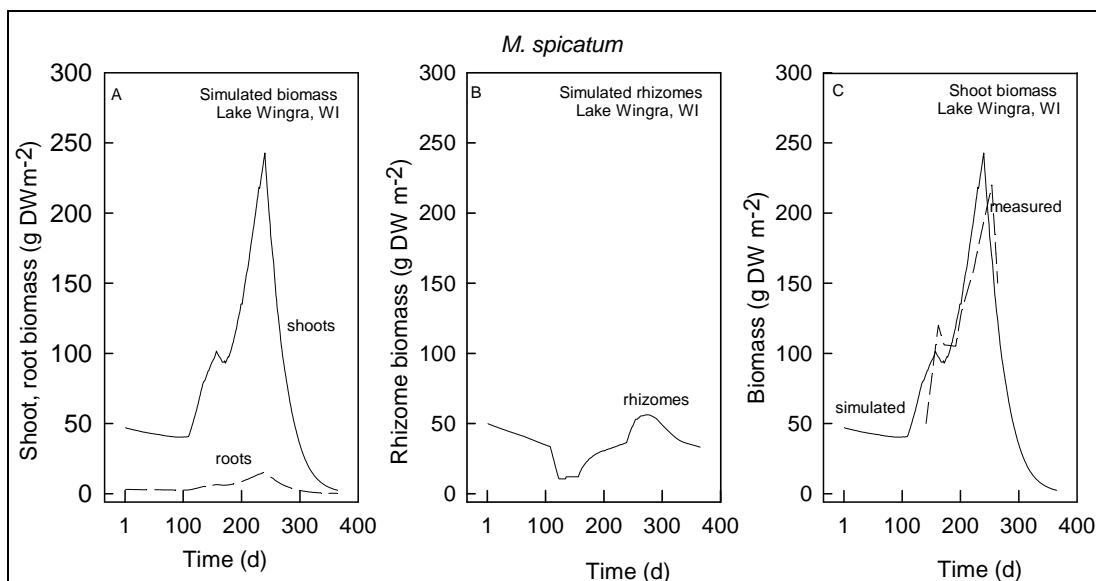


Figure 22. Simulated biomass of shoots, roots (A), rhizomes/root crowns (B), and measured shoot biomass (C) of *M. spicatum* in Lake Wingra, WI. Nominal run. Field data on shoot biomass, 1970, from Adams and McCracken (1974), and on initial rhizomes/root crown biomass, 1970, from Smith and Adams (1986); climatological data 1970, Lake Wingra, WI (lat 43° 08' N, long 89° 20' W); water depth 1.5 m; light extinction coefficient 1.15-2.00 (Lee and Kluesener 1972).

Running MILFO with the low assimilate requirements suggested as typical for SAV by Spencer et al. (1997), showed that peak biomass of *M. spicatum* shoots would increase by approximately 20 percent, oscillations in biomass of the rhizome/root crown system would be greater, and final biomass of the rhizome/root crown system would be somewhat increased (Figure 23). However, as indicated under "Maintenance, growth, and assimilate partitioning," a construction cost of 0.99 to 1.11 for *M. spicatum* plant tissues is on the low side, taking the usually high N concentrations of shoots into consideration.

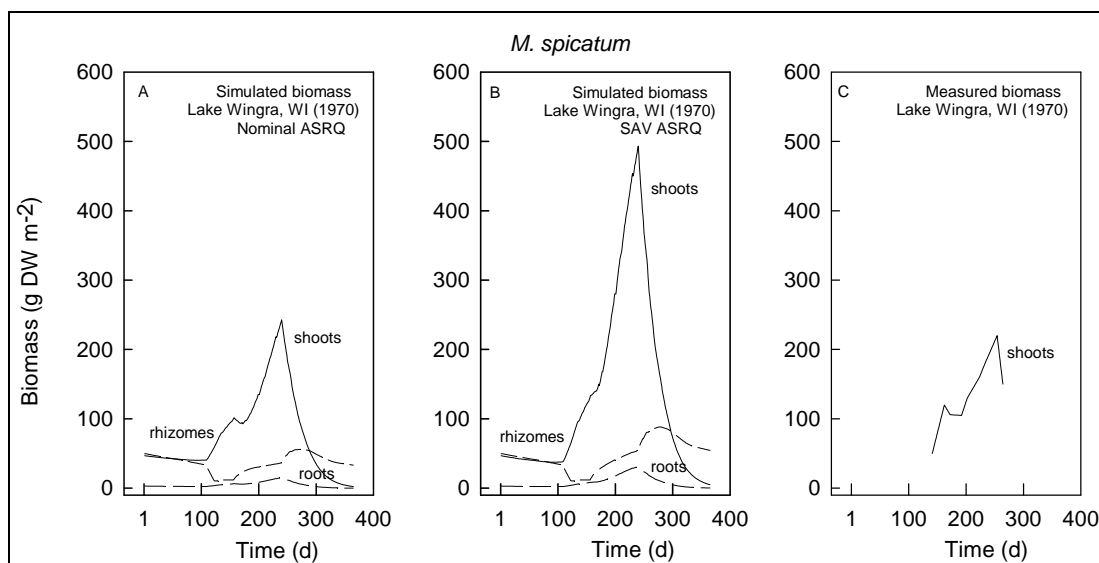


Figure 23. Simulated biomass with assimilate requirement for growth (ASRQ) value nominal (A) or as suggested for SAV (B), and measured shoot biomass (C) of a *M. spicatum* community in Lake Wingra, WI (SAV ASRQ data; Spencer et al. 1997). Initial biomass and climatological data as in nominal run.

#### MILFO validation: Simulated and measured behavior of a *M. spicatum* community at a more southern latitude

To investigate whether MILFO could be used to simulate behavior of a *M. spicatum* community at other sites, runs were made for a site at a more southern latitude, Lake Guntersville, AL. Behavior of *M. spicatum* in this lake is particularly interesting because the lake is long, oriented from northeast to southwest, and situated at a latitude of 34° N, being very close to tropical (33° N). The biomass dynamics of *M. spicatum* communities in this lake have been described as highly variable in time and space (Grace and Wetzel 1978; Stanley et al. 1976); unfortunately, in these descriptions no attention was paid to differences in latitude of the various sites within the lake nor to local differences in temperature or other environmental factors. It was mentioned, however, that flowering and subsequent sloughing periods were less predictable in southern locales than in northern ones.

Initial plant biomass values measured at a site in this lake studied in 1990 were very low, possibly due to grass carp herbivory the previous year (M. S. Stewart, personal communication, Waterways Experiment Station, Vicksburg), and initial rhizome/root crown mass for the simulation has, therefore, been set at the critical value of 12 g DW m<sup>-2</sup>. Rooting depth in the simulation was kept at 1.5 m, although actual water depth may have

varied over  $1.0 \pm 0.7$  m within a year (Stanley et al. 1976). Simulated biomass of the first plant cohort remained low (Figure 24). Only one apparent biomass peak could be distinguished, which originated from the second plant cohort. Simulated shoot biomass coincided in timing with measured shoot biomass, but the simulated peak was lower than the measured one. The latter difference was attributed to temporal decreases in water depth in the lake, while water depth was kept constant in the simulation, leading to an underestimate of simulated plant biomass. Relatively small changes in water depth can cause large changes in net assimilation and biomass production (See “Sensitivity Analysis of the Models” and “Discussion”). To investigate which consequences a warm year for the *M. spicatum* community in this lake might have, when three instead of two plant cohorts are expected to be active, a model run was made with the same initial biomass and climatological data but with a third plant cohort activated. It turned out that such a SAV was able to generate far higher shoot biomass values of approximately  $950 \text{ g DW m}^{-2}$  in one year, similar in timing and value to maximum biomass values reported for the nearby Melton Hill Lake (Stanley et al. 1976), with rhizome/root crown biomass accumulating towards the end of the year. However, similar biomass values could also be reached earlier in the year when higher initial (nominal) biomass

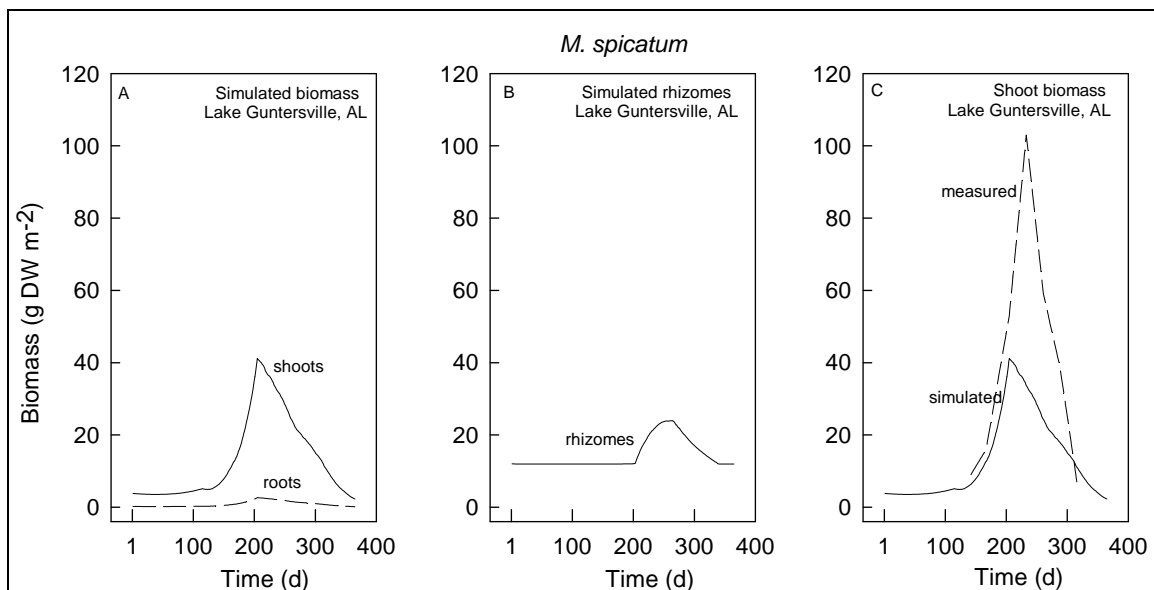


Figure 24. Simulated biomass of shoots, roots (A), rhizomes/root crowns (B), and measured shoot biomass (C) of *M. spicatum* in Lake Guntersville, AL. Field data on shoot and initial rhizomes/root crown biomass from M. S. Stewart 1990, unpublished) extrapolated to Julian day number 1. Climatological data 1990, Lake Guntersville, AL (lat 34° 08' N, long 85° 50' W).

values were used as input, and only two cohorts active; in the latter case, biomass peaks of both plant cohorts could be distinguished and rhizome/root crown biomass was well above the critical level but not accumulating.

### MILFO example application: Simulated and measured behavior of a *M. spicatum* community at other latitudes

Running MILFO with nominal biomass values and climatological data typical for sites representative for temperate, temperate to tropical, and tropical climates (Figure 25) indicated the following: (1) in all climates one clear biomass peak is generated; (2) only in a temperate climate the biomass peak of both first and second cohorts can be distinguished (flowering coinciding with every biomass maximum is always a suitable indicator, but it is often not noted in biomass studies); (3) peak biomass is expected to be highest in the tropics (that highest biomass values have been found at northern latitudes may be because most biomass studies on SAV have been performed at the latter latitudes and biomass data from tropical areas are extremely scarce); and (4) end-of-year accumulation of rhizome/root crown biomass usually occurs in tropical, but not in temperate climates (that is, when three plant cohorts are active).

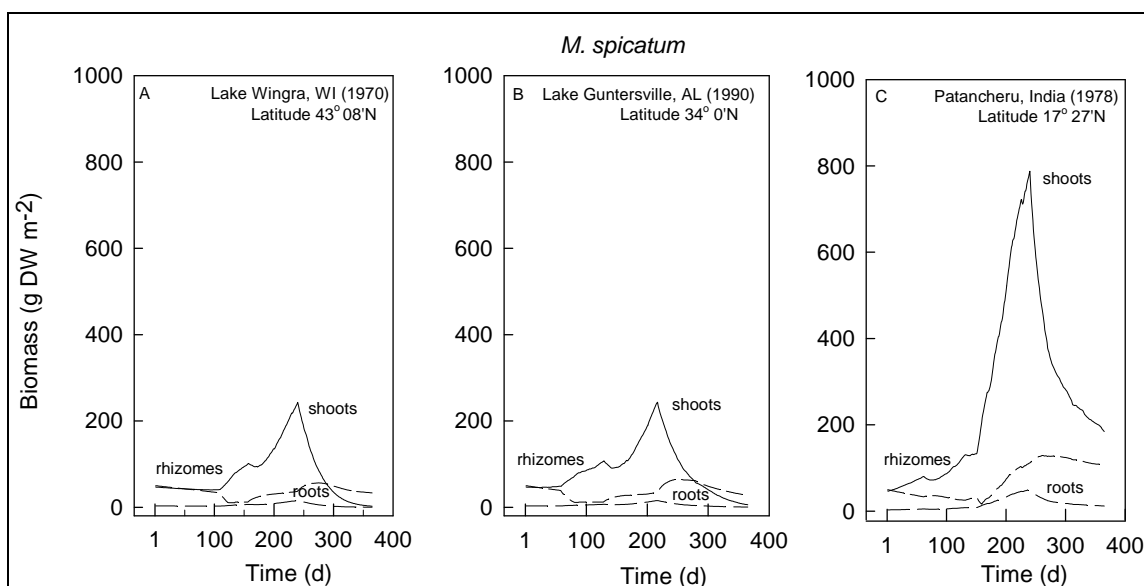


Figure 25. Simulated biomass of shoots, roots, and rhizomes of *M. spicatum* at sites differing in latitude, starting from a nominal initial biomass. (A) Lake Wingra, WI (lat 43° 08' N, long 89° 20' W); climatological data 1970. (B) Lake Guntersville, AL (lat 34° 08' N, long 85° 50' W); climatological data 1990. (C) Patancheru, India, 1978 (lat 17° 27' N, long 78° 28' E); climatological data 1978.

The maximum shoot biomass generated under tropical conditions was somewhat higher than the measured range of 288 to 640 g DW m<sup>-2</sup> and the rhizome/root crown biomass varied over a range close to the measured range of 32 to 160 (Zutschi and Vass 1973). The higher simulated shoot biomass in this case might partly be attributed to the use of climatological data from Patancheru, which is located more south, and thus warmer, than the Kashmir lakes from which the measured biomass values originated (Patancheru 17° N, Kashmir Lake 32° N); however, more northern climatological data from India were not available. It was also investigated whether *M. spicatum* may benefit from adaptation to the tropics by producing thinner leaves. This was done because a higher leaf surface area : dry weight ratio (K value) has been found for milfoil in Japan (0.01 m<sup>2</sup> g DW<sup>-1</sup>; Ikusima 1970) than in WI (0.006 m<sup>2</sup> g DW<sup>-1</sup>; Titus and Adams 1979a). Timing was very similar and simulated plant biomass about ten percent higher using the higher K value (data not shown).

## 5 Sensitivity Analysis of the Models

A sensitivity analysis of a simulation model is required to assess the parameters likely to strongly affect model behavior. The current analysis is based on the effect of a change in one parameter when all other parameters are kept the same. The parameter under study was changed and 1-year simulations were conducted under nominal environmental conditions. As reference level, the nominal parameter values were chosen as presented in Tables 2a, 2b, 2c, and 2d. The results were compared with those of a nominal run. Each parameter was once increased by 20 percent and once decreased by 20 percent. The relative sensitivity (RS) of a parameter was defined as the relative change in the variable on which the effect was tested divided by the relative change in the parameter (Ng and Loomis 1984). The effects of nine parameters on two state variables, representing different plant biomass compartments, were tested. A model variable is considered sensitive to a change in the value of a parameter at  $RS > 0.5$  and  $< -0.5$ .

$$RS = \frac{(yield_1 - yield_2) / yield_r}{(param_i - param_r) / param_r} \quad (7)$$

where

$yield_i$  = value at parameter value  $i$ ;  
 $yield_r$  = value at reference parameter value  $r$ ;  
 $param_i$  and  $param_r$  as above

Among the four models, VALLA was the most and HYDRIL the least sensitive to parameter changes (Table 6). Among the models for tuber-formers, VALLA was far more sensitive than POTAM and HYDRIL. In the models, maximum plant biomass was generally more sensitive to changes in the tested parameter values than end-of-year tuber number in tuber-forming plants or rhizome/root crown biomass in *M. spicatum* (Table 6). Maximum plant biomass was sensitive to changes in all parameters in VALLA, but only to changes in *DVRRRT*, *NPL*, *INTUB*, *AMX* and *EE* in HYDRIL. End-of-year tuber number/rhizome biomass was sensitive to changes in almost all parameters, except increased *NPL* and *ROC*, and decreased

*INTUB*, while it was only sensitive to changed *NPL* and decreased *RTR* in *HYDRIL*.

Table 6. Relative sensitivity (RS) of two state variables to deviations in parameter values from their nominal values as presented in Table 2. The RS of a parameter is the relative change in the variable on which the effect was tested divided by the relative change in the parameter. A model variable is considered sensitive to a change in the value of a parameter at  $RS > 0.5$  and  $< -0.5$ . Results were obtained in 1-year simulations under nominal conditions. Sensitive values shaded.

Parameter Name	Parameter Value	Relative Sensitivity							
		VALLA		POTAM		HYDRIL		MILFO	
		Max. Plant Biomass	EOY <sup>2</sup> Tuber No.	Max. Plant Biomass	EOY <sup>2</sup> Tuber No.	Max. Plant Biomass	EOY <sup>2</sup> Tuber No.	Max. Plant Biomass	EOY <sup>2</sup> Rhiz. Biomass
<i>DVRVT</i>	+20%	0.56	-2.5	-1.36	-3.36	-0.20	0	-0.23	-0.81
	-20%	-6.04	-1.39	-0.91	4.91	-0.44	0	-0.26	-0.99
<i>DVRT</i>	+20%	0.98	-2.47	-0.39	-0.43	-1.04	0	-0.69	-0.89
	-20%	-2.19	0.24	-0.45	-3.12	-2.19	0	-0.79	0.66
<i>NPL</i>	+20%	3.39	-0.01	0.28	1.20	0.62	-0.62	0.16	-0.79
	-20%	-0.82	2.71	0.35	1.14	0.73	-0.54	-0.16	0.79
<i>INTUB</i> <sup>1</sup>	+20%	3.25	-1.79	0.25	0	0.50	0	0.20	0.17
	-20%	-0.92	-0.03	0.34	0.19	0.62	0	0.22	0.18
<i>ROC</i>	+20%	2.65	-0.43	0.09	0	0.02	0	0.19	0.17
	-20%	-1.37	2.33	0.14	0	0.03	0	0.21	0.18
<i>AMX</i>	+20%	5.00	4.46	1.72	-1.58	3.40	0	1.96	2.00
	-20%	3.02	2.04	1.94	5.00	3.16	0	1.97	2.02
<i>EE</i>	+20%	0.50	-0.73	0.25	-0.83	1.47	0	1.10	1.14
	-20%	0.56	1.44	0.33	-3.10	1.61	0	1.22	1.25
<i>RTR</i> <sup>1</sup>	+20%	1.76	-0.77	-0.10	-2.15	-0.11	0	-0.13	0.57
	-20%	-2.62	2.19	-0.10	5.00	-0.10	0.97	-0.14	0.72
<i>RDR</i>	+20%	2.25	0.71	0	0	0	0	-0.62	-1.01
	-20%	-3.03	0.22	0	-2.93	0	0	-0.77	-1.36

Notes: <sup>1</sup> Synonymous terms in MILFO: IWGRIZ and TRAFAC; <sup>2</sup> EOY, end-of-year.

The sensitivity of maximum plant biomass and end-of-year tuber number/rhizome biomass to changes in environmental factors was assessed following the same approach as for sensitivity analysis of the model parameters. For this purpose, parameter changes were based on value ranges taken

from literature, which sometimes differed more than 20 percent from the nominal parameter values presented in Table 2. Also in this analysis, VALLA was the most sensitive among the models (Table 7). In the models, maximum plant biomass was generally more sensitive to changes in the tested parameter values than end-of-year tuber number in tuber-forming plants or rhizome/root crown biomass in *M. spicatum*. Changes in light reflection coefficient at the water surface (*RC*) had no significant effect, whereas the effects of changes in the other tested parameter values decreased in the order of *LT* > *DPTT*.

Table 7. Environmental factor analysis, expressed as relative sensitivity (RS) of two state variables to deviations in parameter values from their nominal values as presented in Table 2. The RS of a parameter is the relative change in the variable on which the effect was tested divided by the relative change in the parameter. A model variable is considered sensitive to a change in the value of a parameter at  $RS > 0.5$  and  $< -0.5$ . Results were obtained in 1-year simulations under nominal conditions. Sensitive values shaded.

Parameter Name	Parameter Value	Relative Sensitivity							
		VALLA		POTAM		HYDRIL		MILFO	
		Max. Plant Biomass	EOY <sup>2</sup> Tuber No.	Max. Plant Biomass	EOY <sup>2</sup> Tuber No.	Max. Plant Biomass	EOY <sup>2</sup> Tuber No.	Max. Plant Biomass	EOY <sup>2</sup> Rhiz. Biomass
Climate <sup>1</sup>	Lat 42° N	-	-						
	Lat 27° N	-0.49	-0.87						
Climate <sup>1</sup>	Lat 52° N			-	-				
	Lat 38° N			-1.54	1.43				
Climate <sup>1</sup>	Lat 29° N					-	-		
	Lat 17° N					1.66	0.47		
Climate <sup>1</sup>	Lat 43° N							-	-
	Lat 34° N							-0.01	0.89
<i>RC</i> <sup>3</sup>	1.00	-0.06	-0.06	-0.06	-0.06	-0.06	-0.03	-0.06	-0.04
	0.00	-0.43	-0.05	-0.02	0.09	-0.09	0	-0.07	-0.07
<i>LT</i>	+20%	2.09	0.04	-0.12	0.18	-0.44	0	0.92	-1.01
	-20%	-2.79	0.66	-0.08	0.43	0.44	0	-1.12	-1.01
<i>DPTT</i>	+20%	1.47	-2.16	-0.02	0	-0.07	0	-0.31	-0.31
	-20%	-2.43	0.48	0.03	0	-0.54	0	-0.34	-0.33

Notes: <sup>1</sup> Climates at Chenango Lake, NY (lat 42° N), Ft. Lauderdale, FL (lat 27° N), De Bilt, NL (lat 52° N), Davis, CA (lat 38° N), Gainesville, FL (lat 29° N), Patancheru, India (lat 17° N), Lake Wingra, WI (lat 43° N) and Lake Guntersville, AL (lat 34° N).

<sup>2</sup> EOY, end-of-year; <sup>3</sup> Light reflection coefficient at water surface; to enable calculation of the relative sensitivity, a very low value of 0.000001 was used.

## 6 Discussion

The models can be used to simulate the daily changes in carbon-flow-based plant processes and biomass under various site-specific conditions and management scenarios over a 1- to 5-year period of four SAV species, in climates varying from temperate to tropical. VALLA, POTAM, and HYDRIL can be run with default or user-specified input values on plant biomass, tuber size/concurrently initiated tuber number, and tuber bank density, and MILFO with user-specified input values on plant and rhizome/root crown biomass. For all runs, climate- and site-specific environmental variable data can be entered by the user, and scenarios interesting to the user can be explored.

### Developmental cycle

In the models, phenology is tied to day-degree sum. This enables simulations for different sites and climates facilitating model operation by users who do not possess a full data set on plant characteristics and environmental variables for the water body for which they desire to run the models. Earlier or later flowering biotypes are suited to different environments. The effect of flowering date can be tested with the model by varying the development rate of the vegetation. Slower rates represent later and faster rates earlier biotypes. Development rate slower or faster than the nominal rate leads to lower biomass. Faster development leads to a shorter growing season and less biomass, incomplete light interception, and lower carbohydrate availability for organ formation. At the same time, however, the rate of organ formation increases but the duration of each organ formation shortens. Intuitive prediction of biotype behavior under such highly variable climatic conditions is, therefore, hazardous. The models show some promise in being able to reproduce some of these complex responses of the vegetation and may be useful in evaluating long term implications of differences in development rate. Because only vegetative reproduction is included in the life cycle formulation, neither the tentative difference in importance of sexual reproduction between climates nor the tentative importance of seeds long-term survival (>5 years) in highly variable environmental conditions such as drought and extreme flooding can be explored with the current model versions.

## Carbon-flow-based aspects

The models are based on the carbon flow through a particular plant community, without limitation by nitrogen and phosphorus. Calibration has been done on field data pertaining to lakes with high alkalinity and relatively high pH, leaving light as major limiting factor followed by DIC. The results of the sensitivity analysis showed that the models are very sensitive to changes in process parameters influencing carbon flow, with VALLA being most sensitive and HYDRIL least. The higher sensitivity of VALLA compared to the other models may be a consequence of its “meadow-type” vertical biomass distribution over the water column that would make it more susceptible to plant-process and environment-related changes in light absorption in the overlying water layers than the “canopy-type” distribution in the other models.

## Unique characteristics of the models

The models contain the following unique descriptions of

1. Species-characteristic vertical distribution of shoot biomass in the water column that enables the calculation of the fraction of irradiance actually available for absorption by the SAV.
2. Recalculation procedures of this vertical distribution with daily changes in water level.
3. Recalculation procedures of this vertical distribution with daily removal of shoot biomass at various levels within the water column.
4. Species-characteristic epiphytic light interception that accommodates accurate estimates of the fraction of irradiance available for absorption by the SAV at sites differing in epiphyte cover.
5. Species-characteristic effects of current velocity on photosynthesis that accommodates accurate estimates of the fraction of *AMX* accomplished by the SAV at sites differing in current velocity.
6. Removal of periodic shoot and tuber/root crown biomass that enables estimates of effects of mechanical control and propagule removal by grazing and dredging on plant biomass.
7. Relationships of plant process parameters with site-specific climate by linkage with formatted weather files and calculation of latitude-specific effects on day length that enables estimates of effects of different climates.

## Application potential

The models can be used to simulate the daily changes in plant processes and biomass under various site-specific conditions and management scenarios over a 1- to 5-year period of four SAV species, in climates varying from temperate to tropical.

Example applications have illustrated how relatively low and high frequency fluctuations in water levels, current velocity, and epiphyte cover might affect submersed plant populations, without taking plant-characteristic adaptation into consideration. Ability of plants to adapt to these changes may be important characteristics for their persistence in rivers, reservoirs, and estuaries. Although this ability is a rather intensively discussed research topic, pertinent ecological data are currently largely lacking.

The models can be run using air or water temperatures as inputs. The relationship between air and water temperature may differ from the model calibration, because temperatures within each water body are influenced by catchment morphometry, wind speed, fetch, mixing processes, and upward seepage. In the authors' experience, a lag period of 7 days is usually a reasonable estimate for shallow lakes.

The models have been developed as stand-alone versions. They can relatively easily be modified to communicate with other models, because they are programmed in FORTRAN77 and their structure is simple. For instance, VALLA version 1.0 was linked via a Geographical Information System through an appropriate interface to hydrodynamic and sediment transport models, and this model combination was used to explore habitat suitability in Peoria Lake, IL, for *V. americana* (Black et al. 2003; Best et al. 2004). VALLA and POTAM versions 1.0 were linked to a decision support system that was used for ecological risk assessment on the UMR (Bartell et al. 2000, 2003). Currently tools are being developed that would greatly facilitate model application by providing links to (1) Websites where standardized weather files can be obtained, and (2) websites where gauging and water quality data required for the input file can be selected/obtained (U.S. only).

Predecessors of the models have been described in technical reports (Versions 1.0; Best and Boyd 1996, 1999a, 1999b, 2001a, 2001b, 2003a, 2003b; Boyd and Best 1996). A summary of the versions 3.0 was published

recently (Best and Boyd 2007). Model versions, user manuals, and executable model versions are available via the internet at

<http://el.erdcl.usace.mil/products.cfm?Topic=model&Type=aquatic>.

## 7 Conclusions

A dynamic simulation modeling approach to describing carbon-flow-based ecophysiological processes and biomass dynamics of freshwater submersed aquatic plant species has been developed.

The models (VALLA, POTAM, HYDRIL, and MILFO) describe major, carbon flow-based ecophysiological processes and biomass dynamics of four common freshwater species and how these are influenced by factors such as light, temperature, current velocity, DIC, availability, oxygen concentration, and human influences such as management measures (changes in turbidity, mechanical harvesting, grazing, flooding).

Model validation results showed a good fit with measured biomass temperate and tropical climates. Validation for tropical climate was limited greatly by the scarcity in available data pertaining to tropical areas. Sensitivity analysis showed that the models are very sensitive to changes in process parameters influencing carbon flow, with VALLA being most sensitive and HYDRIL least.

## References

- Adams, M. S., and M. D. McCracken. 1974. Seasonal production of the *Myriophyllum* component of the littoral of Lake Wingra, Wisconsin. *J. Ecol.* 62: 457-466.
- Adams, M. S., J. E. Titus, and M. D. McCracken. 1974. Depth distribution of photosynthetic activity in a *Myriophyllum spicatum* community in Lake Wingra. *Limnol. Oceanogr.* 19: 377-389.
- Aiken, S. G., P. Newroth, and I. Wile. 1979. The biology of Canadian weeds (34), *Myriophyllum spicatum* L. *Can. J. Plant Sci.* 59: 201-215.
- Aleem, A. A., and A. A. Samaan. 1969. Productivity of Lake Mariut, Egypt. Part II. Primary production. *Internat. Rev. Hydrobiol.* 54: 491-527.
- Ambasht, R. S., and K. Ram. 1976. Stratified primary production of certain macrophytic weeds in a large Indian lake. In *Aquatic weeds in S.E. Asia. Proc. Regional Seminar on Noxious Aquatic Vegetation, New Delhi, 12-17 December 1973*, ed. C. K. Varshney and J. Rzoska, 147-155. The Netherlands : W. Junk, Den Haag.
- Barko, J. W., and G. J. Filbin. 1982. Influences of light and temperature on chlorophyll composition in submersed freshwater macrophytes. *Aquat. Bot.* 15: 249-255.
- Barko, J. W., and R. M. Smart. 1981. Comparative influences of light and temperature on the growth and metabolism of selected submersed freshwater macrophytes. *Ecol. Monogr.* 51: 219-235.
- Bartell, S. M., K. R. Campbell, E. P. H. Best, and W. A. Boyd. 2000. *Interim report for the Upper Mississippi River System - Illinois Waterway System Navigation Study. Ecological risk assessment of the effects of incremental increase of commercial navigation traffic (25, 50, 75, and 100% increase of 1992 baseline traffic) on submerged aquatic plants in the main channel borders.* ENV Report 17. U.S. Army Corps of Engineers, Rock Island District, St. Louis District, St. Paul District.
- Bartell, S. M., K. R. Campbell, E. M. Miller, S. K. Nair, E. P. H. Best, and D. J. Schaeffer. 2003. *Interim report for the Upper Mississippi River System - Illinois Waterway System Navigation Study. Ecological models and approach to ecological risk assessments.* ENV Report 38. U.S. Army Corps of Engineers, Rock Island District, St. Louis District, St. Paul District.
- Bellrose, F. C., S. P. Havera, F. L. Paveglio, and D. W. Steffeck. 1983. Fate of the lakes in the Illinois River valley. *Ill. Nat. Hist. Survey Biol. Note* 119.
- Best, E. P. H. 1981. A preliminary model for growth of *Ceratophyllum demersum* L. *Verh. Internat. Verein. Limnol.* 21: 1484-1491.
- Best, E. P. H., and W. A. Boyd. 1996. *A simulation model for growth of the submersed aquatic macrophyte Hydrilla verticillata L.* Technical Report A-96-8. Vicksburg, MS: U.S. Army Engineer Waterways Experiment Station.

- Best, E. P. H., and W. A. Boyd. 1999a. *A simulation model for growth of the submersed aquatic macrophyte Myriophyllum spicatum L.* Technical Report A-99-3. Vicksburg, MS: U.S. Army Engineer Research and Development Center.
- \_\_\_\_\_. 1999b. *MILFO (version 1.0): A simulation model for growth of Eurasian watermilfoil – User's guide.* Instruction Report A-99-1. Vicksburg, MS: U.S. Army Engineer Research and Development Center.
- \_\_\_\_\_. 2001a. *A simulation model for growth of the submersed aquatic macrophyte American wildcelery (Vallisneria americana Michx.).* ERDC/EL TR-01-5. Vicksburg, MS: U.S. Army Engineer Research and Development Center.
- \_\_\_\_\_. 2001b. *VALLA (version 1.0): A simulation model for growth of American wildcelery.* ERDC/EL SR-01-1. Vicksburg, MS: U.S. Army Engineer Research and Development Center.
- \_\_\_\_\_. 2003a. *A simulation model for growth of the submersed aquatic macrophyte Sago pondweed (Potamogeton pectinatus L.).* ERDC/EL TR-03-6. Vicksburg, MS: U.S. Army Engineer Research and Development Center.
- \_\_\_\_\_. 2003b. *POTAM (version 1.0): a simulation model for growth of Sago pondweed.* ERDC/EL SR-03-1. Vicksburg, MS: U.S. Army Engineer Research and Development Center.
- \_\_\_\_\_. 2003c. Appendix C: Biomass characteristics and photosynthetic activity of sago pondweed populations in the Western Canal near Zandvoort, The Netherlands. In *A simulation model for growth of the submersed aquatic macrophyte sago pondweed (Potamogeton pectinatus L.).* ERDC/EL TR-03-6. Vicksburg, MS: U.S. Army Engineer Research and Development Center.
- \_\_\_\_\_. 2007. Expanded simulation models (Version 3.0) for growth of the submersed aquatic plants American wildcelery, sago pondweed, hydrilla, and Eurasian watermilfoil. ERDC/TN SWWRP-07-XX. Vicksburg, MS: U.S. Army Engineer Research and Development Center.
- Best, E. P. H., and F. H. H. Jacobs. 1990. Potential and actual production of submersed aquatic angiosperms common in temperate regions. *Proc. EWRS/AAB 8th Symp. on Aquatic Weeds* 39-47.
- Best, E. P. H., C. P. Buzzelli, S. M. Bartell, R. L. Wetzel, W. A. Boyd, R. D. Doyle, and K. R. Campbell. 2001. Modeling submersed macrophyte growth in relation to underwater light climate: Modeling approaches and application potential. *Hydrobiologia* 444: 43-70.
- Best, E. P. H., A. H. Teeter, and S. K. Nair. 2004. *Modeling the impacts of suspended sediment concentration and current velocity on submersed vegetation in an Illinois River pool,* ERDC/TN APCRP-EA-07. Vicksburg, MS: U.S. Army Engineer Research and Development Center.
- Best, E. P. H., G. A. Kiker, B. A. Rycyzyn, K. P. Kenow, J. Fischer, S. K. Nair, and D. B. Wilcox. 2005. *Aquatic plant growth model refinement for the Upper Mississippi River-Illinois Waterway System Navigation Study.* ENV Report 51. U. S. Army Corps of Engineers, Rock Island District, St. Louis District, St. Paul District.

- Bick, H., and A. W. J. Van Schaik. 1980. *Ecological vision border lakes*. Advice of the Natural Science Committee of the Nature Conservation Council, 291 pp. (in Dutch).
- Black, P., E. P. H. Best, E. A. Newcomb, T. Birkenstock, B. Boyt, R. Heath, and W. F. James. 2003. *Assessing hydraulic modifications on Vallisneria americana in Peoria Lake, Illinois. A pilot study using data sharing protocols to integrate legacy models*. ERDC/CRREL TR-03-18. Hanover, NH: U.S. Army Engineer Research and Development Center.
- Blanch, S. J., G. G. Ganf, and K. F. Walker. 1998. Growth and recruitment in *Vallisneria americana* as related to average irradiance in the water column. *Aquat. Bot.* 61: 181-205.
- Bowes, G., T. K. Van, L. A. Garrard, and W. T. Haller. 1977. Adaptation to low light levels by Hydrilla. *J. Aquat. Plant Manage.* 15: 32-35.
- Bowes, G., A. C. Holaday, and W. T. Haller. 1979. Seasonal variation in the biomass, tuber density and photosynthetic metabolism in three Florida lakes. *J. Aquat. Plant Manage.* 17: 61-65.
- Boyd, W.A., and E. P. H. Best. 1996. *HYDRIL (version 1.0): A simulation model for growth of Hydrilla. User Manual*. Instruction Report A-96-1. Vicksburg, MS: U.S. Army Engineer Waterways Experiment Station.
- Budd, J., R. A. Lillie, and P. Rasmussen. 1995. Morphological characteristics of the aquatic macrophyte, *Myriophyllum spicatum* L., in Fish Lake, Wisconsin. *J. Freshwat. Ecol.* 10: 19-31.
- Carpenter, S. R. 1980. The decline of *Myriophyllum spicatum* in a eutrophic Wisconsin USA lake. *Can. J. Bot.* 58: 527-535.
- Carr, G. M., H. C. Duthie, and W. D. Taylor. 1997. Models of aquatic plant productivity and growth: A review of the factors that influence growth. *Aquat. Bot.* 59: 195-215.
- Chambers, P. A., E. E. Prepas, H. R. Hamilton, and M. L. Bothwell. 1991. Current velocity and its effects on aquatic macrophytes in flowing waters. *Ecol. Appl.* 1: 249-257.
- Choudhuri, G. N. 1966. Seed germination and flowering in *Vallisneria spiralis*. *Northwest Sci.* 40: 31-35.
- Collins, C. D., and J. H. Wlosinski. 1985. A macrophyte submodel for aquatic ecosystems. *Aquat. Bot.* 33: 191-206.
- Crow, G. E., and C. B. Hellquist. 2000. *Aquatic and wetland plants of North America*. Vol. 2, p. 36.
- Den Hartog, C. 1982. Architecture of macrophyte-dominated aquatic communities. In *Studies on aquatic vascular plants*, ed. J. J. Symoens, S. S. Hoooper, and P. Compere, 222-224. Brussels: Royal Botanical Society of Belgium.

- Donnermeyer, G. N. 1982. The quantity and nutritive quality of *Vallisneria americana* biomass, in Navigation Pool No. 9 of the Upper Mississippi River. MS thesis, University of Wisconsin, La Crosse.
- Donnermeyer, G. N., and M. M. Smart. 1985. The biomass and nutritive potential of *Vallisneria americana* Michx. in Navigation Pool 9 of the Upper Mississippi River. *Aquat. Bot.* 22: 33-44.
- Giesen, W. B. J. T., M. M. Van Katwijk, and C. Den Hartog. 1990. Eelgrass condition and turbidity in the Dutch Wadden Sea. *Aquat. Bot.* 37: 71-85.
- Gijzen, H. 1985. *Simulatie van drogestof-productie en de Leaf Area Index van cassave*. MS thesis, Department of Tropical Crop Science, Wageningen Agricultural University, The Netherlands (In Dutch).
- Godfrey, R. K., and J. W. Wooten. 1997. *Aquatic and wetland plants of Southeastern United States, monocotyledons*. Athens: The University of Georgia Press, 711 pp.
- Golterman, H. L. 1975. *Physiological limnology. An approach to the physiology of lake ecosystems*. Amsterdam: Elsevier Scientific Publishing Company, 489 pp.
- Goudriaan, J. 1986. A simple and fast numerical method for the computation of daily totals of crop photosynthesis. *Agricult. Forest Meteorol.* 38: 251-255.
- Goudriaan, J., H. Van Keulen, and H. H. Van Laar. 1992. Crop growth model for potential production (SUCROS1). Simulation of crop growth for potential and water-limited production situations (as applied to spring wheat). Post-graduate course "Simulation of plant growth and crop production." Pontignano, Siena, Italy, 3-12 November 1992, 1-25.
- Grace, J. B., and R. G. Wetzel. 1978. The production biology of Eurasian watermilfoil (*Myriophyllum spicatum* L.): A review. *J. Aquat. Plant Manage.* 16: 1-11.
- Griffin, K. L. 1994. Caloric estimates of construction cost and their use in ecological studies. *Funct. Ecol.* 8: 551-562.
- Gupta, R. K. 1968. *Flora Nainitalenses*. New Delhi: Mawagag Traders Publishing.
- Hahn, S. K., and Y. Hozyo. 1983. Sweet potato and yam. In *Potential productivity of field crops under different environments*, 319-340. Los Banos: Internat. Rice Res. Inst.
- Haller, W. T. 1974. Photosynthetic characteristics of the submersed aquatic plants *Hydrilla*, southern naiad, and *Vallisneria*. Ph.D. diss., University of Florida.
- Haller, W. T., J. L. Miller, and L. A. Garrard. 1976. Seasonal production and germination of *Hydrilla* vegetative propagules. *J. Aquat. Plant Manage.* 16: 26-29.
- Haller, W. T., and D. L. Sutton. 1975. Community structure and competition between *Hydrilla* and *Vallisneria*. *Hyacinth Control J.* 3: 48-50.
- Hammer, U. T., and J. M. Heseltine. 1988. Aquatic macrophytes in saline lakes of the Canadian prairies. *Hydrobiologia* 158: 101-116.

- Herb, W. R., and H. G. Stefan. 2003. Integral growth of submersed macrophytes in varying light regimes. *Ecol. Modell.* 168: 77-100.
- Hootsmans, M. J. M. 1994. A growth analysis model for *Potamogeton pectinatus* L. In *Lake Veluwe, a macrophyte-dominated system under eutrophication stress. Geobotany 21*, ed. W. Van Vierssen, M. Hootsmans, and J. Vermaat, 250-286. Dordrecht/Boston/London: Kluwer Academic Publishers.
- Hootsmans, M. J. M., and J. E. Vermaa. 1994. Intraspecific variation in *Potamogeton pectinatus* L.: A controlled laboratory experiment. In *Lake Veluwe, a macrophyte-dominated system under eutrophication stress, Geobotany 21*, ed. W. Van Vierssen, M. Hootsmans, and J. Vermaat, 26-39. Dordrecht/Boston/London: Kluwer Academic Publishers.
- Howard-Williams, C. 1978. The growth and reproduction of aquatic macrophytes in a south temperate saline lake. *Verh. Internat. Verein. Limnol.* 20: 1153-1158.
- Hunt, R. 1982. *Plant growth curves*. London: Arnold.
- Ikusima, I. 1970. Ecological studies on the productivity of aquatic plant communities. IV. Light condition and community photosynthetic production. *Bot. Mag. Tokyo* 83: 330-340.
- Ingram, K. T., and D. E. McCloud. 1984. Simulation of potato crop growth and development. *Crop Sci.* 24: 21-27.
- Kautsky, L. 1987. Life cycles of three populations of *Potamogeton pectinatus* L. at different degrees of wave exposure in the Asko area, Northern Baltic proper. *Aquat. Bot.* 27: 177-186.
- Kimber, A., C. E. Korschgen, and A. G. Van der Valk. 1995. The distribution of *Vallisneria americana* seeds and seedling light requirements in the Upper Mississippi River. *Can. J. Bot.* 73: 1966-1973.
- Kooman, P. L., 1995. Genotype-environment interaction in potato 2: Dry matter allocation and duration of the growth cycle. Yielding ability of potato crops as influenced by temperature and daylength. PhD diss., Agricultural University Wageningen. Chap. 5, 71-89.
- Korschgen, C. E., and W. L. Green. 1988. *American wildcelery (Vallisneria americana): Ecological considerations for restoration*. Fish and Wildlife Technical Report 19. Washington DC: U.S. Department of the Interior, Fish and Wildlife Service.
- Korschgen, C. E., W. L. Green, and K. P. Kenow. 1997. Effects of irradiance on growth and winter bud production by *Vallisneria americana* and consequences to its abundance and distribution. *Aquat. Bot.* 58: 1-9.
- Lapirov, A. G., and L. V. Petukhova. 1985. The rhythm of development of fennel-leaved pondweed in the Uglitch reservoir. *Biol vnutr. vod, Inform. Bull.* 66: 10-13 (In Russian).
- Lee, G. F., and J. W. Kluesener. 1972. *Nutrient transport and transformation in Lake Wingra, Wisconsin*. Eastern Deciduous Forest Biome Memo-Report 72-42.

- Lind, C. T., and G. Cottam. 1969. The submerged aquatics of University Bay: A study in eutrophication. *Amer. Midl. Natur.* 81: 353-369.
- Lohammar, G. 1938. Wasserchemie und höhere Vegetation Schwedischer Seen. *Symb. Bot. Upsal.* 3: 1-252.
- Lovvorn, J. R. 1989. Distributional responses of canvasback ducks to weather and habitat change. *J. Appl. Ecol.* 26: 113-130.
- Lovvorn, J. R., and M. P. Gillingham. 1996. Food dispersion and foraging energetics: A mechanistic synthesis for field studies of avian benthivores. *Ecol.* 77: 435-451.
- Lowden, R. M. 1982. An approach to the taxonomy of *Vallisneria* L. (Hydrocharitaceae). *Aquat. Bot.* 13: 269-298.
- Madsen, J. D. 1997. Seasonal biomass and carbohydrate allocation in a southern population of Eurasian watermilfoil. *J. Aquat. Plant Manage.* 35: 15-21.
- Madsen, J. D., and M. S. Adams. 1988. The seasonal biomass and productivity of the submerged macrophytes in a polluted Wisconsin stream. *Freshwat. Biol.* 20: 41-50.
- Madsen, J. D., L. W. Eichler, and C. W. Boylen. 1988. Vegetative spread of Eurasian watermilfoil in Lake George, New York. *J. Aquat. Plant Manage.* 26: 47-50.
- McFarland, D., and J. W. Barko. 1990. Temperature and daylength effects on growth and tuber formation in *Hydrilla*. *J. Aquat. Plant Manage.* 28: 15-19.
- Ng, E., and R. S. Loomis. 1984. *Simulation of growth and yield of the potato crop*. Simulation Monographs. Wageningen: Pudoc Scientific Publishing.
- Nichols, S. A., 1971. *The distribution and control of macrophyte biomass in Lake Wingra*. Publ. Water Resources Center, Hydraulic Sanitary Laboratory, University of Wisconsin, 111 pp.
- Penning de Vries, F. W. T. 1975. The cost of maintenance processes in plant cells. *Ann. Bot.* 39: 77-92.
- Penning de Vries, F. W. T., D. M. Jansen, H. F. M. Ten Berge, and A. Bakema. 1989a. Morphological development and assimilate partitioning. In *Simulation of ecophysiological processes of growth in several annual crops*, chap. 3, 49-56. Wageningen: Pudoc Scientific Publishing.
- \_\_\_\_\_. 1989b. Morphological development and assimilate partitioning. In *Simulation of ecophysiological processes of growth in several annual crops*, chap. 3, 73-115. Wageningen: Pudoc Scientific Publishing.
- Penning de Vries, F. W. T., and H. H. Van Laar. 1982a. Simulation of growth processes and the model BACROS. In *Simulation of plant growth and crop production*, 99-102. Wageningen: Pudoc Scientific Publishing.
- \_\_\_\_\_. 1982b. Simulation of growth processes and the model BACROS. In *Simulation of plant growth and crop production*, 114-131. Wageningen: Pudoc Scientific Publishing.

- Pilon, J. 1999. Progress report 1998 Netherlands Institute of Ecology. Nieuwersluis, The Netherlands: Royal Dutch Academy of Sciences.
- Pilon, J., and L. Santamaria. 2002. Clonal variation in the thermal response of the submerged aquatic macrophyte *Potamogeton pectinatus*. *J. Ecol.* 90: 141-152.
- Rabbinge, R., and C. T. De Wit. 1989. Theory of modelling and systems management. In *Simulation and systems management in crop protection*, ed. R. Rabbinge, S. A. Ward, and H.H. Van Laar. Chapter 1. Simulation Monographs 32, pp. 1-12. Wageningen: Pudoc Scientific Publishing.
- Ramirez, C., and J. San Martin 1984. Hydrophilous vegetation of a coastal lagoon in central Chile. *Internat. J. Ecol. Environ. Sci.* 10: 93-110.
- Rogers, S. J. 1994. Preliminary evaluation of submersed macrophyte changes in the Upper Mississippi River. *Lake Reservoir Manage.* 10: 35-38.
- Sahai, R., and A. B. Sinha. 1973. Productivity of submerged macrophytes in polluted and non-polluted regions of the eutrophic Lake Ramgarh (U.P.). In *Aquatic weeds in S.E. Asia. Proc. regional seminar on noxious aquatic vegetation, New Delhi, 12-17 December 1973*, ed. C. K. Varshney and J. R. Zosha, 131-140. The Netherlands: W. Junk, Den Haag.
- Scannel, M. J. P., and D. A. Webb. 1976. The identity of the Renvyle *Hydrilla*. *Irish Natur. J.* 18: 327-331.
- Scheffer, M. 1991. On the prediction of aquatic vegetation in shallow lakes. *Mem. Istit. Ital. Idrobiol.* 48: 207-217.
- Scheffer, M., A. H. Bakema, and F. G. Wortelboer. 1993. MEGAPLANT: A simulation model of the dynamics of submerged plants. *Aquat. Bot.* 45: 341-356.
- Sher-Kaul, S., B. Oertli, E. Castella, and J. B. Lachavanne. 1995. Relationship between biomass and surface area of six submerged aquatic plant species. *Aquat. Bot.* 51: 147-154.
- Sinha, A. B. 1970. Studies on the bioecology and production in Ramgarh Lake, Gorakhpur. PhD diss., Gorakhpur University, India.
- Smith, C. S., and M. S. Adams. 1986. Phosphorus transfer from sediments by *Myriophyllum spicatum*. *Limnol. Oceanogr.* 31: 1312-1321.
- Spencer, D. F. 1987. Tuber size and planting depth influence growth of *Potamogeton pectinatus* L. *Amer. Midl. Natur.* 118: 77-84.
- Spencer, D. F., and L. W. J. Anderson. 1986. Photoperiod responses in monoecious and dioecious *Hydrilla verticillata*. *Weed Sci.* 34: 551-557.
- Spencer, D. F., and L. W. J. Anderson. 1987. Influence of photoperiod on growth, pigment composition and vegetative propagule formation for *Potamogeton nodosus* Poir. and *Potamogeton pectinatus* L. *Aquat. Bot.* 28: 102-112.
- Spencer, D. F., F. J. Ryan, and G. G. Ksander. 1997. Construction costs for some aquatic plants. *Aquat. Bot.* 56: 203-214.

- Spencer, D. F., G. G. Ksander, and L. C. Whitehand. 1994. Estimating the abundance of subterranean propagules of submersed aquatic plants. *Freshwat. Biol.* 31: 191-200.
- Spink, A., and S. Rogers. 1996. The effects of a record flood on the aquatic vegetation of the Upper Mississippi River System: Some preliminary findings. *Hydrobiologia* 340: 51-57.
- Spitters, C. J. T. 1986. Separating the diffuse and direct component of global radiation and its implications for modeling canopy photosynthesis. II. Calculation of canopy photosynthesis. *Agricult. Forest Meteorol.* 38: 231-242.
- Stanley, R. A., and A. W. Nailor. 1972. Photosynthesis in Eurasian watermilfoil (*Myriophyllum spicatum* L.). *Plant Physiol.* 50: 149-151.
- Stanley, R. A., E. Shackelford, D. Wade, and C. Warren. 1976. Effects of season and water depth on Eurasian watermilfoil. *J. Aquat. Plant Manage.* 14: 32-36.
- Steward, K. K., and T. K. Van. 1986. Physiological studies of monoecious and dioecious *Hydrilla* biotypes in the USA. *Proc. EWRS/AAB 7th Symp. on Aquatic Weeds*, 333-344.
- Sutton, D. L., and K. M. Portier. 1992. Growth of dioecious and monoecious *Hydrilla* from single tubers. *J. Aquat. Plant Manage.* 30: 15-20.
- Thornley, J. H. M., and I. R. Johnson. 1990a. Temperature effects on plant and crop processes. *Plant and crop modelling. A mathematical approach to plant and crop physiology*. Oxford: Clarendon Press, pp. 139-144.
- \_\_\_\_\_. 1990b. Plant growth functions. *Plant and crop modelling. A mathematical approach to plant and crop physiology*. Oxford: Clarendon Press, pp. 74-89.
- Titus, J. E. 1977. *The comparative physiological ecology of three submersed macrophytes*. PhD diss., University of Wisconsin.
- Titus, J., and M. A. Adams. 1979a. Coexistence and the comparative light relations of the submersed macrophytes *Myriophyllum spicatum* L. and *Vallisneria americana* Michx. *Oecologia* 40: 273-286.
- \_\_\_\_\_. 1979b. Comparative storage utilization patterns in the submersed macrophytes, *Myriophyllum spicatum* and *Vallisneria americana*. *Amer. Midl. Natur.* 102: 263-272.
- Titus, J. E., R. S. Feldman, and D. Grise. 1990. Submersed macrophyte growth at low pH. I. CO<sub>2</sub> enrichment effects with fertile sediment. *Oecologia* 84: 307-313.
- Titus, J., R. A. Goldstein, M. A. Adams, J. B. Mankin, R. V. O'Neill, P. R. Weiler, H. H. Shugart, and R. S. Booth. 1975. A production model for *Myriophyllum spicatum* L. *Ecol.* 56: 1129-1138.
- Titus, J. E., and M. D. Stephens. 1983. Neighbor influences and seasonal growth patterns for *Vallisneria americana* in a mesotrophic lake. *Oecologia* 56: 23-29.

- Titus, J. E., and W. H. Stone. 1982. Photosynthetic response of two submersed macrophytes to dissolved inorganic carbon concentration and pH. *Limnol. Oceanogr.* 27: 151-160.
- Van, T. K., and K. K. Steward. 1990. Longevity of monoecious *Hydrilla* propagules. *J. Aquat. Plant Manage.* 28: 74-76.
- Van, T. K., W. T. Haller, and G. Bowes. 1976. Comparison of the photosynthetic characteristics of three submersed aquatic plants. *Plant Physiol.* 58: 761-768.
- Van, T. K., W. T. Haller, G. Bowes, and L. A. Garrard. 1977. Effects of light quality on chlorophyll composition in *Hydrilla*. *J. Aquat. Plant Manage.* 15: 29-31.
- Van, T. K., W. T. Haller, and G. Bowes. 1978a. Some aspects of the competitive biology of *Hydrilla*. In *Proc. 5th EWRS Internat. Symp. on Aquatic Weeds, Amsterdam (The Netherlands)*, pp. 117-126.
- Van, T. K., W. T. Haller, and L. A. Garrard. 1978b. The effect of daylength and temperature on *Hydrilla* growth and tuber production. *J. Aquat. Plant Manage.* 16: 57-59.
- Van der Bijl, L., K. Sand-Jensen, and A. L. Hjerminde. 1989. Photosynthesis and canopy structure of a submerged plant *Potamogeton pectinatus*, in a Danish lowland stream. *J. Ecol.* 77: 947-962.
- Van der Zwerde, W. 1981. Research of the influence of light intensity and day length on the formation of turions in the aquatic macrophyte *Hydrilla verticillata* Royle. Student Report, Centre for Agrobiological Research, Wageningen (In Dutch).
- Van Dijk, G. M., and E. P. Achterberg. 1992. Light climate in the water column of a shallow eutrophic lake (Lake Veluwe) in The Netherlands. *Arch. Hydrobiol.* 125: 257-278.
- Van Dijk, G. M., A. W. Breukelaar, and R. Gijlstra. 1992. Impact of light climate history on seasonal dynamics of a field population of *Potamogeton pectinatus* L. during a three year period (1986-1988). *Aquat. Bot.* 43: 17-41.
- Van Kraalingen, D. W. G. 1995. *The FSE System for Crop Simulation*. AB-DLO Report. Wageningen, The Netherlands, 53 pp.
- Van Wijk, R. J. 1988. Ecological studies on *Potamogeton pectinatus* L. I. General characteristics, biomass production and life cycles under field conditions. *Aquat. Bot.* 31: 211-258.
- Van Wijk, R. J. 1989. Ecological studies on *Potamogeton pectinatus* L. III. Reproductive strategies and germination ecology. *Aquat. Bot.* 33: 271-299.
- Van Wijk, R. J., E. Van Goor, and J. A. C. Verkley. 1988. Ecological studies on *Potamogeton pectinatus* L. II. Autecological characteristics with emphasis on salt tolerance, intraspecific variation and isoenzyme patterns. *Aquat. Bot.* 32: 239-260.

- Vogt, K. A., D. J. Vogt, and J. Bloomfield. 1991. Input of organic matter to the soil by tree roots. In *Plant roots and their environment*, ed B. L. MicMichael and H. Persson pp. 171-190. Elsevier Science Publications.
- Voss, E. 1972. *Michigan Flora. Part I – Gymnosperms and monocots*. Bloomfield Hills, Michigan: Cranbrook Institute of Science, 488 pp.
- Westlake, D. F. 1965. Light extinction, standing crop and photosynthesis within weed beds. *Verh. Internat. Verein. Limnol.* 15: 415-425.
- Wetzel, R. L., and H. A. Neckles. 1996. A model of *Zostera marina* L. photosynthesis and growth: simulated effects of selected physical-chemical variables and biological interactions. *Aquat. Bot.* 26: 307-323.
- Williams, K., F. Percival, J. Merino, and H. A. Mooney. 1987. Estimation of tissue construction cost from heat combustion and organic nitrogen content. *Plant Cell Environ.* 10: 725-734.
- Yeo, R. R. 1965. Life history of sago pondweed. *Weeds* 13: 314-321.
- Zutschi, D. P., and K. K. Vass 1973. Ecology of macrophyte vegetation of Kashmir lakes. In *Aquatic weeds in S.E. Asia. Proc. regional seminar on noxious aquatic vegetation, New Delhi, 12-17 December 1973*, ed. C. K. Varshney and J. R. Zosha, 141-146. The Netherlands: W. Junk, Den Haag.

# REPORT DOCUMENTATION PAGE

*Form Approved*  
OMB No. 0704-0188

Public reporting burden for this collection of information is estimated to average 1 hour per response, including the time for reviewing instructions, searching existing data sources, gathering and maintaining the data needed, and completing and reviewing this collection of information. Send comments regarding this burden estimate or any other aspect of this collection of information, including suggestions for reducing this burden to Department of Defense, Washington Headquarters Services, Directorate for Information Operations and Reports (0704-0188), 1215 Jefferson Davis Highway, Suite 1204, Arlington, VA 22202-4302. Respondents should be aware that notwithstanding any other provision of law, no person shall be subject to any penalty for failing to comply with a collection of information if it does not display a currently valid OMB control number. **PLEASE DO NOT RETURN YOUR FORM TO THE ABOVE ADDRESS.**

<b>1. REPORT DATE (DD-MM-YYYY)</b> September 2007		<b>2. REPORT TYPE</b> Final report		<b>3. DATES COVERED (From - To)</b>		
<b>4. TITLE AND SUBTITLE</b>  Carbon-Flow-Based Modeling of Ecophysiological Processes and Biomass Dynamics of Submersed Aquatic Plants				<b>5a. CONTRACT NUMBER</b>		
				<b>5b. GRANT NUMBER</b>		
				<b>5c. PROGRAM ELEMENT NUMBER</b>		
<b>6. AUTHOR(S)</b>  Elly P. H. Best and William A. Boyd				<b>5d. PROJECT NUMBER</b>		
				<b>5e. TASK NUMBER</b>		
				<b>5f. WORK UNIT NUMBER</b>		
<b>7. PERFORMING ORGANIZATION NAME(S) AND ADDRESS(ES)</b>  Environmental Laboratory U.S. Army Engineer Research and Development Center 3909 Halls Ferry Road Vicksburg, MS 39180-6199				<b>8. PERFORMING ORGANIZATION REPORT NUMBER</b>  ERDC/EL TR-07-14		
<b>9. SPONSORING / MONITORING AGENCY NAME(S) AND ADDRESS(ES)</b>  U.S. Army Corps of Engineers Washington, DC 20314-1000				<b>10. SPONSOR/MONITOR'S ACRONYM(S)</b>		
				<b>11. SPONSOR/MONITOR'S REPORT NUMBER(S)</b>		
<b>12. DISTRIBUTION / AVAILABILITY STATEMENT</b>  Approved for public release, distribution unlimited.						
<b>13. SUPPLEMENTARY NOTES</b>						
<b>14. ABSTRACT</b> A dynamic simulation modeling approach to describing carbon-flow-based, ecophysiological processes and biomass dynamics of fresh-water submersed aquatic plant species has been developed. The models describe major, carbon-flow-based ecophysiological processes and biomass dynamics of four common freshwater species and how these are influenced by factors such as light, temperature, current velocity, dissolved inorganic carbon availability, oxygen concentration, and human influences such as management measures (changes in turbidity, mechanical harvesting, grazing, flooding). The model species are <i>Vallisneria americana</i> [model VALLA], <i>Potamogeton pectinatus</i> [POTAM], <i>Hydrilla verticillata</i> [HYDRIL], and <i>Myriophyllum spicatum</i> [MILFO]. These plant species are similar in growth strategy but differ significantly in morphology and physiology. The same modeling approach was followed for all species, with species-characteristic morphology and physiology incorporated in four separate models. <i>V. americana</i> and <i>P. pectinatus</i> are considered as desirable, and <i>H. verticillata</i> and <i>M. spicatum</i> as invasive species in parts of the United States. In the models, phenology is tied to day-degree sum. This enables simulations for different sites and climates facilitating model operation. The models contain unique descriptions of (1) species-characteristic vertical distribution of shoot biomass in the water column; (2) recalculation procedures  <div style="text-align: right;">(Continued)</div>						
<b>15. SUBJECT TERMS</b> Biomass carbon flow		<i>Hydrilla</i> <i>Myriophyllum</i> Persistence	<i>Potamogeton</i> <i>Vallisneria</i> Modeling	VALLA POTAM HYDRIL	MILFO	
<b>16. SECURITY CLASSIFICATION OF:</b>			<b>17. LIMITATION OF ABSTRACT</b>	<b>18. NUMBER OF PAGES</b>  109	<b>19a. NAME OF RESPONSIBLE PERSON</b>	
<b>a. REPORT</b>  UNCLASSIFIED	<b>b. ABSTRACT</b>  UNCLASSIFIED	<b>c. THIS PAGE</b>  UNCLASSIFIED			<b>19b. TELEPHONE NUMBER (include area code)</b>	

#### 14. ABSTRACT (Concluded).

of vertical distribution with daily changes in water level; (3) *ibidem* with daily removal of shoot biomass at various levels within the water column; (4) species-characteristic epiphytic light interception; (5) species-characteristic effects of current velocity on photosynthesis; (6) removal of periodic shoot and tuber/root crown biomass; and (7) relationships of plant process parameters with site-specific climate by linkage with formatted weather files and calculation of latitude-specific effects on day length. Sensitivity analysis showed that the models are very sensitive to changes in process parameters influencing carbon flow. A good fit was found between simulated and measured biomass in the field. The models can be used to simulate the daily changes in plant processes, biomass, and persistence under various site-specific conditions and management scenarios over a 1- to 5-year period of four submersed aquatic vegetation species, in climates varying from temperate to tropical.